The Duality of Oxidative Stress-Inducing Non-Thermal Plasma for Cancer Treatment

From Regulated Cell Death to Enhanced Migration

Eline Biscop

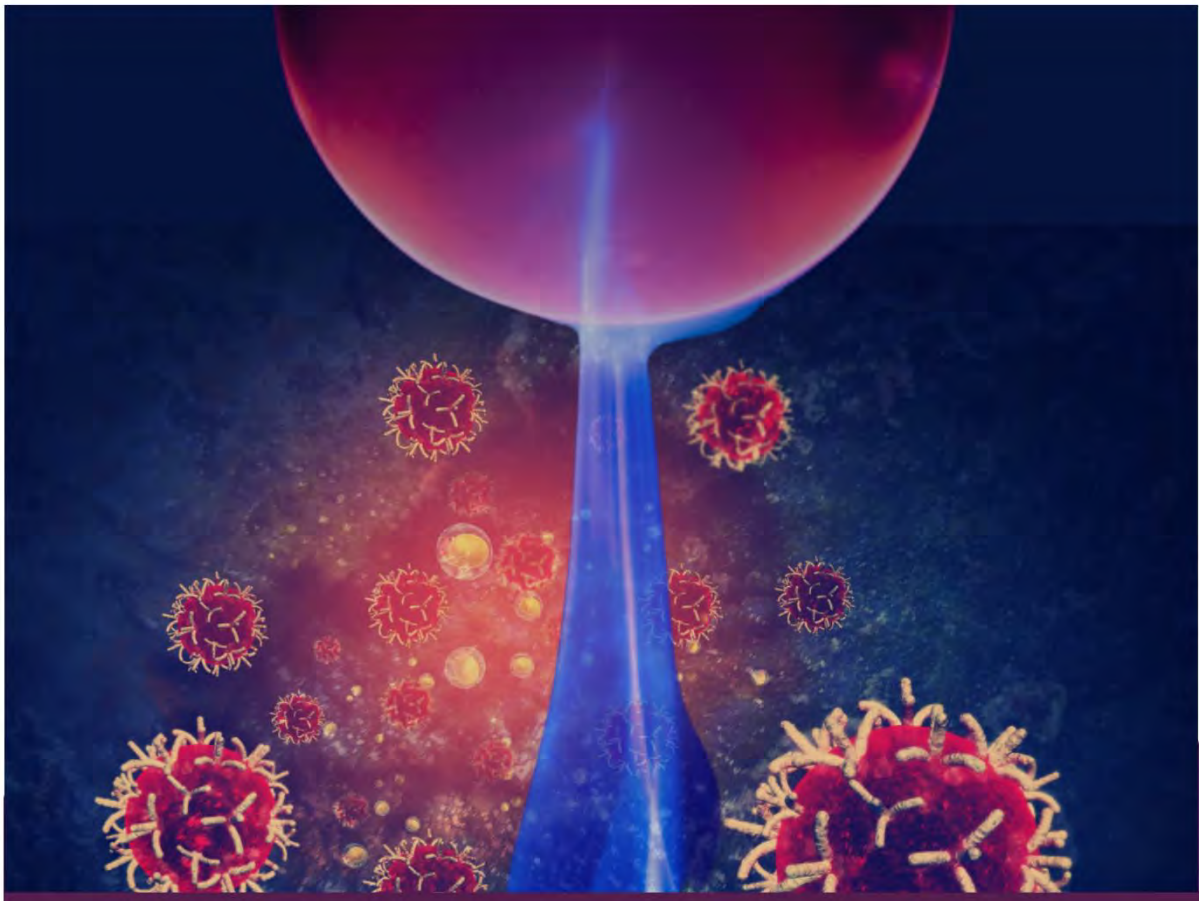

Promotors **Prof. Dr. Annemie Bogaerts | Prof. Dr. Evelien Smits | Dr. Abraham Lin**

Thesis submitted for the degree of Doctor of Science: Chemistry
Faculty of Science at the University of Antwerp | Antwerp, 2023

University of Antwerp

The Duality of Oxidative Stress-Inducing Non-Thermal Plasma for Cancer Treatment

From Regulated Cell Death to Enhanced Migration

Het Duale Karakter van Oxidatieve Stress-Gemedieerde Plasmabehandeling voor Kanker

Van gereguleerde celdood tot verhoogde migratie

Proefschrift voorgelegd tot het behalen van de graad van *Doctor in de Wetenschappen: Chemie* aan de Universiteit Antwerpen te verdedigen door

Eline Biscop

Promotoren

Prof. Dr. Annemie Bogaerts

Prof. Dr. Evelien Smits

Dr. Abraham Lin

Antwerpen
2023

Members of the Jury

CHAIRMAN

Prof. Dr. Erik Neyts, University of Antwerp

PROMOTORS

Prof. Dr. Annemie Bogaerts, University of Antwerp

Prof. Dr. Evelien Smits, University of Antwerp

Dr. Abraham Lin, University of Antwerp

INTERNAL JURY

Prof. Dr. Paul Cos, University of Antwerp

Prof. Dr. An Wouters, University of Antwerp

EXTERNAL JURY

Prof. Dr. Cristina Canal, Technical University of Catalonia (UPC)

Prof. Dr. Ana Sobota, Eindhoven University of Technology (TU/e)

Acknowledgements

I can hardly believe that I've reached the end of this incredible 4-year PhD journey. It has been quite an adventure, filled with so many wonderful memories and, like any journey, a few less enjoyable ones *kuch* Corona *kuch*. Luckily it all ended happily though, which would not have been possible without the support of so many amazing people in my life.

First of all I want to thank my promotors Annemie and Evelien for giving me the opportunity to start my PhD in their two amazing research groups PLASMANT and CORE. Your kindness and guidance over the past four years have been invaluable and I can honestly say that I couldn't have wished for better promotors to guide me through my PhD!

And then of course Abraham. You took me under your wing as a first year PhD student and shaped me into the researcher I am today. I couldn't have dreamed of a better mentor than you. You guided me through all the ups and downs in the lab and you were always there when I needed some advice. You recently told me you were very proud of me and what I accomplished, but honestly it is largely because of your support and guidance that I've been able to successfully finish this PhD. So, in reality, you should be very proud of yourself and the major role you played in my journey.

Secondly, I want to thank my colleagues, with a special shoutout to a few individuals:

Claudia, Senne and Elise, you have been part of my daily life for almost ten years, and I'm incredibly grateful that we got to share the past four years of this PhD adventure together. It simply would have never been the same without you guys. And of course Callie, who could not have been a better match to our office. You are so kind and supporting and I really enjoyed sharing an office with you (not only because you know all the gossip hehe).

Then I also want to thank Björn and Joachim. I won't forget our often random but always enjoyable conversations in the office. Those chats were the perfect breaks I didn't always need but always appreciated.

Furthermore, I want to thank Ruben and Hanne, “the three plasmateers”. We had some amazing times together, with Perry, Patsy and Pingy to prove it. I could always count on you guys to vent my frustrations if my experiments failed (again) or if the plasma devices gave a completely different result than the first repeat (again). And also to the rest of the former and current plasma-onco team – Angela, Abraham, Lisa, Jana, Edgar, Jinthe, Joey, and Priyanka – I really enjoyed our interesting discussions as well as our many fun teambuildings outside of work.

And of course I want to extend my thanks to all the other colleagues of PLASMANT and CORE for all the nice moments we shared. I feel really privileged to have worked in such amazing research groups.

Finally, I also want to thank my friends and family, who might not realize how much they contributed to my PhD by being there for my when I needed them. Especially my mom and my sister, who have supported me unconditionally. Even in difficult times, you were always there for me and pushed me to be the best person I could be, for which I will be eternally grateful!

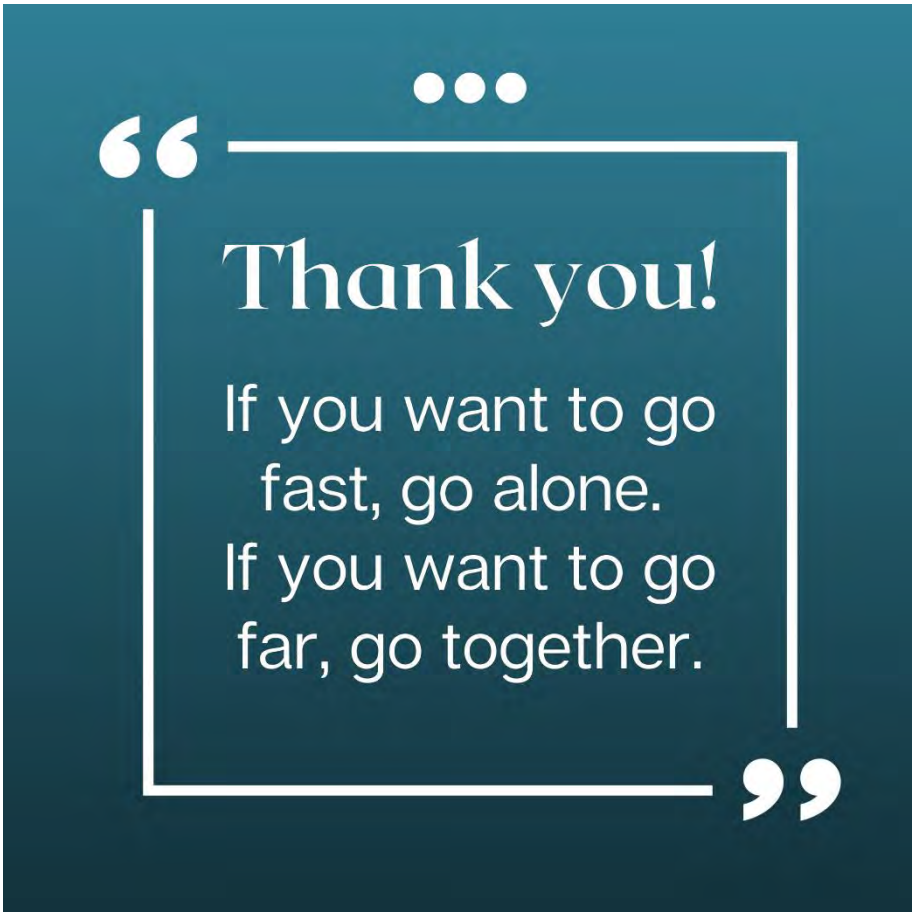

Table of Contents

CHAPTER 1

General Introduction and Aims of this Thesis

1.1 Cancer, The Silent Killer of the 21st Century

Although cancer was already documented about 5000 years ago in ancient Egypt, it still remains one of the leading causes of death today, accounting for around 10 million deaths in 2020 worldwide[1]. In general, cancer is a complex disease involving dynamic changes in the genome leading to unregulated cell division. Over the years, thousands of researchers have made significant contributions to uncovering more insights into this intricate disease, resulting in the creation of the Hallmarks of cancer, which are distinctive characteristics of cancer cells that define their behavior[2]. These Hallmarks were originally proposed by researchers Douglas Hanahan and Robert Weinberg in 2000, and have been expanded since. Initially, they proposed six hallmarks, after which they added four more in 2011, and four more in 2022, bringing the total to 14 Hallmarks[2–4]. (Figure 1.1) While numerous characteristics are shared among various cancer types, each type possesses unique mutations that result in varying responses to specific triggers[5]. This complexity makes it impossible to find a universal treatment that could effectively address all types of cancer. Due to the increasing number of mutations leading to the development of resistance against therapies, the development of innovative therapies remains critical in the fight against this horrible disease.

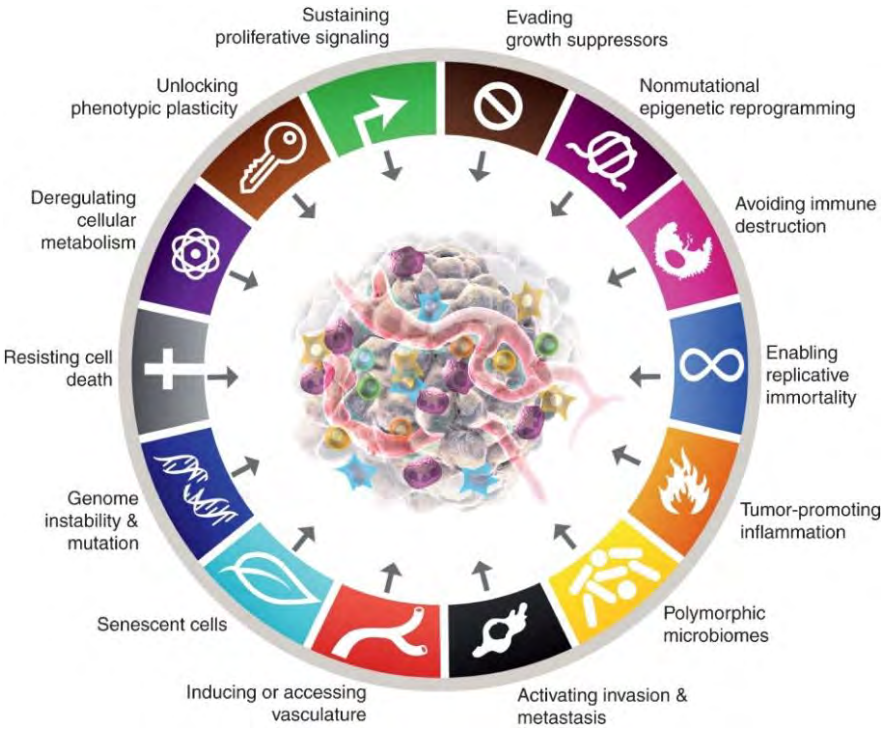

Figure 1.1: Overview of all 14 Hallmarks of cancer as proposed by Douglas Hanahan and Robert Weinberg[4]

1.1.1 Melanoma, current state-of-the-art and ongoing challenges

Melanoma is the most aggressive form of skin cancer, originating from malignant genetic mutations of melanocytes in the skin, and the leading cause of death among cutaneous cancers. Despite the significant advances in cancer therapies in recent years, the occurrence and mortality rates of melanoma keep rising annually[6]. In 2020, there were 324,635 new cases and 57,043 mortalities reported worldwide[7]. When diagnosed early, melanoma is in most cases successfully treatable, whereas when diagnosed at an advanced stage, it exhibits a more limited response to conventional anti-cancer therapies, resulting in a 5-year survival rate of only 30%[8]. Although this still remains low, the 5-year survival rate has already doubled

since 2017, where it was only 15%, due to the significant advancements in targeted therapies and immunotherapies. Analysis of the genetic landscape in melanoma has revealed an exceptionally high level of mutations when compared to other types of cancer, exceeding 10 mutations per megabase[9]. The primary cause of these mutations is UV exposure. Among the most frequently encountered mutations in melanoma is one in the BRAF gene, specifically the V600E mutation, which is prevalent in approximately 50% of melanoma patients[9,10]. The BRAF gene is an oncogene that functions as a serine/threonine protein kinase and plays a crucial role in the RAS-RAF-MEK-ERK mitogen-activated protein kinase (MAPK) cell signaling pathway. Additionally, mutations in the MEK gene, also a component of the MAPK signaling pathway, have been identified in around 10% of melanoma cases[10]. Currently, several targeted therapies focusing on the combination of BRAF and MEK inhibitors are clinically approved[10]. However, despite these targeted therapies, immunotherapy has emerged as the most promising approach for treating advanced melanoma due to its potential for achieving sustained therapeutic effects[9,10]. Melanoma's high immunogenicity and mutational burden render it an ideal candidate for immunotherapies. The FDA has approved three types of immunotherapies for advanced melanoma treatment: immune-checkpoint inhibitors (ICIs) targeting PD-1 and CTLA4 to mitigate T-cell exhaustion, T-cell-stimulating cytokines such as interferon-α2b and interleukin-2, and an oncolytic virus called T-VEC that activates dendritic cells (DC)[11]. Combining immunotherapy (anti-PD-1 or anti-CTLA4 ICI) with targeted therapy (BRAF+MEK inhibition) holds significant promise due to the advantages of both treatment

modalities. Currently, there are three ongoing phase II and phase III clinical trials that explore combinations of anti-PD-1, BRAF, and MEK inhibitors, showing encouraging enhancements in response rates, duration of response, progression-free survival, and overall survival[10]. However, despite the notable successes of targeted therapies and immunotherapy, challenges remain in the form of resistance to targeted therapies and the side effects associated with immunotherapy. Consequently, the search for alternative treatment strategies for advanced melanoma remains a critical priority [10].

1.2 Basic Principles of Non-Thermal Plasma

1.2.1 What is non-thermal plasma?

Plasma, often referred to as the fourth state of matter, is a (partially) ionized gas consisting of a large number of reactive species, such as electrons, ions, radicals and excited species[11–13]. While plasma is a relatively rare phenomenon on Earth, it dominates the composition of the universe, accounting for over 99% of its visible matter. In a controlled environment, plasma can be created by applying a high electric field between two electrodes, which leads to an acceleration of the electrons, initiating a cascade of collisions that gives rise to a diverse range of reactive species[11,13]. This process can be characterized by a wide range of temperatures and pressures, and plasmas are therefore generally subdivided into two major groups: thermal and non-thermal plasmas[11,13]. In thermal plasmas, the energy and temperature of the electrons, ions and neutral species are in equilibrium, resulting in overall high gas temperatures exceeding 1000 K. In contrast, non-thermal plasmas (NTP) transfer the applied energy primarily to the electrons, while the bulk gas containing the

heavier species, maintains a relatively low temperature, akin to room temperature. This overall low temperature of the gas makes NTP particularly interesting for the treatment of heat-sensitive materials. Consequently, NTP rapidly gained increasing interest for various biomedical applications, including sterilization, wound healing, dentistry and most recently cancer therapy[11,12].

1.2.2 Non-thermal plasma sources

In the research area of plasma for medical applications, various types of plasma sources are being used, with the dielectric barrier discharge (DBD) and the plasma jet emerging as the two most extensively investigated ones[14,15]. Both have a distinct configuration and operating conditions, providing them with unique advantages and disadvantages, dependent on the intended application. Up until now, several NTP sources have been officially approved for medical and cosmetic use (listed in Table 1.1). Overall, there are currently more clinically approved plasma jets compared to DBD devices, being primarily used for wound healing and cosmetic purposes. Yet, recent advances in the plasma medicine field led to an increasing interest in the use of plasma devices for cancer therapy. Presently, only the kINPen MED and Canady Helios Cold Atmospheric Scalpel have been used in clinical trials focused on cancer treatment.

1.2.2.1 Dielectric barrier discharge (DBD)

DBD plasma sources consist of two electrodes of which at least one is covered by a dielectric material, often quartz, but also glass, ceramics or polymers can be used (shown in Figure 1.2A)[13,15]. When an electric field is applied between the two electrodes, the dielectric surface gets locally charged. These charge accumulations at the

dielectric surface reduce the electric field, locally reducing it to zero, which terminates the discharge within nanoseconds after breakdown. The short duration of these discharges, or so-called pulses, leads to an efficient energy transfer to the electrons while minimally affecting the temperature of the bulk gas, resulting in a thermal non-equilibrium between the electrons and heavy species[16]. In order to continuously create the short-lived discharges over the whole surface of the electrodes, a high voltage alternating current (AC) or pulse is applied with frequencies generally in the kHz range. For the use in medical applications like wound healing and cancer therapy, generally a floating-electrode DBD (FE-DBD) is used[15]. In this DBD set-up, the second, grounded, electrode is replaced by a biological target like human skin (shown in Figure 1.2B). To create a discharge between the insulated high voltage electrode and the biological target, it is necessary to maintain a relatively small gap (<3 mm) between the two.

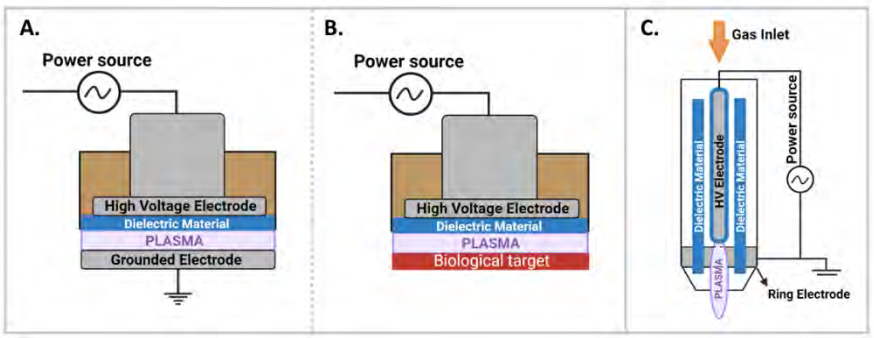

Figure 1.2 Schematic overview of the two main types of NTP sources. A. a dielectric barrier discharge. B. a floating-electrode dielectric barrier discharge. C. a plasma jet

A major benefit of utilizing a DBD plasma source is its capability to deliver a uniform and widespread treatment across the target area due to the large surface area covered by micro-discharges.

Additionally, DBD electrodes can be designed in different geometries, allowing adaptation for various medical applications. However, the requirement for short distances during discharges may impose limitations on effectively reaching and treating specific target areas within the body [17,18].

1.2.2.2 Plasma jet

Similarly to a DBD plasma source, a plasma jet consists of two electrodes, usually a central rod-like electrode connected to a HV power source and a grounded ring electrode (shown in Figure 1.2C). The electrodes are typically surrounded by a metal housing through which a carrier gas, such as helium or argon, flows. When an electric field is applied between the electrodes, a highly energized electron flow is created causing excitation and ionization of the carrier gas. Due to the inefficient energy transfer from the energetic electrons to the heavier particles from the carrier gas, the heavy particles remain relatively cold, resulting in a low overall gas temperature. Additional cooling of the plasma can be achieved by using pulsed excitation patterns or increased fluxes of the carrier gas[11,15,19].

One of major advantages of a plasma jet is the tunability of the treatment parameters. By introducing small amounts of molecular gases like oxygen or nitrogen into the carrier gas, the composition of the reactive species generated by the plasma can be tailored according to the specific medical application. Furthermore, while the DBD is highly effective in treating larger surface areas, the plasma jet is more suitable to treat smaller, harder-to-reach areas in the body[15,18].

Table 1.1 List of certified NTP devices with their main applications in medicine and year of medical approval.

Name	Type	Application	Year	Ref.
Rhytec Portrait®	Plasma jet	Skin Rejuvenation	2008	[20]
Bovie J-Plasma®	Plasma jet	Surgery	2020	[21]
Canady Helios Cold Plasma® Scalpel	Plasma jet	Cancer therapy	2019	[22]
Canady Hybrid and APC Plasma® Scalpel	Plasma jet	Surgery	2019	[22]
kINPen® MED	Plasma jet	Wound healing, Cancer therapy	2013	[19]
PlasmaDerm®	DBD	Wound healing	2012	[23]
SteriPlas®	Plasma jet	Wound healing	2017	[24]
Plasma Care®	DBD	Wound healing, Dermatology	2019	[25]
Plasma One®	DBD	Wound healing, Dentistry	2013	[26]

1.3 Non-Thermal Plasma, from Thunderbolt to Therapy

1.3.1 Basic principles and treatment modalities

As mentioned above, NTP is a partially ionized gas consisting of highly energetic electrons and other reactive species. Since NTP sources for medical applications operate in an open atmospheric environment, NTP can interact with the surrounding ambient air (O_2 and N_2), generating reactive oxygen and nitrogen species (RONS)[11,18]. NTP-derived RONS are generally subdivided into long-lived RONS (lifetimes ≥ 1 s), such as hydrogen peroxide (H_2O_2), nitrate (NO_3^-) and nitrite (NO_2^-), and short-lived RONS (lifetimes < 1 s), such as hydroxyl radicals ($^\bullet OH$), atomic oxygen (O), ozone (O_3), singlet oxygen ($^1O_2$), nitric oxide ($^\bullet NO$) and peroxynitrite ($ONOO^-$

)[11,27]. Although NTP also exposes the cells to a variety of physical components (UV, high electric/magnetic field), it is demonstrated in numerous studies that the anti-cancer effect of NTP is predominantly due to the formation of these highly reactive RONS. It is, however, important to note that the mixture of RONS reaching the cells is highly dependent on the NTP source and more specifically on the treatment modality used to deliver the RONS to the biological target. At present, two major NTP treatment modalities are being studied: direct and indirect NTP treatment (shown in Figure 1.3)[17,28].

With direct NTP treatment, NTP is generated in direct contact with the biological target, resulting in the delivery of both long-lived and short-lived RONS. While this modality is highly efficient in delivering a plethora of biologically active RONS, this approach is constrained to surfaces that can be accessed by the device[28].

With the indirect NTP treatment method, a physiological solution is treated with NTP and enriched with RONS for a specific duration before being introduced to the target substrate[28]. This treatment modality allows for the treatment of deeper tissue layers via delivery of the RONS-enriched physiological solution, but the longer intervals between the NTP enrichment of the solution and its administration onto the target substrate, consequently, limits the RONS delivered. Only the long-lived RONS are able to reach the cells, which may potentially restrict certain biological responses.

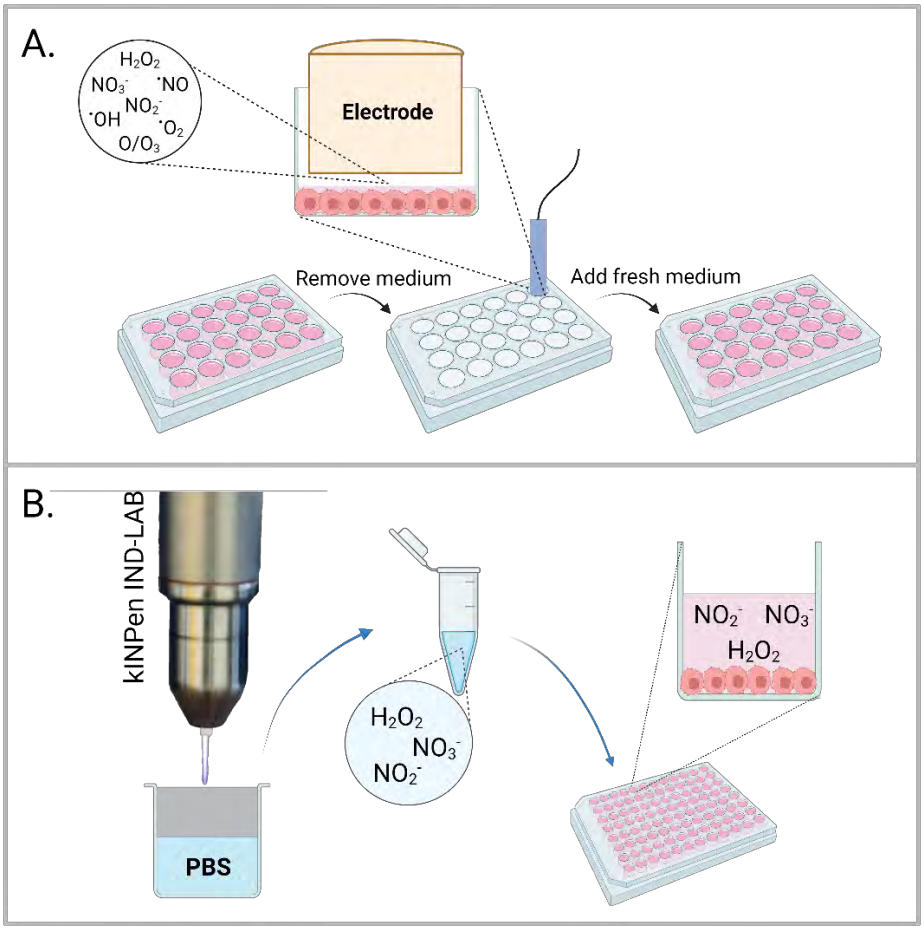

Figure 1.3 Schematic representation of the two major NTP treatment modalities. A. Direct NTP treatment; B. Indirect NTP treatment

1.3.2 Mechanism of action

Currently, the main, accepted hypothesis regarding the mechanism by which NTP can eliminate cancer cells is through the induction of oxidative stress, which refers to an imbalance between oxidants and antioxidants in favor of the oxidants[29,30]. The NTP-derived RONS can penetrate or interact with the cellular membrane, potentially triggering secondary effects inside the cell that can amplify the NTP-induced biological effects. This process leads to an increase in

intracellular RONS concentrations, activating several redox signaling cascades and response mechanisms within the cell[18,30]. However, due to the complex mixture of RONS interacting with the cells, a comprehensive understanding of the redox biology responses following NTP treatment is challenging. In the next paragraph, I will try to summarize the main redox reactions initiated following NTP treatment.

The cellular membrane plays a key role in the biological responses triggered by NTP-derived RONS as this is the first barrier they have to penetrate or interact with (presented in Figure 1.4). Among the NTP-derived RONS, $^{\bullet}OH$ is one of the most reactive[30]. Despite its inability to diffuse through the cellular membrane, it can interact with cholesterol, resulting in the formation of hydroperoxyl radicals ($HO_2^{\bullet}$) and the corresponding superoxide anion radicals ($^{\bullet}O_2^-$), which can elicit multiple responses in cells[31]. In addition to its interaction with cholesterol, $^{\bullet}OH$ plays a significant role as an inducer of lipid peroxidation, leading to the generation of additional pores in the cell membrane[30]. Within the cell, $^{\bullet}OH$ is formed from H_2O_2 through the Fenton reaction. Besides $^{\bullet}OH$, $^{\bullet}O_2^-$ also plays an important role in cellular redox biology. Other than being generated by NTP, $^{\bullet}O_2^-$ is formed by converting O_2 with NADPH oxidase and as a byproduct of mitochondrial respiration. It reacts with $^{\bullet}NO$, forming $ONOO^-$, which acts as a highly potent oxidant. Furthermore, $^{\bullet}O_2^-$ can be converted into H_2O_2 by superoxide dismutases (SODs) or undergo self-dismutation with another $^{\bullet}O_2^-$ molecule[30]. H_2O_2 is a relatively stable ROS which can enter the cell through aquaporins[18]. Once inside the cell, it has the potential to transform into highly reactive OH radicals through the Fenton reaction or can be converted into oxygen and

water by catalase. In general, $^{\bullet}O_2^-$ and H_2O_2 are considered major signaling molecules in cell physiology[30,32]. Additionally, other RONS, including $^{\bullet}NO$, O and O_3, have the ability to diffuse through the cell membrane, leading to elevated intracellular ROS levels and inducing oxidative stress[31]. Enhanced RONS concentrations can subsequently trigger endoplasmic reticulum (ER) stress, resulting in increased Ca^{2+} concentrations, which in turn adversely affect mitochondrial functions[30]. Alongside ER stress, oxidative stress can induce DNA damage through strand breaks and base oxidation[30].

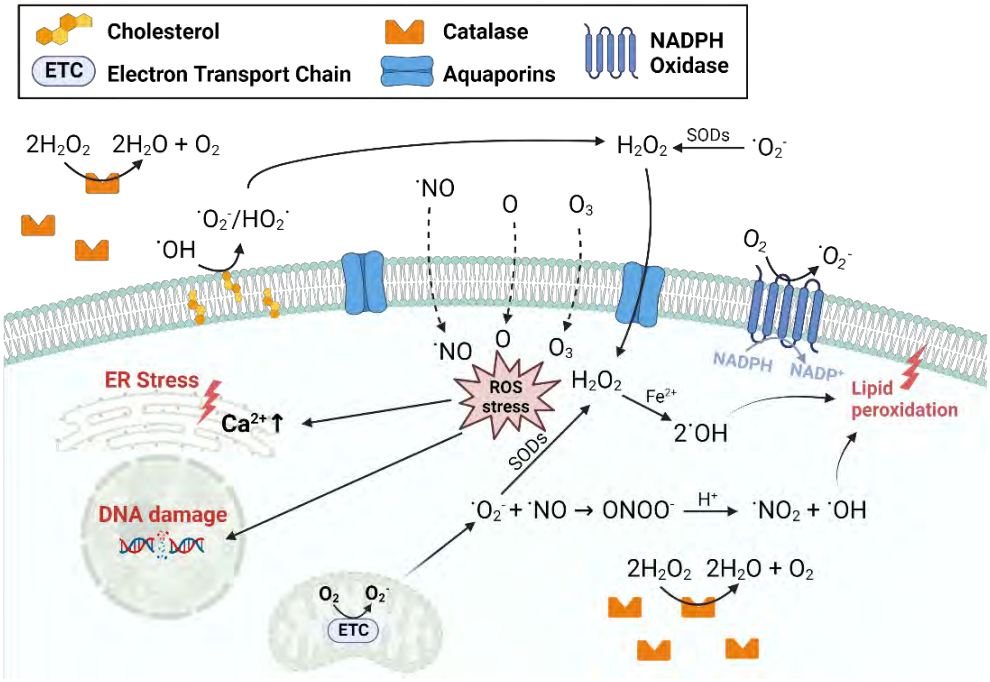

Figure 1.4 Overview of the main NTP-derived RONS and their impact on redox biology

1.3.3 Targeting RONS in cancer

RONS have long been associated with cancer, where different types of cancer cells have been shown to produce higher levels of RONS compared to their normal counterparts. In response to this intrinsic oxidative stress, cancer cells have evolved protective mechanisms and adaptation strategies by upregulating pro-survival molecules and their antioxidant defense systems to maintain redox balance[33]. Conversely, when RONS levels exceed a certain threshold, they can overwhelm the defense antioxidant system of the cancer cells, leading to cell death.

Indeed, the initial report on NTP as a novel oxidative stress-inducing therapy for cancer emerged in 2007, revealing its pro-apoptotic effects on human melanoma cancer cells[34]. Subsequently, numerous studies followed, providing compelling evidence of NTP's anticancer effects across various cancer types, such as glioblastoma, melanoma, breast cancer, colorectal cancer, lung cancer, cervical cancer, pancreatic cancer, leukemia, liver cancer, and head and neck cancer[18,35,36]. Moreover, due to the higher basal RONS levels in cancer cells, they will reach their threshold for oxidative stress faster than healthy cells, indicating that targeting oxidative stress can trigger a selective killing response. This hypothesis was further supported by the higher amounts of aquaporins and lower amounts of cholesterol in the cell membrane of cancer cells compared to healthy cells, facilitating the diffusion of additional RONS inside the cell. Therefore, if the treatment can be applied within a range in which tumor cells reach their threshold but healthy cells can still recover from the oxidative stress, a selective treatment can be achieved. Several researchers indeed claimed that NTP induces a

selective killing response, however these results should be interpreted with caution since discrepancies were found in several biological factors and culturing methods. I will elaborate more on the importance of these factors in Chapter 2.

However, in recent years it has become clear that to ensure a long-lasting anticancer effect, it is often not sufficient for a cancer treatment to solely induce a cytotoxic response. In order to provide a more systemic approach, a cancer treatment should also promote anti-tumor immunity, which can be achieved through immunogenic cell death (ICD)[37,38]. This is a unique type of cell death characterized by the release of damage-associated molecular patterns (DAMPs). These are stress-released endogenous danger signals acting as alarm signals for the innate immune system, leading to the effective presentation of tumor antigens and subsequent priming of antigen-specific T cells. This process enhances the elimination of tumor cells and generates an immune memory against the tumor antigens, thereby reducing the chance of recurrence[18]. In literature, there are already multiple studies showing that tumor cells undergoing oxidative stress-induced cell death have the capacity to trigger ICD[27,38–41]. Moreover, preclinical research has reported the ability of NTP to stimulate ICD in numerous cancer types via the release of damage-associated molecular patterns (DAMPs), increase in activation of dendritic cells (DCs) and phagocytosis activity in co-culture settings, the gold-standard 'vaccination assay', and even demonstration of abscopal effects[27,39–41]. Furthermore, our lab has previously traced the activation of the cancer-immunity cycle over time in a melanoma mouse model following NTP treatment. The cancer immunity cycle describes the sequence of events through

which the immune system recognizes, attacks, and eliminates cancer cells. It involves steps such as cancer cell recognition, antigen presentation, T cell activation, tumor infiltration, destruction of cancer cells, and memory cell formation. We demonstrated that local NTP treatment of the tumor resulted in greater DC and T cell activation in not only the tumor microenvironment (TME) but also in the tumor-draining lymph nodes[39].

While the potential of NTP treatment in cancer treatment seems promising, it is important to acknowledge that oxidative stress-inducing therapies can be a double-edged sword[42,43]. Extensive research from both experimental and clinical studies indicates that RONS can also play an important role in promoting various stages of tumor formation and progression, dependent on their mutagenic potential and ability to interact with signaling pathways regulating cell proliferation, motility, invasiveness and survival[33]. For instance, H_2O_2 can reversibly oxidize the cysteine thiol groups of phosphatase and tension homolog (PTEN), causing its inactivation and, consequently, promoting the activation of the PI3K/Akt/mTOR survival pathway, ultimately supporting tumor cell survival[42]. Indeed, it was shown that inactivation of PTEN is found frequently in a variety of cancers including breast cancer, endometrial cancers, glioblastoma, melanoma and prostate cancer[42]. Furthermore, the oxidative stress-induced Ca^{2+} release can activate kinases such as protein kinase C (PKC), which plays an important role in the proliferation of cancer cells[44]. Moreover, increasing evidence demonstrates that RONS play a crucial role in promoting cell invasion and metastasis through the activation of stimuli associated with epithelial-mesenchymal transition (EMT)[45]. Finally, DNA oxidation and double-strand breaks

generated by high levels of intracellular ROS leads to an accumulation of multiple mutations, contributing to an increased risk of tumor cells developing resistance against cancer therapies[33]. Indeed, several studies show that oxidative stress frequently causes mutations in the genes encoding the NRF2 transcription factor and its negative regulator, KEAP1, which is associated with poor prognosis and correlates with therapy resistance and tumor recurrence[46].

Taken together, targeting oxidative stress in cancer can be a very efficient anticancer strategy, but several dual aspects need to be taken into account when investigating novel oxidative stress-inducing therapies.

1.4 Aims and Outline of this Thesis

Because of its very promising preclinical results, NTP has gained great interest as a novel therapy for cancer. However, to realize larger clinical trials using NTP, some important gaps in knowledge have to be investigated. The general aim of this research study was therefore to answer several key questions regarding the dual effects of NTP-induced oxidative stress in melanoma skin cancer.

This thesis is organized into 6 different chapters (Figure 1.5). Chapter 1 provides comprehensive introduction and background information. Chapters 2-5 each address a specific research question, as described below. Concluding the thesis, Chapter 6 presents a general summary along with future prospects concerning NTP treatment.

Research question 1: Can NTP selectively target cancer cells while leaving their normal counterparts unharmed?

Since cancer cells have a higher basal ROS level, it is hypothesized that by further increasing these intracellular ROS levels, they will reach their cytotoxic threshold faster in comparison to healthy cells. Moreover, they have more aquaporins and less cholesterol in their cell membrane, allowing for a faster uptake of exogenous RONS, providing additional support to this hypothesis. Indeed, when looking into literature, there are several reports claiming NTP to be selective. However, retrospective analysis of these studies revealed discrepancies in several biological factors and culturing methods. Before NTP can be conclusively stated as a selective cancer treatment, the importance of these factors must be investigated. In this study, we evaluated the influence of the cell type, cancer type, and cell culture medium on direct and indirect NTP treatment.

Research question 2: What is the stability of the most important NTP-derived RONS in a more clinical setting?

The results from my first research question raised some additional questions regarding the stability of RONS in a more clinical setting. Since NTP-derived RONS will almost inevitably come into contact with blood in several clinical settings, understanding their stability in this system is crucial. Thus, I examined the stability of the most important RONS in three aqueous solutions with increasing organic complexities: phosphate-buffered saline (PBS), blood plasma and processed whole blood. Based on our results, we discussed the scavenging capacity of different blood components as well as the

necessary considerations to choose the most optimal NTP modality for the desired clinical application.

Research question 3: Which regulated cell death mechanisms are activated following NTP treatment?

NTP has shown promising anti-cancer effects, but there is still limited knowledge about the underlying cell death mechanisms induced by NTP and inherent differences between direct and indirect NTP treatment. As previously discussed, the interaction of different RONS with the cancer cells varies between the two NTP modalities. With the direct NTP treatment, both long-lived and short-lived RONS can interact with cancer cells, whereas with the indirect NTP treatment, only the long-lived RONS can reach the cells. This study aimed to investigate four major regulated cell death (RCD) pathways, namely apoptosis, pyroptosis, necroptosis, and ferroptosis, and provide an overview of the mechanistic differences between the two major NTP treatment modalities.

Research question 4: Does NTP-induced oxidative stress trigger EMT?

As mentioned in section 1.3.3 above, despite its great potential to selectively kill cancer cells, oxidative stress can trigger some undesired side effects. Increasing evidence suggests that RONS play a crucial role in promoting cell invasion and metastasis through the activation of stimuli associated with EMT. In light of this connection between oxidative stress and EMT, we sought to investigate whether NTP would initiate this transition and whether we could modify the response by altering the NTP treatment parameters. To do this, we performed a comprehensive study of six key EMT biomarkers to

analyze their expression post NTP treatment and, moreover, looked into a change in migratory capacities of the cancer cells in two different 3D cancer models, the spheroid model and the *in ovo* model.

Overall, this thesis will provide valuable insights into the NTP-induced activation of molecular pathways related to cytotoxicity and migration, and will enable researchers to make more strategic choices for combination cancer therapies in the future.

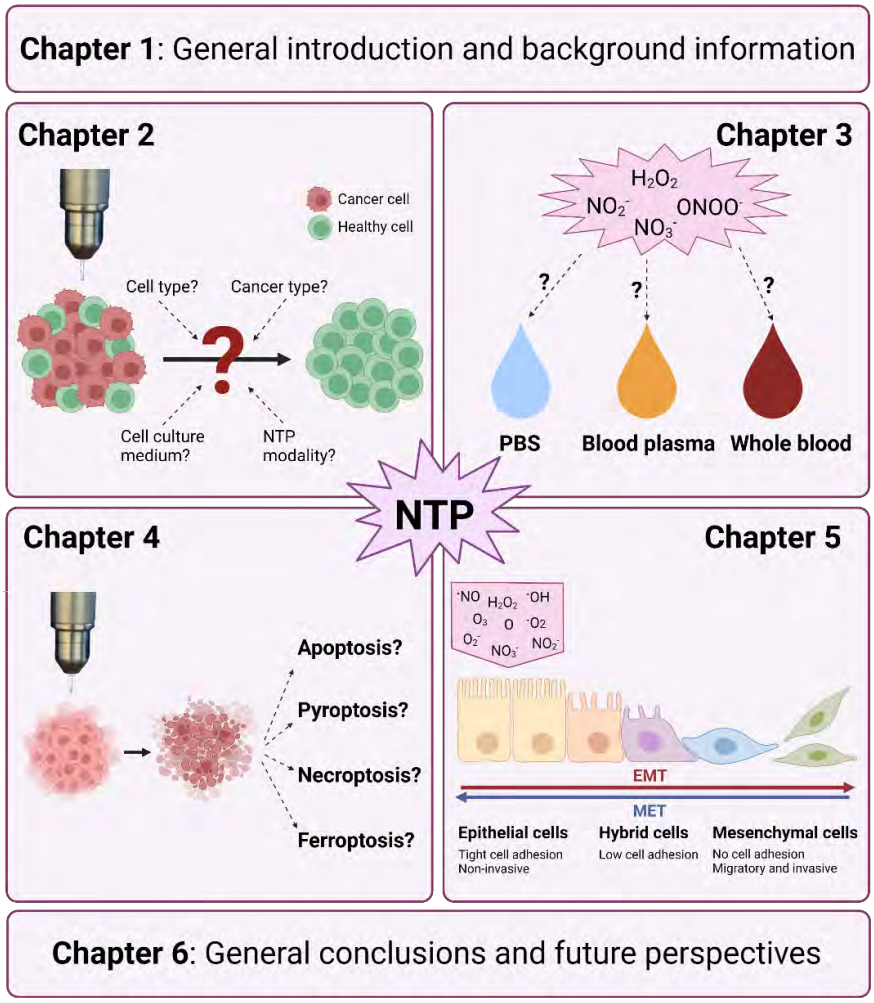

Figure 1.5 Outline of the doctoral thesis

1.5 References

1. Cancer Research UK. Worldwide Cancer Statistics.
2. Hanahan D, Weinberg RA. *The Hallmarks of Cancer*. Vol 100.; 2000.
3. Hanahan D. Hallmarks of Cancer: New Dimensions. *Cancer Discov*. 2022;12(1):31-46. doi:10.1158/2159-8290.CD-21-1059
4. Hanahan D, Weinberg RA. Hallmarks of cancer: The next generation. *Cell*. 2011;144(5):646-674. doi:10.1016/j.cell.2011.02.013
5. Hao D, Wang L, Di LJ. Distinct mutation accumulation rates among tissues determine the variation in cancer risk. *Sci Rep*. 2016;6. doi:10.1038/srep19458
6. Arnold M, Singh D, Laversanne M, et al. Global Burden of Cutaneous Melanoma in 2020 and Projections to 2040. *JAMA Dermatol*. 2022;158(5):495-503. doi:10.1001/jamadermatol.2022.0160
7. The Global Cancer Observatory. *Melanoma of the Skin Fact Sheet*.; 2020.
8. Cancer Research UK. Melanoma skin cancer - Survival.
9. Schadendorf D, van Akkooi ACJ, Berking C, et al. Melanoma. *The Lancet*. 2018;392(10151):971-984. doi:10.1016/S0140-6736(18)31559-9
10. Switzer B, Puzanov I, Skitzki JJ, Hamad L, Ernstoff MS. Managing Metastatic Melanoma in 2022: A Clinical Review. *JCO Oncol Pract*. 2022;18(5):335-351. doi:10.1200/OP.21.00686
11. Ernst M, Giubellino A. The Current State of Treatment and Future Directions in Cutaneous Malignant Melanoma. *Biomedicines*. 2022;10(4). doi:10.3390/biomedicines10040822
12. Keidar M. *Plasma Cancer Therapy*.; 2020. http://www.springer.com/series/411
13. Fridman AA, Friedman G (Gary G). *Plasma Medicine*. John Wiley & Sons; 2013.
14. Fridman AA. *Plasma Chemistry*. Cambridge University Press; 2008.
15. Yan D, Sherman JH, Keidar M. Cold atmospheric plasma, a novel promising anti-cancer treatment modality. *Oncotarget*. 2017;8(9):15977-15995. doi:10.18632/oncotarget.13304

16. Isbary G, Shimizu T, Li YF, et al. Cold atmospheric plasma devices for medical issues. *Expert Rev Med Devices*. 2013;10(3):367-377. doi:10.1586/erd.13.4

17. Kogelschatz U. *Dielectric-Barrier Discharges: Their History, Discharge Physics, and Industrial Applications*. Vol 23.; 2003.

18. Tanaka H, Mizuno M, Ishikawa K, et al. New Hopes for Plasma-Based Cancer Treatment. *Plasma*. 2018;1(1):150-155. doi:10.3390/plasma1010014

19. Faramarzi F, Zafari P, Alimohammadi M, Moonesi M, Rafiei A, Bekeschus S. Cold Physical Plasma in Cancer Therapy: Mechanisms, Signaling, and Immunity. *Oxid Med Cell Longev*. 2021;2021. doi:10.1155/2021/9916796

20. Bekeschus S, Schmidt A, Weltmann KD, von Woedtke T. The plasma jet kINPen – A powerful tool for wound healing. *Clin Plasma Med*. 2016;4(1):19-28. doi:10.1016/j.cpme.2016.01.001

21. Kilmer S, Semchyshyn N, Shah G, Fitzpatrick R. A pilot study on the use of a plasma skin regeneration device (Portrait® PSR3) in full facial rejuvenation procedures. *Lasers Med Sci*. 2007;22(2):101-109. doi:10.1007/s10103-006-0431-9

22. Filis K, Galyfos G, Sigala F, Zografos G. Utilization of low-temperature helium plasma (J-Plasma) for dissection and hemostasis during carotid endarterectomy. *J Vasc Surg Cases Innov Tech*. 2020;6(1):152-155. doi:10.1016/j.jvscit.2020.01.008

23. Ly L, Jones S, Shashurin A, et al. A New Cold Plasma Jet: Performance Evaluation of Cold Plasma, Hybrid Plasma and Argon Plasma Coagulation. *Plasma*. 2018;1(1):189-200. doi:10.3390/plasma1010017

24. Wandke D, Busse B, Helmke A. DBD-CAP PlasmaDerm Flex and Dress. In: Metelmann HR, Von Woedtke T, Weltmann KD, Emmert S, eds. *Textbook of Good Clinical Practice in Cold Plasma Therapy*. Springer; 2022:307-321.

25. Arndt S, Schmidt A, Karrer S, von Woedtke T. Comparing two different plasma devices kINPen and Adtec SteriPlas regarding their molecular and cellular effects on wound healing. *Clin Plasma Med*. 2018;9:24-33. doi:10.1016/j.cpme.2018.01.002

26. Zimmermann JL, Roskopf CC, Cantzler S, et al. Plasma Care. In: *Textbook of Good Clinical Practice in Cold Atmospheric Plasma*. Springer; 2022:363-387.

27. Zashev M, Donchev D, Ivanov I, Gornev R. Efficacy of Plasma ONE apparatus for disinfection of S. aureus, P. aeruginosa and E. coli bacteria from the solid surface. *Journal of Theoretical and Applied Physics*. 2020;14:41-49. doi:10.1007/s40094-020-00401-5

28. Lin A, Gorbanev Y, De Backer J, et al. Non-Thermal Plasma as a Unique Delivery System of Short-Lived Reactive Oxygen and Nitrogen Species for Immunogenic Cell Death in Melanoma Cells. *Advanced Science*. 2019;6(6). doi:10.1002/advs.201802062

29. Malyavko A, Yan D, Wang Q, et al. Cold atmospheric plasma cancer treatment, direct: Versus indirect approaches. *Mater Adv*. 2020;1(6):1494-1505. doi:10.1039/d0ma00329h

30. Turrini E, Laurita R, Stancampiano A, et al. Cold Atmospheric Plasma Induces Apoptosis and Oxidative Stress Pathway Regulation in T-Lymphoblastoid Leukemia Cells. *Oxid Med Cell Longev*. 2017;2017. doi:10.1155/2017/4271065

31. Von Woedtke T, Laroussi M, Gherardi M. Foundations of plasmas for medical applications. *Plasma Sources Sci Technol*. 2022;31(5). doi:10.1088/1361-6595/ac604f

32. Privat-Maldonado A, Schmidt A, Lin A, et al. ROS from Physical Plasmas: Redox Chemistry for Biomedical Therapy. *Oxid Med Cell Longev*. 2019;2019. doi:10.1155/2019/9062098

33. Lu X, Naidis G V., Laroussi M, Reuter S, Graves DB, Ostrikov K. Reactive species in non-equilibrium atmospheric-pressure plasmas: Generation, transport, and biological effects. *Phys Rep*. 2016;630:1-84. doi:10.1016/j.physrep.2016.03.003

34. Hayes JD, Dinkova-Kostova AT, Tew KD. Oxidative Stress in Cancer. *Cancer Cell*. 2020;38(2):167-197. doi:10.1016/j.ccell.2020.06.001

35. Fridman G, Shereshevsky A, Jost MM, et al. Floating electrode dielectric barrier discharge plasma in air promoting apoptotic behavior in Melanoma skin cancer cell lines. *Plasma Chemistry and Plasma Processing*. 2007;27(2):163-176. doi:10.1007/s11090-007-9048-4

36. Dubuc A, Monsarrat P, Virard F, et al. Use of cold-atmospheric plasma in oncology: a concise systematic review. *Ther Adv Med Oncol*. 2018;10. doi:10.1177/1758835918786475

37. Yan D, Malyavko A, Wang Q, Lin L, Sherman JH, Keidar M. Cold atmospheric plasma cancer treatment, a critical review. *Applied Sciences (Switzerland)*. 2021;11(16). doi:10.3390/app11167757

38. Van Loenhout J, Peeters M, Bogaerts A, Smits E, Deben C. Oxidative stress-inducing anticancer therapies: Taking a closer look at their immunomodulating effects. *Antioxidants*. 2020;9(12):1-19. doi:10.3390/antiox9121188

39. Živanić M, Espona-Noguera A, Lin A, Canal C. Current State of Cold Atmospheric Plasma and Cancer-Immunity Cycle: Therapeutic Relevance and Overcoming Clinical Limitations Using Hydrogels. *Advanced Science*. 2023;10(8). doi:10.1002/advs.202205803

40. Lin A, De Backer J, Quatannens D, et al. The effect of local non-thermal plasma therapy on the cancer-immunity cycle in a melanoma mouse model. *Bioeng Transl Med*. 2022;7(3). doi:10.1002/btm2.10314

41. Lin A, Truong B, Fridman G, Fridman A, Miller V. *Immune Cells Enhance Selectivity of Nanosecond-Pulsed DBD Plasma Against Tumor Cells*. Vol 7.; 2017. www.begellhouse.com

42. Van Loenhout J, Boullosa LF, Quatannens D, et al. Auranofin and cold atmospheric plasma synergize to trigger distinct cell death mechanisms and immunogenic responses in glioblastoma. *Cells*. 2021;10(11). doi:10.3390/cells10112936

43. Moloney JN, Cotter TG. ROS signalling in the biology of cancer. *Semin Cell Dev Biol*. 2018;80:50-64. doi:10.1016/j.semcdb.2017.05.023

44. Gupta SC, Hevia D, Patchva S, Park B, Koh W, Aggarwal BB. Upsides and downsides of reactive oxygen species for Cancer: The roles of reactive oxygen species in tumorigenesis, prevention, and therapy. *Antioxid Redox Signal*. 2012;16(11):1295-1322. doi:10.1089/ars.2011.4414

45. Perillo B, Di Donato M, Pezone A, et al. ROS in cancer therapy: the bright side of the moon. *Exp Mol Med*. 2020;52(2):192-203. doi:10.1038/s12276-020-0384-2

46. Giannoni E, Parri M, Chiarugi P. EMT and oxidative stress: A bidirectional interplay affecting tumor malignancy. *Antioxid Redox Signal*. 2012;16(11):1248-1263. doi:10.1089/ars.2011.4280

47. Kim SJ, Kim HS, Seo YR. Understanding of ROS-Inducing Strategy in Anticancer Therapy. *Oxid Med Cell Longev*. Published online 2019. doi:10.1155/2019/5381692

CHAPTER 2

The Influence of Cell Type and Culture Medium on Determining Cancer Selectivity of Non-Thermal Plasma Treatment

This Chapter is published as:

Eline Biscop, Abraham Lin, Wilma Van Boxem, Jinthe Van Loenhout, Joey De Backer, Christophe Deben, Sylvia Dewilde, Evelien Smits and Annemie Bogaerts. The Influence of Cell Type and Culture Medium on Determining Cancer Selectivity of Non-Thermal Plasma Treatment. Cancers, 11 (9) (2019) (15 pages)

Abstract

Increasing the selectivity of cancer treatments is attractive, as it has the potential to reduce side-effects of therapy. As mentioned in previous Chapter, NTP is a novel cancer treatment that disrupts the intracellular oxidative balance. Several reports claim NTP treatment to be selective, but retrospective analysis of these studies revealed discrepancies in several biological factors and culturing methods. Before NTP can be conclusively stated as a selective cancer treatment, the importance of these factors must be investigated. In this Chapter, we evaluated the influence of the cell type, cancer type, and cell culture medium on direct and indirect NTP treatment. Comparison of cancerous cells with their non-cancerous counterparts was performed under standardized conditions to determine selectivity of treatment. Analysis of seven human cell lines (cancerous: A549, U87, A375, and Malme-3M; non-cancerous: BEAS-2B, HA, and HEMa) and five different cell culture media (DMEM, RPMI1640, AM, BEGM and DCBM) revealed that the tested parameters strongly influence indirect NTP treatment, while direct treatment was less affected. Taken together, the results of our study demonstrate that cell type, cancer type, and culturing medium must be taken into account before selectivity of NTP treatment can be claimed and overlooking these parameters can easily result in inaccurate conclusions of selectivity.

2.1 Introduction

As explained in Chapter 1, the current understanding of NTP mechanisms for effecting biological response, is that the RONS generated by NTP elicit oxidative damage to the cell, resulting in cell death[1,2]. According to this understanding, NTP treatment has been hypothesized to be selective for cancer, as the disturbance of the oxidative balance occurs more easily in cancer cells compared to healthy cells[3,4]. Additionally, cancer cells have more aquaporins and less cholesterol in their cellular membrane, which contributes to the diffusion of certain NTP-generated RONS through the membrane and facilitates pore formation, respectively[5-8]. Furthermore, Bauer and Graves proposed a theory where the initial concentration of singlet oxygen, produced by the plasma, triggers cells to generate higher concentrations of secondary singlet oxygen, which leads to the inactivation of catalase in the cell membrane[9]. The inactivation of catalase can also play an important role in the selectivity, as this allows reactivation of intercellular ROS/RNS-dependent, apoptosis-inducing signaling within the population of tumor cells[9]. To date, however, the underlying mechanisms of NTP selectivity are not yet fully understood, and furthermore, the selectivity has not been fully validated.

While several papers claim that NTP selectively kills cancer cells in vitro, retrospective analysis of these papers reveals that definitive proof is rather scarce. This is largely due to the discrepancies between treatment conditions for cancerous and non-cancerous cells. In several cases, the cell culture media used for cancerous and non-cancerous cells were not the same, while in other studies, the cell culture media were not specified at all[10-15]. It is understandable that non-cancerous cells normally require more advanced cell culture media with additional organic compounds compared to cancer cells, but the different media

have disparate buffering and antioxidant capacities[16]. In fact, the stability of RONS in different liquids has been thoroughly investigated[17,18] and Yan, et al. showed that the presence of cysteine and methionine can significantly degrade NTP-generated RONS[16]. Since the working mechanism of NTP involves disrupting the oxidative balance of cells via RONS generation, changes in medium composition could impede their production and delivery, subsequently affecting biological outcome. Therefore, the observed selectivity of NTP treatment could actually result from variation in media and not from intrinsic sensitivity of cancerous and normal cells. In other studies, the selectivity of NTP treatment was claimed, but comparisons were made with different cell types (e.g. epithelial cancer cells with non-cancerous fibroblast cells) and even tissue types (e.g. comparison of ovarian cancer cells with non-cancerous lung cells)[11,15,19-21]. Due to the different physiological characteristics of distinct tissues[22], comparisons between equivalent cell types must also be made before selectivity of treatment can be claimed[22].

Taken together, in order to avoid false claims of selectivity for NTP treatment, the potentially confounding factors found in previous work must be investigated. Therefore, our goals in this study were to address the following: What are the influences of the cell and cancer types on selectivity experiments? What are the influences of cell culture medium on selectivity experiments? Finally, when the proper comparisons are made, is NTP treatment more selective against cancerous cells compared to their normal, non-cancerous counterparts? In this study, two well-established methods of NTP treatment were studied—'direct' and 'indirect' treatment[23]. In the direct case, NTP was generated directly onto cells, while in the indirect case, a liquid (e.g., saline) was enriched with RONS following NTP treatment, and this plasma-treated liquid (PTL)

was then delivered to cells or tissue. The selectivity of both treatment methods for three different cancer types (lung cancer, skin cancer, and brain cancer) was analyzed by comparing their survival 24 hours after treatment with that of their non-cancerous counterparts. Next, the cytotoxic effects of NTP treatment on cells using five different cell culture media, i.e., two 'standard' cell culture media and three 'more advanced' cell culture media for cancerous and non-cancerous cells, respectively, were analyzed. Our results show that both the cell type and cancer type, as well as the cell culture medium, can have a substantial influence on the outcome of experiments. When analyzing selectivity of NTP treatment in the correct way (with cancerous and non-cancerous cells from the same tissue, the same cell type, and cultured in the same medium), appreciable selectivity was not observed in this study.

2.2 Materials and Methods

Cell culture and plating

To evaluate the selectivity of the NTP treatment, we used three non-cancerous human cell lines as a model for healthy tissue (BEAS-2B - lung epithelial cell line, HA - human astrocytes, and HEMa – human epidermal melanocytes) and four cancer human cell lines (A549 – non-small-cell lung cancer cell line, U87 – glioblastoma cell line, and A375 and Malme-3M – melanoma cell lines). A549 and U87 were cultured in Dulbecco's Modified Eagle Medium (DMEM) (Life Technologies, 10938025), A375 and Malme-3M were cultured in Roswell Park Memoriam Institute 1640 (RPMI1640) (Life Technologies, 52400025), BEAS-2B was cultured in Bronchial Epithelial Growth Medium (BEGM) (Lonza, CC-3170), the astrocytes were cultured in Astrocyte Medium (AM) (Sciencell, 1801) and the melanocytes were cultured in Dermal Cell Basal Medium DCBM (ATCC®, PCS-200030TM). DMEM and

RPMI1640 were supplemented with 10% Fetal Bovine Serum (FBS) (Gibco™ FBS, Life Technologies, 10270098), 2 mM L-glutamine (Gibco™, Life Technologies, 25030081), 100 units/mL penicillin and 100 µg/mL streptomycin (Life Technologies, 15140163). According to the manufacturer's protocol, BEGM was supplemented with 2 mL Bovine Pituitary Extract (BPE), 0.50 mL insulin, 0.50 mL hydrocortisone, 0.50 mL GA-1000, 0.50 mL retinoic Acid, 0.50 mL transferrin, 0.50 mL triiodothyronine, 0.50 mL epinephrine and 0.50 mL human Epidermal Growth Factor (hEGF) (Lonza, CC-4175), AM was supplemented with 2% Fetal Bovine Serum (Sciencell, 0010), 5 mL astrocyte growth supplement (Sciencell, 1852) and 5 mL of a penicillin/streptomycin solution (Sciencell, 0503). Finally, DCBM was supplemented with 5 µg/mL recombinant human insulin, 50 µg/mL ascorbic acid, 1 µM epinephrine, 1.5 mM calcium chloride, 1 mL peptide growth factor and 5 mL M8 supplement (ATCC®, PCS-200042TM). The cells were incubated at 37°C in a 5% CO_2 humidified atmosphere. All media were prepared according to the recommendation for each cell line[24-26].

For the indirect treatment, the cells were seeded in 96-well plates with a density of 2500 cells per well for A549, BEAS-2B and A375, 3000 cells per well for U87, and 6000 cells per well for the astrocytes and melanocytes, in 150 µL of cell culture medium. The densities were chosen for each cell line based on their growth rate, in order to achieve comparable densities for all cell lines at the time of treatment. For the direct treatment, the cells were seeded in a 24-well plate with a density of 8333 cells per well for A549, BEAS-2B and A375, 10,000 cells per well for U87, and 20,000 cells per well for the astrocytes and melanocytes, in 500 µL of cell culture medium.

Plasma sources

We studied both direct and indirect plasma treatment. For the indirect treatment, we used the kINPen®IND plasma jet (INP Greifswald/Neoplas tools GmbH, Greifswald, Germany). This is an atmospheric pressure argon plasma jet, made of a central pin electrode (1 mm diameter), shielded by a dielectric quartz capillary (internal diameter 1.6 mm and outer diameter 2 mm), which is connected to a grounded ring electrode. The distance from the tip of the central electrode to the exit nozzle is about 3.5 mm (Figure 2.1). Plasma is generated by applying a sinusoidal voltage to the central electrode with a frequency between 1.0 and 1.1 MHz, and a maximum power of 3.5 W. This voltage creates a gas discharge between both electrodes, which generates the reactive species inside the capillary. These species are carried out with the argon gas flow, creating a plasma effluent with a length of 9 – 12 mm and a diameter of about 1 mm.

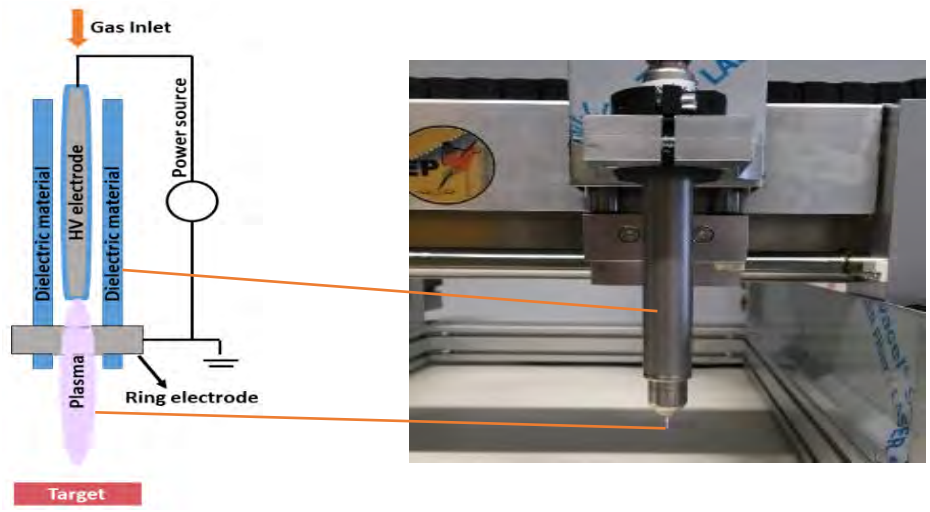

Figure 2.1 Schematic representation and picture of the kINPen®IND used in the experiments

For the direct NTP treatment, we used a FE-DBD. A DBD normally consists of a pair of electrodes, of which at least one is shielded with a dielectric material, separated by a small gap filled with a gas[73]. High voltage (HV) is applied to one electrode, while the target, in our case cells in a well on a grounded metal plate, functions as the second electrode. As the discharge takes place in the gap between the HV electrode and the target, no additional carrier gas was used with this plasma source (Figure 2.2). The plasma was generated by applying microsecond-pulses to the HV electrode from a pulse generator (Advanced Plasma Solutions, Malvern, USA) with an amplitude in the range of 17 kV and a varying frequency between 100 Hz and 500 Hz in our experiments.

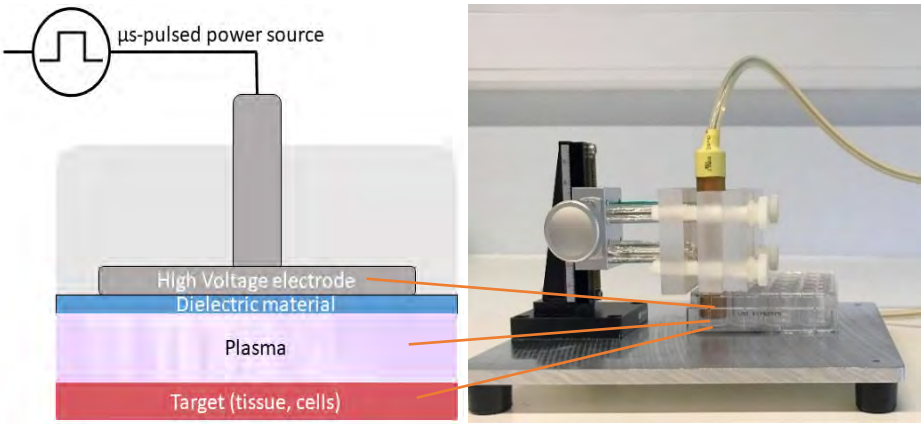

Figure 2.2 Schematic representation and picture of the FE-DBD used in the experiments

Indirect NTP treatment

We used the kINPen®IND to treat 2 mL phosphate-buffered saline (PBS) (pH 7.3) in a 12-well plate. A gap of 6 mm between the tip of the NTP source and the liquid, a gas flow rate of 1 slm, and a treatment time of 5 minutes were used. In this case, the gap was small enough to have

discharges at the liquid surface, as discharge streamers were visible between the head of the plasma jet and the liquid interface. Here, the liquid surface acts as a third electrode, and the electrons interact with the liquid, resulting in electron impact reactions, which affect the generation of RONS. In our experiments comparing all cell culture media on cancer cells, a gap of 30 mm, a gas flow rate of 3 slm and a treatment time of 7 minutes were used. Here, the gap was sufficiently large to avoid the generation of these discharges at the liquid surface. Before treatment of cells with plasma-treated PBS (pPBS), the cells were seeded in a 96 well-plate and incubated for 24h at 37°C and 5% CO_2. For treatment, we applied 30 µL of (diluted) pPBS to each well of the 96-well plate. We also used a control sample, where 30 µL of untreated PBS was added.

Direct NTP treatment

After cell seeding into 24-well plates and incubating for 24h at 37°C and 5% CO_2, the cells were treated with the FE-DBD as stated in our previous work [74]. The cell culture medium was first removed, after which cells were washed with PBS and treated for 10 seconds at a distance of 1 mm and a frequency varying between 100 Hz and 500 Hz. Immediately after NTP treatment, 500 µL of fresh cell culture medium was added to each well. The control sample was handled in exactly the same way, but without turning on the power source and applying high voltage.

Cell viability assay

After treatment, the cells were incubated for 24h at 37°C and 5% CO_2 before the further viability analysis with the sulforhodamine B-method (SRB). The cell culture medium was removed from each well and the cells were first fixed to the plate using 10% trichloro acetic acid (TCA) (Fischer Scientific, A322), 100 µL for a 96-well plate and 400 µL for a

24-well plate. The plates were placed at 4°C for 1h, after which the TCA was thoroughly washed away with deionized water. The wells were dried, and a SRB-solution (0.1 wt/vol% in 1% (vol/vol) acetic acid, Sigma-Aldrich®, s1402) was added (100 µL for a 96-well plate and 400 µL for a 24-well plate). After 30 minutes, the SRB was washed away with 1% acetic acid. The cells were dried again, and tris(hydrocymethyl)aminomethane (TRIS)-buffer (Sigma-Aldrich®, 252859) was added to each well (100 µL for a 96 well-plate and 400 µL for a 24-well plate). After 30 minutes, the absorbance was measured at 540 nm, using a BIO-RAD iMark™ Microplate reader for the 96-well plates and a Tecan Infinite F Plex Microplate reader for the 24-well plates. The cell viability was determined by comparing the absorbance of the treated groups with the untreated control sample.

Analysis of the influence of the cell culture medium

Since the cancerous cell lines and non-cancerous cell lines have different optimal culture media, it was important to analyze the influence of the media on the plasma treatment results. For this purpose, we tested two of the cancer cell lines, i.e., A549 and A375, with the five different cell culture media (DMEM, RPMI1640, BEGM, AM and DCBM). We cultured the cells in their recommended medium, but at the moment of seeding, we seeded them in the different media. Both the direct (FE-DBD at 500 Hz) and indirect (pPBS, condition 2) treatment were tested.

Statistical analysis

All experiments were performed in triplicate, and the results are expressed as the mean with associated standard error of the mean. Statistical significance was calculated using the generalized linear mixed model and displayed on the figure plots as *$p \leq 0.05$, **$p \leq 0.01$, ***$p \leq 0.001$ and ****$p \leq 0.0001$.

2.3 Results

2.3.1 Influence of cell type and cancer type on cell viability

Since different cell types have different responses to oxidative stress[29], we first investigated the cytotoxic effect of NTP on two human malignant melanoma cell types: an epithelial cell line (A375, derived from skin) and a fibroblast cell line (Malme-3M, derived from a metastatic site on the lung), according to the American Type Culture Collection (ATCC). As these cells were cultured in the same medium and under the same conditions, the cell type was the only variable in this experiment. Our results show that while there was no significant difference in sensitivity for the cell lines with direct NTP treatment, the epithelial cells were more sensitive to indirect treatment compared to malignant fibroblasts (Figure 2.3a). To further evaluate the cytotoxic effects of NTP on different cancer types, we treated two additional human epithelial cells, U87 glioblastoma and A549 lung carcinoma. All cancer types were more or less equally sensitive to direct NTP treatment, but the U87 was less sensitive to indirect treatment (Figure 2.3b). Therefore, it is clear that cell sensitivity to indirect NTP treatment is influenced by both cell type and cancer type, while this impact seems not present with direct treatment.

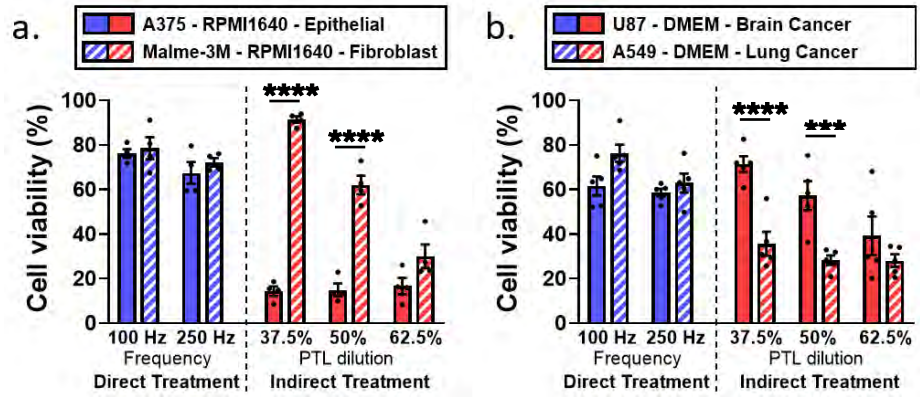

Figure 2.3 Analysis of the influence of the cell type and cancer type on both direct treatment (FE-DBD at two different frequencies) and indirect treatment (pPBS in three different dilutions). a. Comparison of an epithelial cell line (A375) with a fibroblast cell line (Malme-3M), which are both skin cancer cell lines. b. Comparison of a brain cancer cell line (U87) with a lung cancer cell line (A549). For both figures, the cells were cultured in the same cell culture medium and treated with exactly the same conditions. Therefore, the only variable tested was a) cell type and b) cancer type. Data are represented as mean ± standard error of mean (SEM) of at least three independent experiments with at least two replicates. Statistical significance was calculated using the generalized linear mixed model. ***p ≤ 0.001, **** p ≤ 0.0001

2.3.2 Influence of cell culture media on cell viability

To determine the importance and influence of cell culture medium when assessing selectivity of treatment, we evaluated the cytotoxicity of both direct and indirect treatment for the A549 and A375 cell lines, in five different media. In order to ensure that the different media alone did not significantly affect cell growth and death, the cytotoxicity assay was performed on cells 24 hours after incubation and cell density in the different media was compared to that of their recommended medium: DMEM for A549 and RPMI for A375 (See Appendix 1, Figure A1.1). The A375 cells were able to grow in all media with a similar growth rate to that in RPMI1640. However, there was a statistically significant decrease in cell growth of the A549 cells in BEGM compared to DMEM. This suggests that even without NTP treatment, certain cell processes are

strongly influenced by the components of the cell culture medium. Due to this discrepancy on cell growth, selectivity of treatment cannot be determined for cases where normal, non-cancerous cells are grown in the BEGM medium. This was further validated when A549 and their normal counterparts (BEAS-2B) were cultured in the BEGM medium and treated with direct and indirect NTP (See Appendix 1, Figure A1.2). Therefore, this medium was removed from all subsequent experiments. For the other three media, the difference in growth rate was not significant ($P>0.05$, details in Appendix 1).

The effect of direct NTP treatment was unaffected by the cell culture medium (Figure 2.4a), as the cell culture medium was removed during treatment. These results further indicate that the effect of direct NTP treatment was initiated during treatment and unaffected by the scavenging effects of the cell culture media added immediately afterwards. For the indirect treatment, cytotoxicity was significantly influenced by the cell culture media (Figure 2.4b). Cancer cells treated in the standard media (DMEM and RPMI1640) resulted in ≥50% cytotoxicity but were unaffected when treated in advanced media used to culture normal, non-cancerous cells (AM and DCBM).

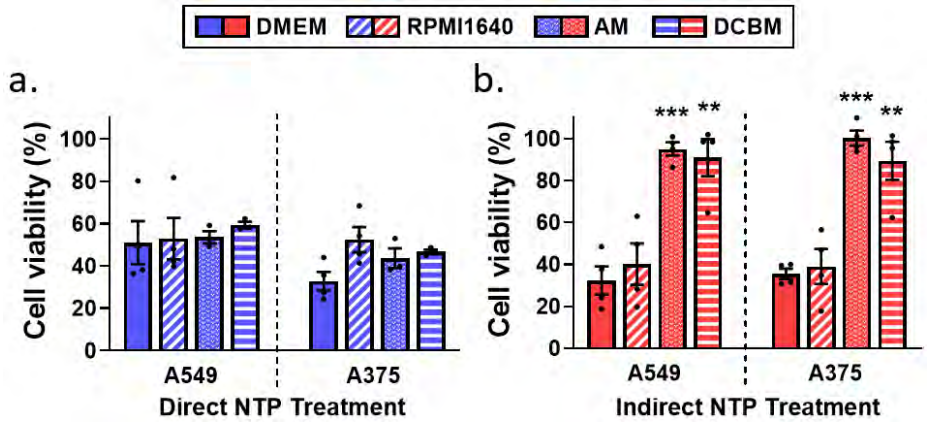

Figure 2.4 Influence of the cell culture medium on the direct and indirect plasma treatment of two cancer cell lines. (a) The direct plasma treatment was performed for 10 seconds, with a frequency of 500 Hz and a gap of 1 mm. (b) The indirect treatment was performed for 7 minutes treatment, with a gas flow rate of 3 slm and a gap of 10 mm. Data are represented as mean ± standard deviation (SD) of three independent experiments with at least two replicates. Statistical significance was calculated using the generalized linear mixed model. **p ≤ 0.01, ***p ≤ 0.001

2.3.3 Influence of cell culture media on selectivity evaluation of indirect NTP treatment

To further validate selectivity of indirect NTP treatment and the influence of cell culture media, we compared cytotoxicity for the cancerous cell lines with their non-cancerous, complimentary cell lines (astrocytes and melanocytes for glioblastoma and melanoma, respectively) in both standard and advanced media. Experiments were performed with cells seeded in their recommended medium and with cells seeded in the same medium. As non-cancerous cells were incapable of being cultured in standard media, cancerous cells were grown in the more advanced media of their non-cancerous counterparts. When cultured and treated in their recommended media (different media), as commonly done in literature, it would appear that pPBS treatment resulted in significant selectivity (Figure 2.5). However, when both cell lines were cultured in the same media, selectivity was diminished. Only the A375 cell line

showed cytotoxic effect in the more advanced media, but this was also reduced compared to treatment in standard media.

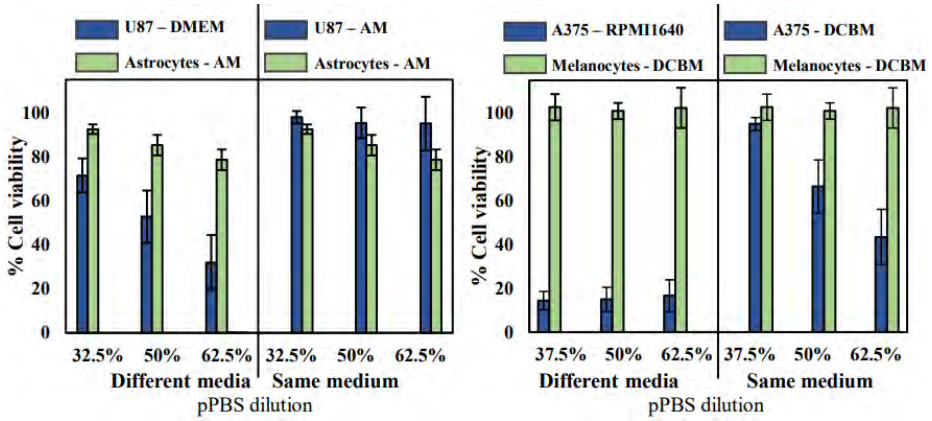

Figure 2.5 Analysis of the selectivity with the indirect treatment for brain cancer and skin cancer. A 5-minute treatment with a gas flow rate of 1 slm and a gap of 6 mm was used to create the pPBS, which we further diluted. Comparison of a) brain and b) skin cancer cells in their common medium (blue solid bars on the left side) with non-cancerous cells in their common medium (green solid bar on the left side) appeared to show selectivity in all cases. However, when compared to the cancer cells in the advanced media (on the right side of the graph), the selectivity was not found. Hence, this clearly shows that the selectivity was affected by the cell culture medium. This is important to realize, to avoid drawing false conclusions. Data are represented as mean ± standard deviation (SD) of three independent experiments with at least two replicates.

2.3.4 Influence of cell culture media on selectivity evaluation of direct NTP treatment

Following previous sections 2.3.1-2.3.3, it is clear that cell type, cancer type, and culture media are critical parameters for indirect NTP treatment. These parameters were also standardized for direct NTP treatment to evaluate their effect on selectivity.

Though we observed that the influence of different cell culture medium was not pronounced for direct NTP treatment, as described in section 2.3.2, to be correct, we still performed our selectivity analysis of cancerous versus non-cancerous cell lines in both the same and different culture media. No selectivity was observed when cancerous and normal cells were cultured in their own recommended medium

(Figure 2.6, different media), but when cancer cells were cultured and treated in the medium used for their non-cancerous counterparts, slight selectivity was observed in the U87 glioblastoma cell line and the A375 melanoma cell line at lower intensity NTP treatment (Figure 2.6, same medium). However, at higher intensity treatment (250 Hz), no such selectivity was observed, as the difference was within error. Interestingly, our results suggest that there is an optimal regime for direct NTP treatment where selectivity can be achieved, above which the oxidative burden becomes too overwhelming for even normal cells to manage.

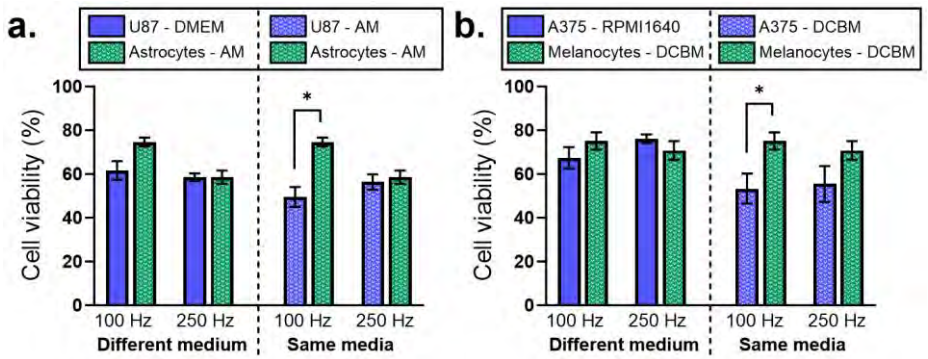

Figure 2.6 Analysis of the selectivity with the direct treatment for brain cancer and skin cancer. A 10 second treatment with a gap of 1 mm and a frequency of either 100 Hz or 250 Hz was used to treat a. brain and b. skin cancer and non-cancerous cells. Data are represented as mean ± standard deviation (SEM) of three independent experiments with at least two replicates. Statistical significance was calculated using the generalized linear mixed model. *$p \leq 0.05$

2.4 Discussion

Selectivity of NTP treatment for cancer is an important topic of research, but it has often been misconcluded. Multiple research groups claim to have found treatment conditions which selectively kill cancerous cells and leave non-cancerous cells unharmed. When examining those articles in more detail, we found critical discrepancies between the treatment conditions and origins of the cancerous and non-cancerous cells[10-15, 19, 20]. To ensure that these comparisons are not confounded by the discrepancies we identified, we analyzed their influence on cell viability after NTP treatment.

An important parameter often neglected in past studies, is the difference in cell type or cancer type[11,15,19,20]. For example, in one article, the authors compared ovarian cancer cells with non-cancerous lung cells[20]. In comparing the responses of two cell lines for both ovarian adenocarcinoma and non-cancerous lung tissue, they concluded that the cancer cell lines were more sensitive to the treatment than the non-cancerous cell line. However, Giordano *et al*. has reported a difference in gene expression profiles between lung cancer and ovarian cancer[30], which can result in differential responses to NTP treatment. Furthermore, the cell type of the cancerous cell lines and non-cancerous cell lines was different. The two ovarian cancerous cell lines used in that study, SKOV-3 and HRA, were epithelial cell lines, while the two non-cancerous lung cell lines, WI-38 and MRC-5, were fibroblasts. Epithelial cells and fibroblasts show different gene expression levels and can therefore give a different response to NTP treatment[31]. To analyze the influence of these parameters, we examined the difference in cell type and cancer type by comparing an epithelial and fibroblast cell line from the same cancer type and by comparing two epithelial cell lines from different cancer types. According to our results, both cell type and

cancer type had an effect on sensitivity to NTP treatment. In light of these findings, it is clear that for analyzing selectivity, cells of the same cancer type and cell type should be chosen, and discrepancies between these two biological parameters could lead to misdirected conclusions of selectivity.

The influence of the cell culture medium is another important parameter often overlooked when determining the selectivity of NTP treatment. Therefore, the influence hereof on cell viability after NTP treatment was also investigated. The effect of two commonly used cell culture media (DMEM and RPMI1640) was compared with two more advanced cell culture media required for culturing non-cancerous cells (AM and DCBM). Our results show that, when cells were cultured in the more advanced media, indirect NTP treatment was ineffective. This was likely in part due to the presence of more organic components in the advanced media, as non-cancerous cells require more nutrients and are much harder to grow *in vitro*[29]. RONS produced by NTP can react with these organic components before reaching the cells[16] One component commonly added to most advanced media is sodium pyruvate, a known H_2O_2-scavenger[32,33]. For DMEM and RPMI1640, we ensured that no sodium pyruvate was present, but for the other two cell culture media, the composition was not specified by the manufacturer[24-26]. This would also explain why the cell culture media did not significantly influence cell viability following direct NTP treatment, as it was removed prior to treatment. These results highlight the influence of cell culture media on downstream biological effects following indirect NTP treatment. Taken together, it is clear that selectivity of NTP treatment cannot be evaluated for indirect plasma treatment when the cancer cells are cultured in medium different to that of non-cancerous cells.

Several papers claiming that NTP selectively kills cancerous cells, cultured their cells in different media[10-15]. For example, one study cultured the A549 cells in DMEM, while their normal BEAS-2B cells were cultured in BEGM[11]. Since the authors saw more response to the treatment in their A549 cell line compared to the BEAS-2B cell line, they stated that their indirect NTP treatment was more selective. However, as evident from our results above, the sensitivity of A549 cells to indirect NTP treatment was reduced when cultured in BEGM compared to DMEM (See Appendix 1, Figure A1.2). Therefore, the reported selectivity was not cell line specific, but due to the different medium used to culture the cells. This strongly highlights the fact that cell culture medium plays an important role in indirect NTP treatment and must be standardized before claims of selectivity can be made. Since the influence of the cell culture medium was less important for direct NTP treatment, we used this treatment method to analyze the selectivity of treatment for two cancer types: melanoma and glioblastoma. Interestingly we observed that direct treatment preferentially affected cancer cells at lower intensity treatments (Figure 2.6), suggesting that selectivity depends on optimizing NTP treatment conditions that exploit the differences between normal and cancerous tissue. It is widely known that cancer cells have a higher proliferation rate, compared to non-cancerous cells. Healthy cells primarily produce energy through mitochondrial oxidative phosphorylation, while cancer cells predominantly produce their energy through a high rate of glycolysis followed by lactic acid fermentation, which benefits this high proliferation rate[34,35]. To sustain this fast growth rate, cancer cells require a 'hyper metabolism', which results in a higher level of basal intracellular ROS[36,37]. Simultaneously, cancer cells also maintain a high level of antioxidant activity, mainly reduced nicotinamide adenine

dinucleotide phosphate (NADPH) and glutathione (GSH), to prevent build-up of ROS[38-40]. However, once the levels of ROS become excessively high through the addition of extra ROS, detrimental oxidative stress can occur, leading to cell death[41,42]. While randomized control clinical trials using pro-oxidant therapy are still ongoing, increasing evidence suggests that raising ROS levels through small molecules can selectively induce cancer cell death by disabling antioxidants[41,43-45]. Taken together with our observations, this would mean that the aim to reach selectivity of NTP treatment lies in the optimization of parameters and conditions to produce sufficient ROS to overwhelm the oxidative threshold in cancer cells, without reaching this threshold in the healthy cells.

It must be noted here that selectivity of NTP treatment may also depend on the RONS generated and delivered to the biological target. This is particularly important, as direct and indirect NTP treatments generate a different cocktail of reactive species. With the indirect NTP treatment, a liquid is treated with NTP and then transferred to cells or tissue. Due to the time delay between treatment and application, only the long-lived species (mostly H_2O_2, NO_2^-, NO_3^-) remain in the liquid and reach the cells[18]. In the case of direct NTP treatment, the liquid is removed before treatment in order for NTP to be generated directly onto the cells, thereby enabling both the long-lived and short-lived ($^{\bullet}OH$, $^1O_2$, O, O_3, $^{\bullet}NO$, $ONOO^-$) species to interact with the biological target[28]. Several reports have already demonstrated the importance of these short-lived species in direct NTP treatment for effecting cell death[28,46,47], though further fundamental investigations are still required, including the type of cell death modalities elicited.

The experiments performed in this study used cancer cell lines in 2D cultures. Cancer cell lines are derived from primary patient material and

have provided important knowledge for cancer research. However, care must be taken when interpreting the results, as cell lines are genetically manipulated and therefore do not always accurately reflect the responses of primary cells[48]. Furthermore, comparison between two cell lines often involves comparison between two patient sources. To further investigate the selectivity in a more realistic manner, the cancer and healthy cells should be derived from the same patient[48]. Hasse *et al*. analyzed NTP treatment on cancer and healthy human tissue samples from head and neck cancer patients[49]. They found that NTP treatment of tumor tissue induced more apoptotic cells than in healthy tissue. This was accompanied by elevated extracellular cytochrome c levels in the tumor tissue[50]. Though this is probably the most representative *in vitro* model, human tissue samples cannot be preserved long-term and are therefore much more difficult to work with[51]. Another recently developed *in vitro* model are organoids[52,53]. These are 3D self-organizing organotypic structures, grown from tissue-derived adult stem cells. Organoids can be expanded long-term without losing their genetic and phenotypical stability[52,53]. Such 3D cell culture systems feature increased complexity for increased faithfulness to the *in-vivo* environment and are above all fairly easy to work with[49]. When comparing these 3D organoids from healthy and cancerous tissue from the same patient, more representative results concerning the selectivity can be obtained compared to those obtained with 2D models. The results from Hasse *et al*. are encouraging as it suggests that NTP treatment may indeed be selective when operated at certain regimes. As more studies using primary patient tissue and the proper 3D models start to emerge, the selectivity capacity of NTP treatment will become clearer.

2.5 Conclusions

In this Chapter, we evaluated the influence of the cell type, cancer type, and cell culture medium on the cytotoxic effects of both direct and indirect NTP treatment for cancer. In all cases, we found that the influence of these biological parameters was more pronounced for indirect NTP treatment compared to direct NTP treatment.

When analyzing the influence of the cell type, we found that fibroblasts are more resistant to indirect NTP treatment. Also, the different cancer types gave different responses to NTP treatment, where the lung cancer cell line, A549, was more sensitive, compared to the brain cancer cell line, U87.

For the indirect NTP treatment, we observed a large influence of the cell culture medium on cell cytotoxicity, as the more advanced media virtually negated the effects of treatment. Thus, when comparing the viability of cancerous cells in their standard media with the non-cancerous cells in their advanced media, it is tempting to conclude significant selectivity of treatment for all the cancer types. However, when cytotoxicity was compared for cancerous and non-cancerous cells cultured in the same media, it was obvious that this apparent selectivity was due to the cell culture media and genuine differential sensitivity to indirect NTP. This is an important conclusion, which must be kept in mind to avoid drawing false conclusions in cancer cell selectivity studies.

Taken together, the results of our study demonstrate that biological factors, including cell type, cancer type, and culturing medium, must be taken into account before selectivity of NTP treatment can be claimed. Overlooking these parameters can easily result in misdirected conclusions and false claims of selectivity.

2.6 References

1. Fridman A, Friedman G. *Plasma Medicine*.; 2013.
2. Dubuc A, Monsarrat P, Virard F, et al. Use of cold-atmospheric plasma in oncology : a concise systematic review. *Ther Adv Med Oncol*. 2018;10:1-12. doi:10.1177/https
3. Ratovitski EA, Cheng X, Yan D, et al. Anti-cancer therapies of 21st century: Novel approach to treat human cancers using cold atmospheric plasma. *Plasma Processes and Polymers*. 2014;11(12):1128-1137. doi:10.1002/ppap.201400071
4. Keidar M. Plasma for cancer treatment. *Plasma Sources Sci Technol*. 2015;24:1-20. doi:10.1088/0963-0252/24/3/033001
5. Maksudbek Y, Dayun Y, M CR, Bogaerts A. Atomic scale simulation of H2O2 permeation through aquaporin : toward the understanding of plasma-cancer treatment. *J Phys D Appl Phys*. 2018;12.
6. Yan D, Xiao H, Zhu W, et al. The role of aquaporins in the anti-glioblastoma capacity of the cold plasma-stimulated medium. *J Phys D Appl Phys*. 2017;50(5). doi:10.1088/1361-6463/aa53d6
7. Paal J Van Der, Verheyen C, Neyts EC, Bogaerts A. Hampering Effect of Cholesterol on the Permeation of Reactive Oxygen Species through Phospholipids Bilayer : Possible Explanation for Plasma Cancer Selectivity. *Sci Rep*. 2017;7:1-11. doi:10.1038/srep39526
8. Paal J Van Der, Neyts EC, Verlackt CCW, Bogaerts A. Chemical Science permeability of cancer and normal cells subjected to oxidative stress. *Chem Sci*. 2016;7:489-498. doi:10.1039/c5sc02311d
9. Bauer G. Cold Atmospheric Plasma and Plasma-Activated Medium : Antitumor Cell Effects with Inherent Synergistic Potential. *Plasma Med*. Published online 2019.
10. Zucker SN, Zirnheld J, Bagati A, et al. Preferential induction of apoptotic cell death in melanoma cells as compared with normal keratinocytes using a non-thermal plasma torch. *Cancer Biology & Therapyiology & Therapy*. 2012;13(13):1299-1306.
11. Kim SJ, Chung TH. Cold atmospheric plasma jet- generated RONS and their selective effects on normal and carcinoma cells. *Sci Rep*. 2016;6:1-14. doi:10.1038/srep20332
12. Wang M, Holmes B, Cheng X, Zhu W, Keidar M, Zhang LG. Cold Atmospheric Plasma for Selectively Ablating Metastatic Breast Cancer Cells. *PLoS One*. 2013;8(9):1-11. doi:10.1371/journal.pone.0073741

13. Guerrero-preston R, Ogawa T, Uemura M, et al. Cold atmospheric plasma treatment selectively targets head and neck squamous cell carcinoma cells. *Int J Mol Med*. 2014;34:941-946. doi:10.3892/ijmm.2014.1849

14. Tanaka H, Mizuno M, Ishikawa K, et al. Plasma-Activated Medium Selectively Kills Glioblastoma Brain Tumor Cells by Down-Regulating a Survival Signaling Molecule, AKT Kinase. *Plasma Med*. 2011;1(3-4):265-277. doi:10.1615/PlasmaMed.2012006275

15. Georgescu N, Lupu AR. Tumoral and Normal Cells Treatment With High-Voltage Pulsed Cold Atmospheric Plasma Jets. *IEEE Transactions on Plasma Science*. 2010;38(8):1949-1955. doi:10.1109/TPS.2010.2041075

16. Yan D, Nourmohammadi N, Bian K, Murad F, Sherman JH, Kei. Stabilizing the cold plasma- stimulated medium by regulating medium ' s composition. *Sci Rep*. 2016;6. doi:10.1038/srep26016

17. Heirman P, Van Boxem W, Bogaerts A. Reactivity and stability of plasma-generated oxygen and nitrogen species in buffered water solution: a computational study. *Physical Chemistry Chemical Physics*. Published online 2019. doi:10.1039/C9CP00647H.Volume

18. Van Boxem W, Van Der Paal J, Gorbanev Y, et al. Anti-cancer capacity of plasma-treated PBS: Effect of chemical composition on cancer cell cytotoxicity. *Sci Rep*. 2017;7(1):1-15. doi:10.1038/s41598-017-16758-8

19. Kim JY, Kim S o, Wei Y, Li J. A flexible cold microplasma jet using biocompatible dielectric tubes for cancer therapy A flexible cold microplasma jet using biocompatible dielectric tubes. *Appl Phys Lett*. 2010;96. doi:10.1063/1.3431392

20. Iseki S, Nakamura K, Hayashi M, et al. Selective killing of ovarian cancer cells through induction of apoptosis by nonequilibrium atmospheric pressure plasma Selective killing of ovarian cancer cells through induction of apoptosis by nonequilibrium atmospheric pressure plasma. *Appl Phys Lett*. 2012;100. doi:10.1063/1.3694928

21. Laroussi M. Effects of PAM on select normal and cancerous epithelial cells. *Plasma Research Express*. 2019;1:1-7.

22. Zhang L, Zhou W, Velculescu VE, et al. Gene Expression Profiles in Normal and Cancer Cells. *Science (1979)*. 1997;276:1268-1272.

23. Saadati F, Mahdikia H, Abbaszadeh H allah, Abdollahifar M amin, Khoramgah MS, Shokri B. Comparison of Direct and Indirect cold atmospheric-pressure plasma methods in the B 16 F 10 melanoma

cancer cells treatment. *Sci Rep*. 2018;8:1-15. doi:10.1038/s41598-018-25990-9

24. Dermal Cell Basal Medium - ATCC. https://www.lgcstandards-atcc.org/products/all/PCS-200-030.aspx?geo_country=be

25. Bronchial Epithelial Growth Medium - Lonza. https://bioscience.lonza.com/lonza_bs/CH/en/Primary-and-Stem-Cells/p/000000000000185308/BEGM-Bronchial-Epithelial-Cell-Growth-Medium-BulletKit#accept

26. Astrocyte Medium - Sciencell. https://www.sciencellonline.com/astrocyte-medium.html

27. Barrier D, Dbd D, Bibinov N, Rajasekaran P, Mertmann P. Basics and Biomedical Applications of DBD. Published online 2008.

28. Lin A, Gorbanev Y, Backer J De, et al. Non-Thermal Plasma as a Unique Delivery System of Short-Lived Reactive Oxygen and Nitrogen Species for Immunogenic Cell Death in Melanoma Cells. *advanced science*. 2019;6. doi:10.1002/advs.201802062

29. Cooper GM. The Development and Causes of Cancer. In: *The Cell: A Molecular Approach. 2nd Edition*. Sunderland (MA): Sinauer Associates; 2000.

30. Giordano TJ, Shedden KA, Schwartz DR, et al. Organ-Specific Molecular Classification of Primary Lung, Colon, and Ovarian Adenocarcinomas Using Gene Expression Profiles. *Am J Pathol*. 2001;159:1231-1238. doi:10.1016/S0002-9440(10)62509-6

31. Mallinjoud P, Villemin J philippe, Mortada H, et al. Endothelial , epithelial , and fibroblast cells exhibit specific splicing programs independently of their tissue of origin. *Genome Res*. 2014;24:511-521. doi:10.1101/gr.162933.113.

32. Jagtap JC, Chandele A, Chopde BA, Shastry P. Sodium pyruvate protects against H2O2 mediated apoptosis in human neuroblastoma cell line-SK-N-MC. *J Chem Neuroanat*. 2003;26:109-118. doi:10.1016/S0891-0618(03)00037-1

33. Wang X, Perez E, Liu R, Yan L jun, Mallet RT, Yang S hua. Pyruvate protects mitochondria from oxidative stress in human neuroblastoma SK-N-SH cells. *Brain Res*. 2007;1132:1-9. doi:10.1016/j.brainres.2006.11.032

34. Heiden MG Vander, Cantley LC, Thompson CB, Mammalian P, Exhibit C, Metabolism A. Understanding the Warburg Effect : The Metabolic Requirements of Cell Proliferation. *Science (1979)*. 2009;324:1029-1034.

35. Fadaka A, Ajiboye B, Ojo O, Adewale O, Olayide I, Emuowhochere R. Biology of glucose metabolization in cancer cells. *Journal of Oncological Science*. 2017;3:45-51. doi:10.1016/j.jons.2017.06.002

36. Cairns RA, Harris IS, Mak TW. Regulation of cancer cell metabolism. *Nature Reviews*. 2011;11. doi:10.1038/nrc2981

37. Hanahan D, Weinberg RA. Review Hallmarks of Cancer : The Next Generation. *Cell*. 2011;144:646-674. doi:10.1016/j.cell.2011.02.013

38. Hanahan D, Weinberg RA. Hallmarks of cancer: The next generation. *Cell*. 2011;144(5):646-674. doi:10.1016/j.cell.2011.02.013

39. Redza-Dutordoir M, Averill-Bates DA. Activation of apoptosis signalling pathways by reactive oxygen species. *Biochimica et Biophysica Acta (BBA) - Molecular Cell Research*. 2016;1863(12):2977-2992. doi:10.1016/j.bbamcr.2016.09.012

40. Schieber M, Chandel NS. ROS Function in Redox Signaling and Oxidative Stress. *Current Biology*. 2014;24(10):R453-R462. doi:10.1016/j.cub.2014.03.034

41. Schieber M, Chandel NS. ROS Function in Redox Signaling and Oxidative Stress. *Current Biology*. 2014;24:R453-R462. doi:10.1016/j.cub.2014.03.034

42. Redza-dutordoir M, Averill-bates DA. Activation of apoptosis signalling pathways by reactive oxygen species. *Biochemica et Biophysica Acte*. 2016;1863:2977-2992. doi:10.1016/j.bbamcr.2016.09.012

43. Raj L, Ide T, Gurkar AU, et al. Selective killing of cancer cells by a small molecule targeting the stress response to ROS. *Nature*. 2011;475:231-234. doi:10.1038/nature10167

44. Shaw AT, Winslow MM, Magendantz M, Ouyang C, Dowdle J. Selective killing of K-ras mutant cancer cells by small molecule inducers of oxidative stress. *PNAS*. 2011;108. doi:10.1073/pnas.1105941108

45. Glasauer A, Sena LA, Diebold LP, Mazar AP, Chandel NS. Targeting SOD1 reduces experimental non – small-cell lung cancer. *J Clin Invest*. 2014;124:117-128. doi:10.1172/JCI71714DS1

46. Lin A, Truong B, Patel S, et al. Nanosecond-Pulsed DBD Plasma-Generated Reactive Oxygen Species Trigger Immunogenic Cell Death in A549 Lung Carcinoma Cells through Intracellular Oxidative Stress. *Int J Mol Sci*. 2017;18. doi:10.3390/ijms18050966

47. Lin A, Chernets N, Han J, et al. Non-Equilibrium Dielectric Barrier Discharge Treatment of Mesenchymal Stem Cells : Charges and Reactive

Oxygen Species Play the Major Role in Cell Death a. *Plasma Processes and Polymers*. 2015;12:1117-1127. doi:10.1002/ppap.201400232

48. Kaur G, Dufour JM. Cell lines, Valuable tools or useless artifacts. *Spermatogenesis*. 2012;2:1-5.

49. Drost J, Clevers H. Organoids in cancer research. *Nat Rev Cancer*. 2018;18(7):407-418. doi:10.1038/s41568-018-0007-6

50. Hasse S, Seebauer C, Wende K, et al. Cold Argon Plasma as Adjuvant Tumour Therapy on Progressive Head and Neck Cancer : A Preclinical Study. *Applied Sciences*. 2019;9:1-16.

51. Grizzle WE, Bell WC, Sexton KC. Issues in collecting, processing and storing human tissues and associated information to support biomedical research. *Cancer Biomark*. 2010;9:531-549. doi:10.3233/CBM-2011-0183.Issues

52. Xu H, Lyu X, Yi M, Zhao W, Song Y, Wu K. Organoid technology and applications in cancer research. *J Hematol Oncol*. Published online 2018:1-15.

53. Drost J, Clevers H. Organoids in cancer research. *Nat Rev Cancer*. 2018;18:407-418. doi:10.1038/s41568-018-0007-6

Appendix 1

Appendix 1.1 Influence of the cell culture medium on the cell growth

In order to ensure that the different medium alone did not significantly affect cell growth and death, the cytotoxicity assay was performed on cells 24 hours after incubation and cell density of the cells in the different media was compared to that of their recommended medium: DMEM for A549 and RPMI for A375. While A375 were able to grow in all media, equivalent to that of RPMI, A549 growth was significantly impeded by the BEGM medium ($p<0.05$). Since BEGM appears to have an inherent effect on A549 cells, results on selectivity would be confounded when comparisons are made to cells grown in BEGM (e.g. BEAS-2B). While DCBM media also appeared to have an effect on the A549 lung carcinoma cells, the variation was large and statistical analysis did not show a significant difference. However, this difference was not present in the A375 melanoma cells. This is crucial, as DCBM is used to culture melanocytes, and therefore indicates that comparison of NTP selectivity on melanocytes and A375 melanoma cells could be performed.

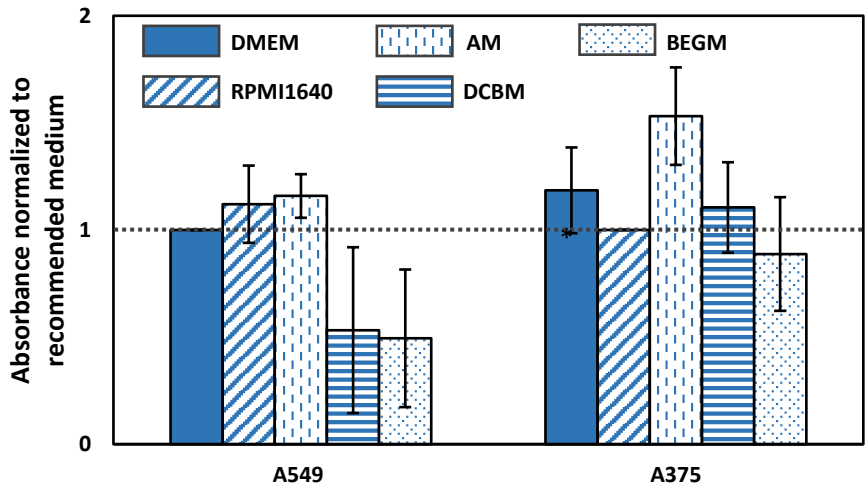

Figure A1.1 Comparison of the cell densities of A375 and A549 in the different cell culture media. The results are normalized to the recommended media for the cell line (DMEM for A549 and RPMI1640 for A375) indicated by the blue bars. Data are represented as mean ± standard deviation (SD) of three independent experiments with at least two replicates. Statistical significance of all treatment conditions was compared to untreated. *$p<0.05$ (One-way ANOVA)

Appendix 1.2 Analysis of the selectivity for A549 and BEAS-2B, for both direct and indirect NTP treatment

A549 in DMEM and BEGM were treated with both direct and indirect NTP and cytotoxicity was compared to that of BEAS-2B treated and cultured in their recommended medium (BEGM). While under different media conditions, NTP treatment appears to be selective for A549, this selectivity becomes revered when the medium was standardized. This is likely due to the inherent effects BEGM has on A549 cells (Figure S1). Taken together, this further highlights the influence of the cell culture medium on observed biological outcome following NTP treatment.

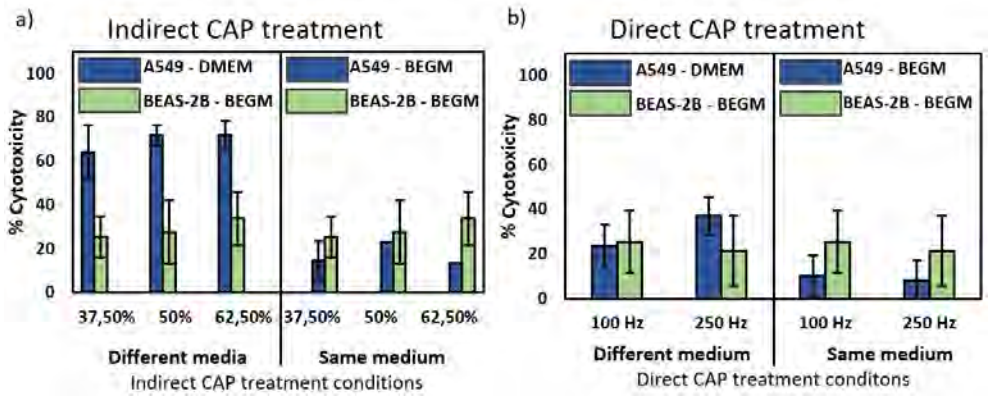

Figure A1.2 Selectivity analysis for lung cancer using a) indirect and b) direct NTP treatment. For the indirect treatment we used different dilutions of plasma-treated PBS (pPBS), using the first condition (5 minute treatment with a gas glow rate of 1 slm and a gap of 6 mm) and for the direct treatment we used a 10 second treatment with a gap of 1 mm and two different frequencies of the FE-DBD.

CHAPTER 3

Critical Evaluation of the Interaction of Reactive Oxygen and Nitrogen Species with Blood to Inform the Clinical Translation of Non-Thermal Plasma

This Chapter is published as:

Eline Biscop, Abraham Lin, Colum Breen, Stephen J. Butler, Evelien Smits and Annemie Bogaerts. Critical Evaluation of the Interaction of Reactive Oxygen and Nitrogen Species with Blood to Inform the Clinical Translation of Non-Thermal Plasma Therapy. Oxidative Medicine and Cellular Longevity 2020, 9750206 (2020) (10 pages)

Abstract

As explained in Chapter 1, through controlled delivery of RONS, NTP can elicit hormetic cellular responses, thus stimulating broad therapeutic effects. To enable clinical translation of the promising preclinical research into NTP therapy, a deeper understanding of NTP interactions with clinical substrates is profoundly needed. Since NTP-generated RONS will inevitably interact with blood in several clinical contexts, understanding their stability in this system is crucial. In this Chapter, two medically relevant NTP delivery modalities were used to assess the stability of NTP-generated RONS in three aqueous solutions with increasing organic complexities: phosphate-buffered saline (PBS), blood plasma (BP), and processed whole blood. NTP-generated RNS collectively (NO_2^-, $ONOO^-$), H_2O_2, and $ONOO^-$ exclusively were analyzed over time. We demonstrated that NTP-generated RNS and H_2O_2 were stable in PBS but scavenged by different components of the blood. While RNS remained stable in BP after initial scavenging effects, it was completely reduced in processed whole blood. On the other hand, H_2O_2 was completely scavenged in both liquids over time. Our previously developed luminescent probe europium(III) was used for precision measurement of $ONOO^-$ concentration. NTP-generated $ONOO^-$ was detected in all three liquids for up to at least 30 seconds, thus highlighting its therapeutic potential. Based on our results, we discuss the necessary considerations to choose the most optimal NTP modality for delivery of RONS to and via blood in the clinical context.

3.1 Introduction

As explained in Chapter 1, the broad range of biological effects is a result of the RONS generated by NTP. While low-dose exposure to RONS can promote regenerative effects, higher doses can induce cellular death[1]. Through controlled delivery of RONS, the clinical benefits of NTP therapy to date have included neutralizing microorganisms, reducing chronic leg ulcers, resolution of dermatological diseases, and palliation for advanced head and neck cancer patients[2–7]. Furthermore, ongoing preclinical research indicates expanding application potential, which includes stopping bleeding and mediating scar formation, alleviating burns, neuroregeneration, and tissue regeneration[8–15]. Two NTP delivery methods are currently considered most applicable for the clinic: direct and indirect NTP treatment[16]. In the direct setting, NTP is generated in direct contact with the target substrate (e.g., blood, wound, and tumor). This modality allows for the most efficient delivery of RONS but is currently limited to superficial areas that are accessible to the device. Indirect NTP treatment is one way to overcome this limitation. Here, NTP is used to enrich a solution with RONS, which can then be transferred to the target substrate. While this allows for treatment of areas deeper in the body, only persistent RONS (lifetimes ≥ s) may reach the target, as short-lived RONS (lifetimes < s) may have off-target reactions or form more stable species during transport[17]. Therefore, investigation of RONS stability is a high priority for successful clinical translation of NTP technology. To date, experimental and *in silico* studies characterizing NTP-generated species in the liquid phase have mainly been performed in water or PBS[18–21], as this reduces the complexity of reactions with supplements and organic molecules found in other solutions (e.g., cell culture medium, blood). While this has led to significant in-depth insight into the fundamental physical and chemical NTP interactions with liquid,

a major gap in current knowledge is on NTP interactions with patient material, as these substrates are far more complex than the models previously used. Since NTP-generated RONS will inevitably interact with blood in several clinical contexts, both deliberately (e.g., hemostasis) or inadvertently (e.g., cancer therapy), understanding their stability in this system is of major importance. In this study, we investigated the stability of NTP-generated RONS in blood as a first step toward elucidating NTP chemistry in clinical material. Both direct and indirect NTP delivery methods, previously used in our lab, were tested [22–24]. We performed analysis of NTP-generated RNS collectively (nitrite, NO_2^-; peroxynitrite, $ONOO^-$), hydrogen peroxide (H_2O_2), and $ONOO^-$ (separately) over time in aqueous solutions with increasing organic complexities: phosphate-buffered saline (PBS), blood plasma (BP), and processed whole blood. Both RNS and H_2O_2, stable in PBS, were scavenged by different components of the blood. The luminescent europium(III) probe, Eu.1 (Figure 3.1(a)), previously developed by our collaborators[25], was also used for precision measurement of $ONOO^-$ and revealed that NTP-generated $ONOO^-$ was present in all three liquids, for at least 30 seconds. Based on our results, we discuss the scavenging capacity of different blood components, as well as the necessary considerations to choose the most optimal NTP modality for the desired clinical application.

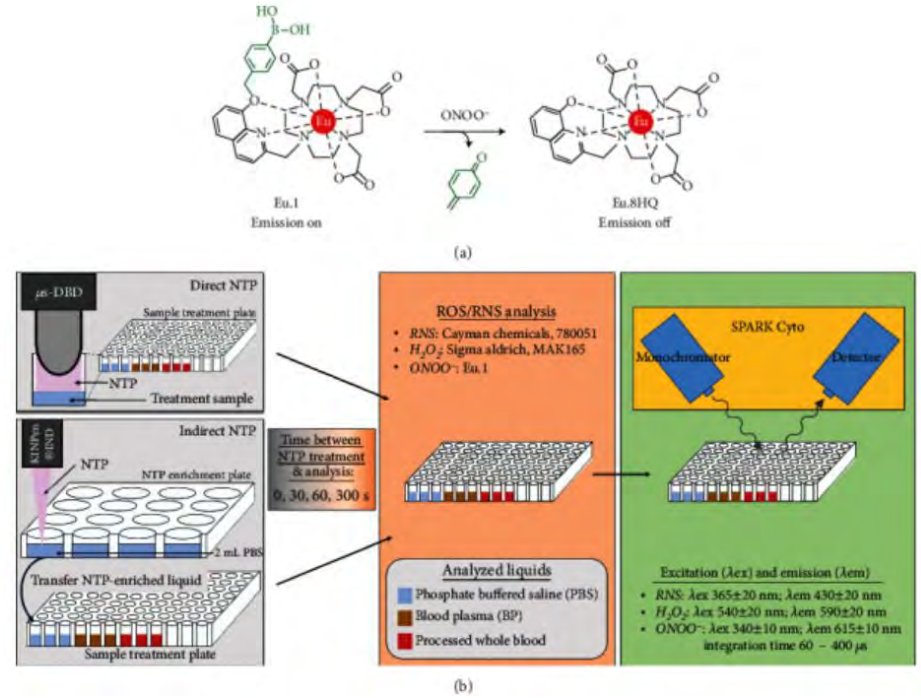

Figure 3.1 Experimental design to determine the stability of persistent ROS/RNS. (a) The mode of action of **Eu.1** for detecting $ONOO^-$ is shown. (b) PBS (blue), BP (brown), and processed whole blood (red) were analyzed following direct and indirect NTP treatment. Following treatment, the sample was either analyzed immediately (0 s) or after a delay (between 30 and 300 s) for RNS, H_2O_2, or $ONOO^-$ (μs-DBD: microsecond-pulsed dielectric barrier discharge; λ_{ex}: excitation wavelength; λ_{em}: emission wavelength)

3.2 Materials and Methods

Aim and Experimental Design

The aim of this study was to evaluate the stability of NTP-generated persistent RONS in clinical substrates (e.g., blood plasma and processed whole blood) to inform on the optimal translation of NTP technology per application. Direct and indirect NTP applications were evaluated and three chemical analysis methods were used (Figure 3.1(b)). The concentration of RONS generated immediately in PBS (0 s) was used as the baseline concentration following NTP treatment. The delay between the end of NTP treatment and the chemical analysis was varied between 30 and 300 seconds to provide insight into RONS stability over time.

Collection of BP and Processed Whole Blood

This study was approved by the Ethics Committee of the University of Antwerp/Antwerp University Hospital (Antwerp, Belgium) under the reference number 19/13/160. Experiments were performed using blood samples from anonymous donors provided by the Blood Service of the Red Cross Flanders (Mechelen, Belgium). The BP was separated from the blood using the following protocol. 25 mL processed whole blood was carefully dispensed onto 15 µL LymphoPrep (1114547, Alerne Technologies SA) and centrifuged for 20 minutes at 2100 rpm at room temperature in a swing-out rotor. After centrifugation, the blood components were separated into four distinct layers with BP at the top. This top layer of BP was then easily collected from the other parts of the blood. The term “processed whole blood” refers to buffy coats that were derived from healthy volunteers' peripheral blood (with citrate phosphate dextrose anticoagulant) donated the day before and stored overnight at room temperature (Red Cross Flanders).

NTP Treatment

We studied both direct and indirect NTP treatment. A single treatment parameter for each method was used based on comparable therapeutic effects from our past studies and published reports[22,23]. For the direct treatment, we used a custom-built microsecond-pulsed dielectric barrier discharge (μs-DBD) operated at atmospheric pressure in air (Megaimpulse Ltd, St. Petersbug, Russia). For these experiments, we used a 700 Hz pulse frequency and treated the samples for 10 seconds, 1 mm above the samples.

For the indirect treatment, we used the kINPen®IND non-thermal plasma jet (INP Greifswald/Neoplas tools GmbH, Greifswald, Germany). This is an atmospheric pressure argon NTP jet, commonly used for plasma medicine research[23,24,26]. We used the kINPen®IND to treat 2 mL phosphate-buffered saline (PBS) (pH 7.3) in a 12-well plate. A gap of 6 mm between the tip of the NTP source and the liquid, a gas flow rate of 1 slm, and a treatment time of 5 minutes were used. Following treatment, the NTP-enriched PBS was transferred to the aqueous solution (PBS, BP, or processed whole blood).

RNS Measurement

To measure RNS concentration in NTP-treated PBS, BP, and processed whole blood, a fluorometric assay was used. The Nitrate/Nitrite Fluorometric Assay kit (780051, Cayman Chemical) was performed according to the manufacturer's instructions. Briefly, for direct treatment, each well contained 10 μL of NTP-treated sample. For the indirect treatment, 10 μL of NTP-enriched PBS (pPBS) was transferred to each well containing 40 μL of PBS, BP, or processed whole blood. The final volume for each sample, both for the direct and indirect NTP treatment, was adjusted to 100 μL with assay buffer. 10 μL of 2,3-

diaminonaphthalene (DAN) reagent was added to each well, either immediately or 30, 60, or 300 seconds after treatment. After 10 minutes of incubation at room temperature, 20 µL of sodium hydroxide (NaOH) was added to each well to enhance the detection of the fluorescent product, 1(H)-naphthotriazole. Immediately after adding NaOH, fluorescence was measured with the Tecan Spark Cyto using an excitation wavelength (λex) of 365 ± 20 nm, an emission wavelength (λem) of 430 ± 20 nm, and a fixed gain (gain 55). The selectivity of the Nitrate/Nitrite Fluorometric Assay Kit used in this study was also evaluated (See Appendix 2, Figure A2.1).

H_2O_2 Measurement

To measure H_2O_2 concentrations in NTP-treated PBS, BP, and processed whole blood, we performed a fluorometric assay (MAK165, Merck) according to the manufacturer's instructions. In short, for analysis of direct NTP treatment, each well contained 25 µL of NTP-treated PBS or 50 µL of NTP-treated BP or processed whole blood. The volume of each sample was adjusted with assay buffer to obtain a final volume of 50 µL. In the case of indirect NTP treatment, each well contained either 2.5 µL of pPBS adjusted with 47.5 µL of PBS, 25 µL of BP, or 25 µL of processed whole blood. Different dilutions were used to stay within the calibration range. 50 µL of master mix (4.75 mL Assay Buffer+50 µL Red Peroxidase Substrate+200 µL 20 units/mL Peroxidase) was then added to each well. After 30 minutes of incubation, fluorescence was measured with the Tecan Spark Cyto, (λex = 540 ± 20 nm, λem of 590 ± 20 nm, fixed gain 34).

$ONOO^-$ Measurement

Here, we used a new luminescent europium(III) probe (Eu.1, Figure 3.1(a)) which was developed previously by our collaborators, for detection of $ONOO^-$ *in vitro* and in living cells[25]. For initial time points, 100 µL of Eu.1 (100 µM) in relevant media was treated with direct NTP and the emission intensity of Eu.1 was measured immediately. For the subsequent time points, Eu.1 (100 µM) was added post-treatment with direct NTP after a certain amount of time (t = 30, 60, 120, and 300 seconds). Emission intensity was measured with a plate reader using time-resolved emission (λex = 340 nm, λem = 615 ± 10 nm, int.time = 60–400 µs). The concentration was determined by comparing the percentage change in emission intensity to the calibration curve (See Appendix 2, Figure A2.2).

Statistical Analysis

All statistical differences were analyzed using the linear mixed model with JMP Pro 13 (SAS software). The fixed effect was set to either the treatment or the time delay between treatment and analysis. When a significant difference was detected, the post hoc Dunnett's test was performed to calculate the adjusted p value compared to the control. For quantification of RONS species, NTP treatment at all time points was compared to the untreated. To determine the scavenging capacity of BP and processed whole blood, delayed analysis (30-300 seconds) of RONS concentration was compared to the initial (0 second). A p value of <0.05 was considered statistically significant. Data in all graphs are represented as mean ± standard error of the mean (SEM), the number of replicates is indicated in the legend, and all figures were prepared in GraphPad Prism (GraphPad Prism 7, GraphPad Prism Software, Inc.).

3.3 Results

3.3.1 NTP-Generated Persistent ROS/RNS Are Stable in PBS, but Scavenged Over Time in BP and Processed Whole Blood

To determine the baseline concentrations of NTP-generated persistent ROS/RNS, direct and indirect NTP was used to treat PBS, using our DBD at atmospheric air and the argon kINPen jet, respectively. While direct NTP generated slightly higher concentrations of RNS compared to the indirect treatment (Figure 3.2(d)), indirect NTP produced over 20 times more H_2O_2 (Figure 3.2(a)). RNS and H_2O_2 analysis was performed immediately after NTP treatment (0 seconds) and delayed between 30 to 300 seconds after treatment. Both these species were stable in PBS up to at least 300 seconds. The pH of the PBS was also measured before and after NTP treatment and remained relatively unchanged following exposure to both direct (7.25 ± 0.01; mean ± SEM) or indirect (7.25 ± 0.01) NTP, compared to untreated (pH: 7.30 ± 0.01).

To examine the stability of NTP-generated RONS in a more complex physiological solution, we treated BP derived from healthy donors. BP accounts for approximately 55% of the volume of blood and consists primarily of water, dissolved electrolytes, proteins, and lipids. Both direct and indirect NTP were used to treat BP, which was collected and analyzed for RNS and H_2O_2 in the same manner as before. Interestingly, the RNS were immediately scavenged to around 15 µM for both direct and indirect NTP treatment, despite direct treatment producing almost twice the amount of RNS in PBS (cf. Figure 3.2(e) vs. Figure 3.2(d)). The remaining RNS were stable up to at least 60 seconds. On the other hand, the H_2O_2 concentration was immediately and significantly reduced compared with that in PBS and continued to decrease over time (Figure 3.2(b)).

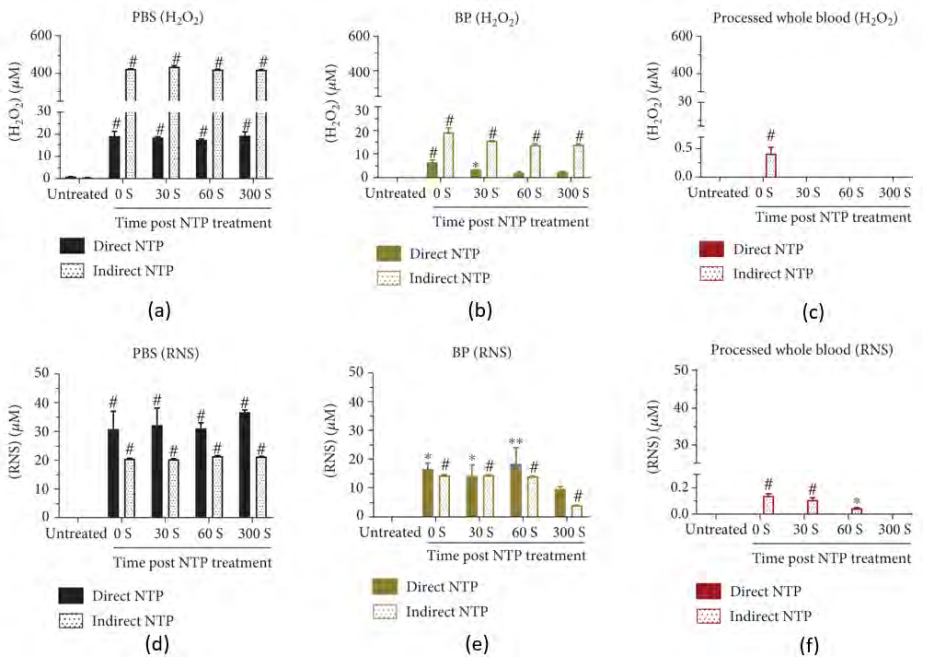

Figure 3.2 Quantification of persistent RNS and H_2O_2 in three aqueous solutions: PBS, blood plasma (BP), and processed whole blood. NTP was generated in direct contact with the target liquid (direct NTP) or used to enrich PBS, which was then transferred to the target liquid (indirect NTP). Following NTP treatment, RNS and H_2O_2 analysis was performed immediately (0 s) or after a delay of 30 to 300 seconds to assess the stability of these species in (a, d) PBS, (b, e) BP, and (c, f) processed whole blood. Data are represented as mean ± SEM. ROS/RNS concentration following NTP treatment at all time points was compared to untreated and statistical significance was determined using the generalized linear mixed model (n = 3). $*p < 0.05$; $**p < 0.01$; #p < 0.001

Processed whole blood, which comprises red and white blood cells and platelets along with BP, was also treated and analyzed as the model for the most complex and complete physiological solution. Both RNS and H_2O_2 generated by direct NTP were immediately reduced to undetectable levels (Figures 3.2(c) and 3.2(f)). For indirect NTP, the RNS were immediately reduced below 0.2 μM and were completely absent by 300 seconds, while H_2O_2 was only detectable immediately after treatment.

While both ROS/RNS were stable in PBS, once introduced to the components of BP, their concentration was significantly diminished (Figure 3.3). In fact, the RNS concentration in BP was reduced to 50-75% of its starting concentration compared with that of PBS and was almost completely absent in processed whole blood (Figures 3.3(a) and 3.3(c)). On the other hand, immediate detection of H_2O_2 in BP displayed a remaining percentage of 33% for direct NTP (Figure 3.3(b)), and 4.5% for indirect NTP (Figure 3.3(d)) compared to baseline levels in NTP-treated PBS. H_2O_2 also decreased slightly over time in BP, which did not occur in PBS. Furthermore, at higher initial concentrations of H_2O_2 from indirect NTP treatment, H_2O_2 was still detectable in processed whole blood when immediately analyzed (Figure 3.3(f)), though the remaining percentage was ≤0.1% (Figure 3.3(d)). Therefore, while the cellular and platelet components may contribute to the H_2O_2 scavenging capacity of the blood, the BP components alone are potent scavengers.

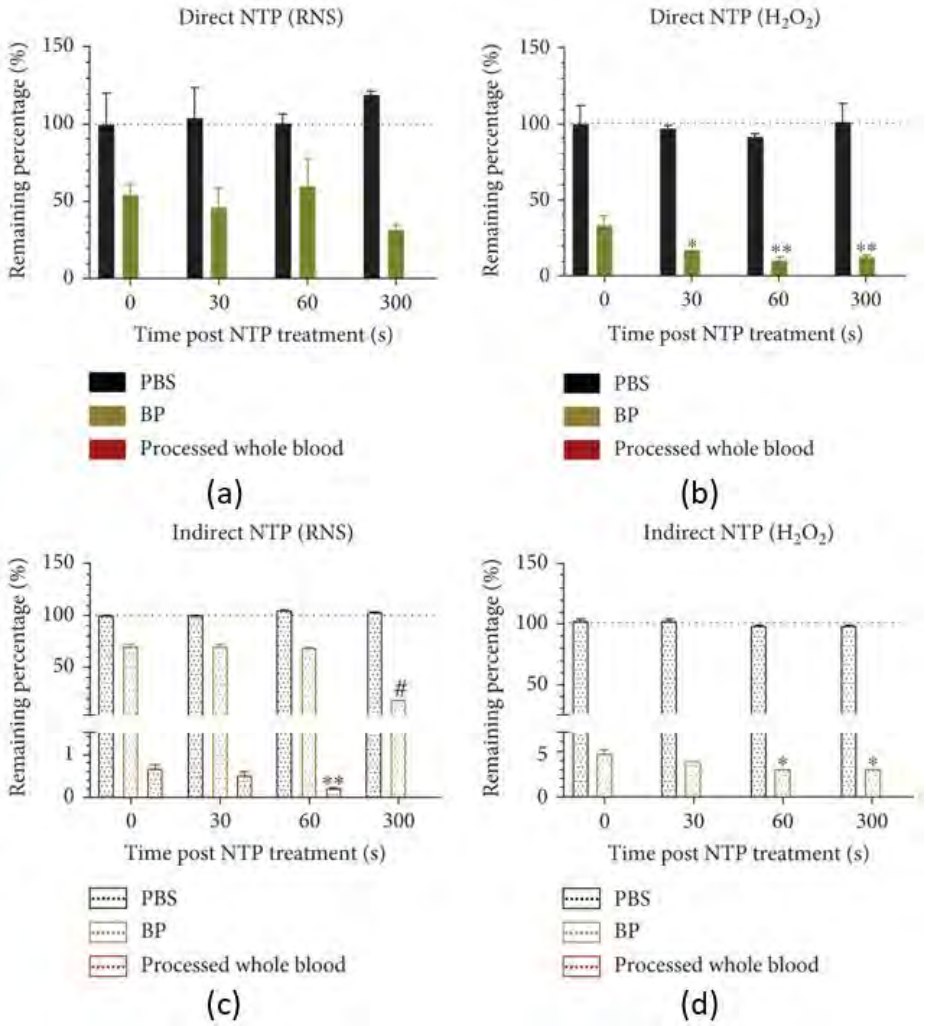

Figure 3.3 Scavenging capacity of BP and processed whole blood for NTP-generated ROS/RNS. RNS and H_2O_2 concentrations at different analysis time points were normalized to their baseline concentrations, measured immediately after treatment in PBS, to determine the remaining percentage following (a, b) direct NTP and (c, d) indirect NTP. Data are represented as mean ± SEM. The ROS/RNS concentration after NTP at time points 30-300 s was compared to the initial concentration (0 s) in the associated liquid. This comparison provides insight into the stability of the species over time in PBS, BP, and processed whole blood. The generalized linear mixed model was used to determine statistical significance (n = 3). $*p < 0.05$; $**p < 0.01$; $\#p < 0.001$

3.3.2 NTP-Generated Peroxynitrite ($ONOO^-$) is Stable in PBS, BP, and Processed Whole Blood for up to at Least 30 Seconds

$ONOO^-$ is a highly reactive RNS involved in cellular signaling and manipulating the $ONOO^-$ concentration has been a strategy for therapy and management of several diseases (e.g., inflammatory disease, vascular diseases, and cancer)[27–29]. Detection of $ONOO^-$ has been particularly challenging in the biomedical setting due to the limited selectivity and applicability of current assays and the slow response times of detection probes, notwithstanding some notable recent developments[30–32]. Here, we used a new luminescent europium(III) probe (Eu.1) to detect direct NTP-generated $ONOO^-$ in PBS, BP, and processed whole blood. This probe, designed and synthesized by our collaborators, has been previously demonstrated to rapidly and selectively detect $ONOO^-$ in a time-resolved manner, in aqueous buffers and human BP[25]. In the current study, the long luminescence lifetime of the Eu(III) probe has been utilized to eliminate any short-lived autofluorescence arising from biomolecules in the BP or processed whole blood, thereby providing high signal-to-noise and accurate measurements of $ONOO^-$ concentration.

It is clear that $ONOO^-$ is generated immediately following direct NTP treatment and the concentration is equivalent in all three aqueous solutions (Figure 3.4(a)). This indicates that direct treatment is initially generating a relatively constant concentration of $ONOO^-$ (~17 μM), regardless of the complexity of the medium. In PBS, the decay of $ONOO^-$ occurs over 300 seconds and could be attributed to the reaction of $ONOO^-$ to form more stable species such as nitrite (NO_2^-) and nitrate (NO_3^-)[33]. It is important to note that degradation of $ONOO^-$ may not be solely and directly responsible for the formation of NO_2^- and NO_3^- and can result in significantly shorter-lived species (e.g., $ONOOCO_2^-$, NO)[19].

Interestingly, following a 30-second delay, $ONOO^-$ in BP and processed whole blood was reduced to approximately the same amount, 7 ± 2 μM and 9 ± 1 μM, respectively, before becoming completely abrogated at higher time delays (≥60 seconds). This indicates that BP components play an important role in scavenging $ONOO^-$, particularly NTP-generated $ONOO^-$. As $ONOO^-$ formation and stability are also highly dependent on the pH of the solution[34], we also evaluated the effect of NTP treatment on pH. Direct NTP did not significantly affect the pH in any of the aqueous solutions (<0.15 pH units) (Figure 3.4(b)). Taken together, this data strongly suggests that the decay of $ONOO^-$ is due to reactions with other biomolecules/organic species in the blood, predominantly in the BP. This is not unexpected, given the potent nitrating and oxidizing nature of $ONOO^-$ and the number of potential reactive partners in both processed whole blood and BP (e.g., amino acids, CO_2, Fe^{2+})[33]. While the reaction of $ONOO^-$ with biomolecules/organic species appears to be the predominant mechanism of decay, the interactions between other ROS/RNS cannot be entirely discounted.

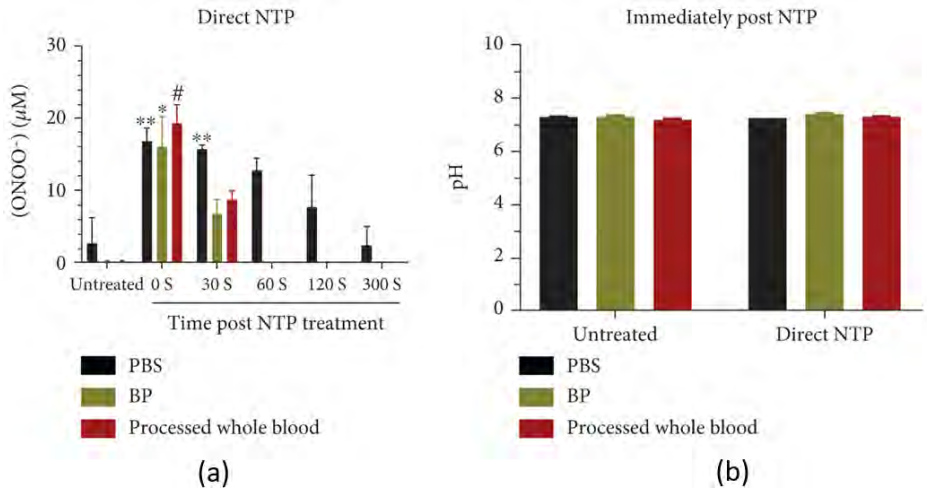

Figure 3.4 Analysis of NTP-generated $ONOO^-$ stability in PBS, BP, and processed whole blood. (a) $ONOO^-$ concentrations were analyzed by the addition of Eu.1 (100 μM) to the solution after a specific time post-NTP treatment. Data are represented as mean ± SEM. The $ONOO^-$ concentration was compared to untreated in corresponding solutions, and statistical significance was determined using the generalized linear mixed model (n = 2-10). $*p < 0.05$; $**p < 0.01$; $\#p < 0.001$. (b) The pH of all aqueous solutions remained largely unchanged after direct NTP treatment (n = 3)

3.4 Discussion

In this study, we tested the scavenging capacity of different components of blood, following treatment with two NTP modalities and using a range of complementary detection methods. Currently, a full understanding of how NTP-generated RONS interact with clinical substrates is lacking, and to our knowledge, this is the first report on the evaluation of NTP-generated RONS in blood.

Since RNS were reduced to a fixed concentration, despite the two NTP modalities producing different starting amounts (Figures 3.2(d) and 3.2(e)), this suggests that dissolved proteins (e.g., albumin, globulins, and fibrinogen) and lipids (e.g., fatty acids, cholesterol) in the BP only have a partial scavenging action. The additional cellular and platelet components of the processed whole

blood further scavenged the RNS (Figures 3.3(a) and 3.3(c)). These data strongly suggest that the RNS are only partially reduced by the BP component of the blood. On the other hand, our results suggest that the BP contains major scavenging capacity for H_2O_2, as the remaining percentage of H_2O_2 was under 40% and 5% for direct and indirect treatment, respectively (Figures 3.3(b) and 3.3(d)). However, this is not to say that the cellular and platelet components of the blood do not contribute to scavenging of H_2O_2, as processed whole blood nearly quenched all H_2O_2 immediately (Figure 3.2(f)). This immediate scavenging effect of H_2O_2 is mostly due to the enzymatic machineries from the red blood cells, protecting hemoglobin from oxidative processes. It should be considered that the iron bound in the hemoglobin can be oxidized by H_2O_2 to ferryl hemoglobin ($HbFe^{4+}$)[34]. With high concentrations of H_2O_2 (6.5 mM), this would decrease the amount of the oxygen-carrying form of hemoglobin, ferrous hemoglobin ($HbFe^{2+}O_2$), leading to toxic responses[34]. When produced in small amounts, $HbFe^{4+}$ will be restored rapidly to ferrous hemoglobin by the red blood cells without any toxic effects. In our case, the amount of H_2O_2 is low enough (≤20 µM for direct treatment and ≤ 400 µM for indirect treatment; Figure 2(b)) to be scavenged by the red blood cells, before large amounts of ferryl hemoglobin will be formed[35]. For NO_2^-, a similar oxidation process can happen with the formation of ferric hemoglobin ($HbFe^{3+}$), instead of ferryl hemoglobin[36]. Taken together, it is clear that evaluation of the concentration of NTP-generated RONS in clinical substrates and the by-products they produce is vital for the safe translation of this technology.

Both direct and indirect NTP modalities have translational potential for the clinic, though they work through different mechanisms due to the different species they deliver. A current limitation of direct NTP is the

requirement of direct access to the target, thus restricting this NTP modality to superficial wounds and cancers (e.g., melanoma, head and neck carcinoma) or during surgery. Indirect NTP treatment is one way to circumvent this limitation, and solutions enriched with RONS by NTP have been delivered to deeper layers of the body for treatment[37–39]. It is essential to highlight that with indirect NTP treatment, only the persistent RONS are delivered to deep tissue, because RONS with shorter lifetimes undergo reactions to form more stable species in the liquid. Based on our results in this study, it appears that intravenous delivery of NTP-enriched solutions for therapy may be difficult, as these species are lost to the blood in-transit. Specifically, $ONOO^-$ was undetectable in under 60 seconds (Figure 3.4(a)), while H_2O_2 was undetectable in under 30 seconds (Figure 3.2(f)). Total RNS was still detectable at 60 seconds, but at very low levels (Figure 3.2(c)). However, considering the location of the injection site to the target and the stability of the RONS species, indirect NTP treatment could be optimized for clinical application. In addition, other indirect NTP delivery methods (e.g., local application, perfusion in body cavities) could also provide promising options. From the data presented herein, it is clear that the clinical benefit of RONS generated by indirect NTP needs to be thoroughly investigated. A comparison with chemically synthesized RONS is also required to determine if indirect NTP provides additional advantages. These fundamental studies must be application-specific (e.g., wound healing, cancer therapy) and concentration-specific due to the pleiotropic effects of RONS[40].

In contrast to indirect NTP, during direct NTP treatment of the target substrate, a unique mixture of short-lived chemical species (e.g., $^{\bullet}OH$, O, and $^{\bullet}NO$) can be delivered along with the persistent RONS (e.g., NO_2^-, H_2O_2, and $ONOO^-$) to induce a biological response[17]. It is important to

note that while short-lived species were not measured in this study, their therapeutic effects cannot be discounted in direct NTP treatment, due to the close proximity of the generation site to the target. Recently, the importance of these short-lived species for direct NTP therapy has surfaced, which is in agreement with current understanding in redox medicine[22,40,41]. While direct treatment is also known to generate UV radiation, several reports have shown that the amount generated by DBDs does not contribute to the overall biological effect[42,43]. As it stands, direct NTP treatment is a valuable method of controllably generating and delivering these short-lived RONS in the clinical setting, which requires further investigation in blood and other biological solutions.

3.5 Conclusions

In summary, we have evaluated the stability of persistent RONS (i.e., NO_2^-, H_2O_2, and $ONOO^-$) in clinically relevant solutions following direct and indirect NTP treatment. A luminescent Eu(III) probe was able to rapidly and selectively detect $ONOO^-$, not only in PBS and BP but also in processed whole blood. NTP-generated $ONOO^-$ was detected in all three liquids for up to at least 30 seconds, thus highlighting its therapeutic potential. Treatment of different components of the blood revealed that mainly the cellular and platelet components of blood are responsible for scavenging RNS. On the other hand, both BP and the other blood components have potent scavenging potential against H_2O_2 and $ONOO^-$. Taken together, our results provide fundamental insight into NTP interactions with blood and suggest that intravenous delivery of NTP-enriched solutions for therapy may be difficult, as a variety of reactive species may be lost to the blood in-transit.

By considering, collectively, the site for introducing NTP-generated RONS, the stability of the therapeutic species, and the distance to the biological target site, more informed decisions on clinical application of direct and indirect NTP therapy can be made. In the field of plasma medicine, this has high translational importance for NTP therapy in diverse clinical contexts and applications.

3.6 References

1. Privat-Maldonado A, Schmidt A, Lin A, et al. ROS from Physical Plasmas: Redox Chemistry for Biomedical Therapy. *Oxid Med Cell Longev*. 2019;2019. doi:10.1155/2019/9062098

2. Schuster M, Seebauer C, Rutkowski R, et al. Visible tumor surface response to physical plasma and apoptotic cell kill in head and neck cancer. *Journal of Cranio-Maxillofacial Surgery*. 2016;44(9):1445-1452. doi:10.1016/j.jcms.2016.07.001

3. Metelmann HR, Seebauer C, Miller V, et al. Clinical experience with cold plasma in the treatment of locally advanced head and neck cancer. *Clin Plasma Med*. 2018;9:6-13. doi:10.1016/j.cpme.2017.09.001

4. Friedman PC, Miller V, Fridman G, Lin A, Fridman A. Successful treatment of actinic keratoses using nonthermal atmospheric pressure plasma: A case series. *J Am Acad Dermatol*. 2017;76(2):349-350. doi:10.1016/j.jaad.2016.09.004

5. Friedman PC, Miller V, Fridman G, Fridman A. Use of cold atmospheric pressure plasma to treat warts: a potential therapeutic option. *Clin Exp Dermatol*. 2019;44(4):459-461. doi:10.1111/ced.13790

6. Isbary G, Heinlin J, Shimizu T, et al. Successful and safe use of 2 min cold atmospheric argon plasma in chronic wounds: results of a randomized controlled trial. *British Journal of Dermatology*. 2012;167(2):404-410. doi:10.1111/j.1365-2133.2012.10923.x

7. Isbary G, Morfill G, Schmidt HU, et al. A first prospective randomized controlled trial to decrease bacterial load using cold atmospheric argon plasma on chronic wounds in patients. *British Journal of Dermatology*. 2010;163(1):78-82. doi:10.1111/j.1365-2133.2010.09744.x

8. Ngo Thi MH, Shao PL, Liao JD, Lin CCK, Yip HK. Enhancement of Angiogenesis and Epithelialization Processes in Mice with Burn Wounds through ROS/RNS Signals Generated by Non-Thermal N_2 /Ar Micro-Plasma. *Plasma Processes and Polymers*. 2014;11(11):1076-1088. doi:10.1002/ppap.201400072

9. Miyamoto K, Ikehara S, Sakakita H, Ikehara Y. Low temperature plasma equipment applied on surgical hemostasis and wound healings. *J Clin Biochem Nutr*. 2017;60(1):25-28. doi:10.3164/jcbn.16-60

10. YAN K, JIN Q, ZHENG C, DENG G, YIN S, LIU Z. Pulsed cold plasma-induced blood coagulation and its pilot application in stanching bleeding during rat hepatectomy. *Plasma Science and Technology*. 2018;20(4):044005. doi:10.1088/2058-6272/aa9b79

11. Jang JY, Hong YJ, Lim J, et al. Cold atmospheric plasma (CAP), a novel physicochemical source, induces neural differentiation through cross-talk between the specific RONS cascade and Trk/Ras/ERK signaling pathway. *Biomaterials*. 2018;156:258-273. doi:10.1016/j.biomaterials.2017.11.045

12. Katiyar KS, Lin A, Fridman A, Keating CE, Cullen DK, Miller V. Non-Thermal Plasma Accelerates Astrocyte Regrowth and Neurite Regeneration Following Physical Trauma In Vitro. *Applied Sciences*. 2019;9(18):3747. doi:10.3390/app9183747

13. Chernets N, Zhang J, Steinbeck MJ, et al. Nonthermal Atmospheric Pressure Plasma Enhances Mouse Limb Bud Survival, Growth, and Elongation. *Tissue Eng Part A*. 2015;21(1-2):300-309. doi:10.1089/ten.tea.2014.0039

14. Xiong Z, Zhao S, Mao X, et al. Selective neuronal differentiation of neural stem cells induced by nanosecond microplasma agitation. *Stem Cell Res*. 2014;12(2):387-399. doi:10.1016/j.scr.2013.11.003

15. Metelmann HR, Vu TT, Do HT, et al. Scar formation of laser skin lesions after cold atmospheric pressure plasma (CAP) treatment: A clinical long term observation. *Clin Plasma Med*. 2013;1(1):30-35. doi:10.1016/j.cpme.2012.12.001

16. Yan D, Sherman JH, Keidar M. Cold atmospheric plasma, a novel promising anti-cancer treatment modality. *Oncotarget*. 2017;8(9):15977-15995. doi:10.18632/oncotarget.13304

17. Lu X, Naidis G V., Laroussi M, Reuter S, Graves DB, Ostrikov K. Reactive species in non-equilibrium atmospheric-pressure plasmas: Generation, transport, and biological effects. *Phys Rep*. 2016;630:1-84. doi:10.1016/j.physrep.2016.03.003

18. Lu X, Naidis G V., Laroussi M, Reuter S, Graves DB, Ostrikov K. Reactive species in non-equilibrium atmospheric-pressure plasmas: Generation, transport, and biological effects. *Phys Rep*. 2016;630(April):1-84. doi:10.1016/j.physrep.2016.03.003

19. Bruggeman PJ, Kushner MJ, Locke BR, et al. Plasma–liquid interactions: a review and roadmap. *Plasma Sources Sci Technol*. 2016;25(5):053002. doi:10.1088/0963-0252/25/5/053002

20. Gorbanev Y, O'Connell D, Chechik V. Non-Thermal Plasma in Contact with Water: The Origin of Species. *Chemistry - A European Journal*. 2016;22(10):3496-3505. doi:10.1002/chem.201503771

21. Gorbanev Y, Verlackt CCW, Tinck S, et al. Combining experimental and modelling approaches to study the sources of reactive species induced in

water by the COST RF plasma jet. *Physical Chemistry Chemical Physics*. 2018;20(4):2797-2808. doi:10.1039/C7CP07616A

22. Lin A, Gorbanev Y, De Backer J, et al. Non-Thermal Plasma as a Unique Delivery System of Short-Lived Reactive Oxygen and Nitrogen Species for Immunogenic Cell Death in Melanoma Cells. *Advanced Science*. 2019;6(6). doi:10.1002/advs.201802062

23. Van Loenhout J, Flieswasser T, Boullosa LF, et al. Cold atmospheric plasma-treated PBS eliminates immunosuppressive pancreatic stellate cells and induces immunogenic cell death of pancreatic cancer cells. *Cancers (Basel)*. 2019;11(10). doi:10.3390/cancers11101597

24. Biscop E, Lin A, Van Boxem W, et al. Influence of cell type and culture medium on determining cancer selectivity of cold atmospheric plasma treatment. *Cancers (Basel)*. 2019;11(9). doi:10.3390/cancers11091287

25. Breen C, Pal R, Elsegood MRJ, et al. Time-resolved luminescence detection of peroxynitrite using a reactivity-based lanthanide probe. *Chem Sci*. 2020;11(12):3164-3170. doi:10.1039/C9SC06053G

26. Bekeschus S, Schmidt A, Weltmann KD, von Woedtke T. The plasma jet kINPen – A powerful tool for wound healing. *Clin Plasma Med*. 2016;4(1):19-28. doi:10.1016/j.cpme.2016.01.001

27. Salvemini D, Wang ZQ, Stern MK, Currie MG, Misko TP. Peroxynitrite decomposition catalysts: Therapeutics for peroxynitrite-mediated pathology. *Proceedings of the National Academy of Sciences*. 1998;95(5):2659-2663. doi:10.1073/pnas.95.5.2659

28. Qiao S, Li W, Tsubouchi R, Haneda M, Murakami K, Yoshino M. Involvement of peroxynitrite in capsaicin-induced apoptosis of C6 glioma cells. *Neurosci Res*. 2005;51(2):175-183. doi:10.1016/j.neures.2004.10.006

29. Pacher P, Beckman JS, Liaudet L. Nitric Oxide and Peroxynitrite in Health and Disease. *Physiol Rev*. 2007;87(1):315-424. doi:10.1152/physrev.00029.2006

30. Li Z, Liu C, Yu C, et al. A highly selective and sensitive red-emitting fluorescent probe for visualization of endogenous peroxynitrite in living cells and zebrafish. *Analyst*. 2019;144(10):3442-3449. doi:10.1039/C9AN00347A

31. Sedgwick AC, Dou WT, Jiao JB, et al. An ESIPT Probe for the Ratiometric Imaging of Peroxynitrite Facilitated by Binding to Aβ-Aggregates. *J Am Chem Soc*. 2018;140(43):14267-14271. doi:10.1021/jacs.8b08457

32. Lee D, Lim CS, Ko G, et al. A Two-Photon Fluorescent Probe for Imaging Endogenous ONOO ⁻ near NMDA Receptors in Neuronal Cells and Hippocampal Tissues. *Anal Chem*. 2018;90(15):9347-9352. doi:10.1021/acs.analchem.8b01960

33. Radi R. Oxygen radicals, nitric oxide, and peroxynitrite: Redox pathways in molecular medicine. *Proceedings of the National Academy of Sciences*. 2018;115(23):5839-5848. doi:10.1073/pnas.1804932115

34. BUEHLER PW, ALAYASH AI. Oxidation of hemoglobin: mechanisms of control in vitro and in vivo. *Transfusion Alternatives in Transfusion Medicine*. 2007;9(4):204-212. doi:10.1111/j.1778-428X.2007.00081.x

35. WHITE DC, TEASDALE PR. THE OXYGENATION OF BLOOD BY HYDROGEN PEROXIDE: IN VITRO STUDIES. *Br J Anaesth*. 1966;38(5):339-344. doi:10.1093/bja/38.5.339

36. Huang KT, Keszler A, Patel N, et al. The Reaction between Nitrite and Deoxyhemoglobin. *Journal of Biological Chemistry*. 2005;280(35):31126-31131. doi:10.1074/jbc.M501496200

37. Yan D, Talbot A, Nourmohammadi N, et al. Principles of using Cold Atmospheric Plasma Stimulated Media for Cancer Treatment. *Sci Rep*. 2015;5(June):1-17. doi:10.1038/srep18339

38. Utsumi F, Kajiyama H, Nakamura K, et al. Effect of indirect nonequilibrium atmospheric pressure plasma on anti-proliferative activity against chronic chemo-resistant ovarian cancer cells in vitro and in vivo. *PLoS One*. 2013;8(12). doi:10.1371/journal.pone.0081576

39. Freund E, Liedtke KR, Gebbe R, Heidecke AK, Partecke LI, Bekeschus S. <i>In Vitro <i> Anticancer Efficacy of Six Different Clinically Approved Types of Liquids Exposed to Physical Plasma. *IEEE Trans Radiat Plasma Med Sci*. 2019;3(5):588-596. doi:10.1109/TRPMS.2019.2902015

40. Sies H, Jones DP. Reactive oxygen species (ROS) as pleiotropic physiological signalling agents. *Nat Rev Mol Cell Biol*. 2020;21(7):363-383. doi:10.1038/s41580-020-0230-3

41. Bekeschus S, Wende K, Hefny MM, et al. Oxygen atoms are critical in rendering THP-1 leukaemia cells susceptible to cold physical plasma-induced apoptosis. *Sci Rep*. 2017;7(1):2791. doi:10.1038/s41598-017-03131-y

42. Lin A, Chernets N, Han J, et al. Non-Equilibrium Dielectric Barrier Discharge Treatment of Mesenchymal Stem Cells: Charges and Reactive Oxygen Species Play the Major Role in Cell Death. *Plasma Processes and Polymers*. 2015;12(10):1117-1127. doi:10.1002/ppap.201400232

43. Lin A, Truong B, Patel S, et al. Nanosecond-Pulsed DBD Plasma-Generated Reactive Oxygen Species Trigger Immunogenic Cell Death in A549 Lung Carcinoma Cells through Intracellular Oxidative Stress. *Int J Mol Sci*. 2017;18(5):966. doi:10.3390/ijms18050966

Appendix 2

Appendix 2.1. Selectivity of Nitrate/Nitrite Fluorometric Assay Kit

The selectivity of the Nitrate/Nitrite Fluorometric Assay Kit (780051, Cayman Chemical) used in this study was also evaluated. According to the literature and the manufacturer, the detection of NO_2^- is based on the reaction with 2,3-diaminonapthalene (DAN), followed by sodium hydroxide (NaOH), to form the fluorescent product 1(H)-napthotriazole. However, since NTP is also known to generate $ONOO^-$, which is molecularly similar to NO_2^-, it is crucial to test its reactivity to DAN to form the fluorescent product. The addition of $ONOO^-$ (18 μM) to DAN and increasing concentrations of NO_2^- (0-10 μM) resulted in higher fluorescent signals (Figure A2.1), thus indicating that this assay is not specific for NO_2^- (or NO_3^-) as the name of the kit would suggest. However, the kit shows a linear response to the concentration of the mixture of NO_2^- and $ONOO^-$. Therefore, the results obtained from using this assay kit reflect the collective RNS concentration following NTP treatment.

Overlooking this potential interference would lead to misinterpretation and oversimplification of results in complex cellular/biological systems. In biological systems, this assay is often used to determine nitric oxide concentrations, as the assay states that NO_2^- and NO_3^- are the stable products of nitric oxide. However, intracellularly, nitric oxide could also react with superoxide and produce $ONOO^-$. As we show here, $ONOO^-$ reacts with DAN to produce the fluorescence signal, much higher than shown in the calibration curve using pure NO_2^-. While intracellularly generated $ONOO^-$ is likely to react with other biological molecules (e.g. amino acids, heme centers), its influence on the assay should be checked and accounted for. In the context of NTP systems, which generate a mixture of RNS, it is clear that this assay can only be used to measure the total amount of RNS, and insight into NO_2^- cannot be delineated without the use of specific $ONOO^-$ scavengers or more specie-specific probes. Here, in our study, we used a specific $ONOO^-$ luminescent probe (**Eu.1**) to investigate direct NTP-generated $ONOO^-$ [28].

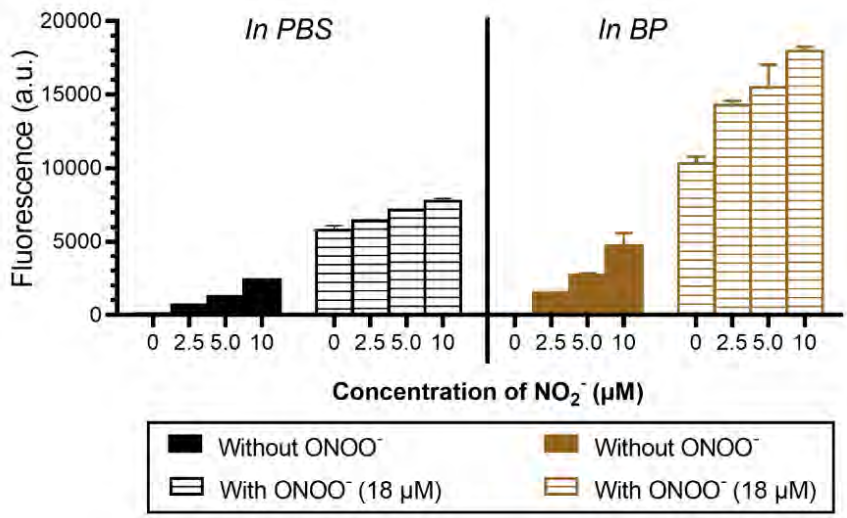

Figure A2.1 The selectivity of the Nitrate/Nitrite Fluorometric Assay Kit (780051, Cayman Chemical) used in this study was determined. The fluorescence signal of the product at increasing NO_2^- concentrations (0-10 μM), with and without the addition of $ONOO^-$ (18 μM), was measured in PBS (left) and BP (right). Data are represented as mean± SEM

Appendix 2.2. $ONOO^-$ measurements

2.1 Plate reader

96 black well plates were used for plate reader-based analysis. For calibration data the plate was read using time-resolved emission (BMG Clariostar, λex = 292 – 366 nm (TR ex filter), λem = 605 – 630 nm, int. time = 60 – 400 μs). All measurements were completed in triplicate. For NTP-generated $ONOO^-$, the plate was read using time-resolved emission (x, λex = 340 nm, λem = 615 ± 10 nm, int. time = 60 – 400 μs).

2.2 General procedure for calibration plots

A known concentration stock solution of $ONOO^-$ was prepared in 0.1 M NaOH and kept at 0°C for the duration of the experiment. A known volume was added to 100 μL of Eu.1 (100 μM) in the relevant solvent (PBS or BP). The concentration of $ONOO^-$ was increased to a total concentration of 200 μM. Total volume addition did not surpass 5 μL. Emission intensity was measured using conditions as described in Section 1.1.

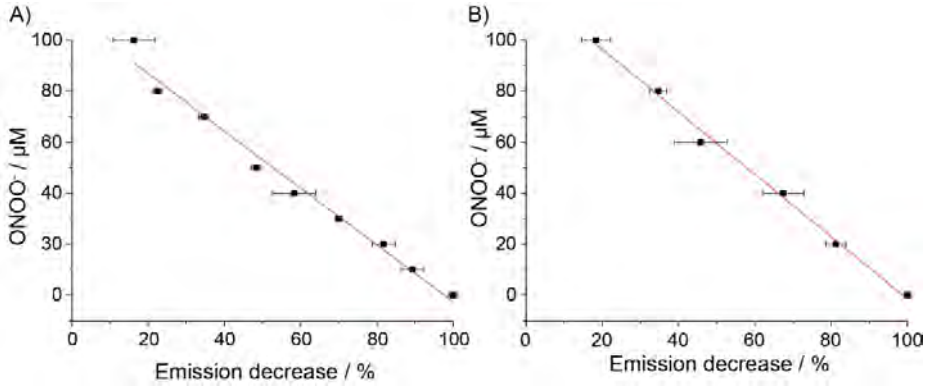

Figure A2.2 Calibration standards for Eu.1 (100 µM) in A) 100 mM PBS, pH 7.4, and in B) human BP. Conditions: λex = 330 nm, λem = 620 ± 20 nm, int. time = 60 – 400 µs. Calibration standards were generated at Loughborough University

CHAPTER 4

Characterization of Regulated Cancer Cell Death Pathways Induced by the Different Modalities of Non-Thermal Plasma Treatment: Apoptosis, Pyroptosis, Necroptosis, and Ferroptosis

This Chapter is submitted to the Journal of Cell Death and Differentiation as:

Eline Biscop, Jana Baroen, Joey De Backer, Wim Vanden Berghe, Evelien Smits, Annemie Bogaerts and Abraham Lin. Characterization of Regulated Cancer Cell Death Pathways Induced by the Different Modalities of Non-Thermal Plasma Treatment: Apoptosis, Pyroptosis, Necroptosis, and Ferroptosis.

Abstract

Non-thermal plasma (NTP) has shown promising anti-cancer effects, but there is still limited knowledge about the underlying cell death mechanisms induced by NTP and inherent differences between NTP treatment modalities. This study aimed to investigate four major regulated cell death (RCD) pathways, namely apoptosis, pyroptosis, necroptosis, and ferroptosis, in melanoma cancer cells following NTP treatment, and to provide an overview of molecular mechanistic differences between direct and indirect NTP treatment modalities. To discriminate which cell death pathways were triggered after treatment, specific inhibitors of apoptosis, pyroptosis, necroptosis, and ferroptosis were evaluated. RCD-specific molecular pathways were further investigated to validate the findings with inhibitors. Both direct and indirect NTP treatment increased caspase 3/7 and Annexin V expression, indicative of apoptosis, as well as lipid peroxidation, characteristic of ferroptosis. Pyroptosis, on the other hand, was only induced by direct NTP treatment, evidenced by increased caspase 1 activity, whereas necroptosis was stimulated in a cell line-dependent manner. These findings highlight the molecular differences and implications of direct and indirect NTP treatment and for cancer therapy. Altogether, activation of multiple cell death pathways offers advantages in minimizing treatment resistance and enhancing therapeutic efficacy, particularly in a combination setting. Understanding the mechanisms underlying NTP-induced RCD will enable the development of strategic combination therapies targeting multiple pathways to achieve cancer lethality.

4.1 Introduction

As mentioned in Chapter 1, promising reports on the anti-cancer and immunological effects of NTP have been demonstrated with a broad range of devices and treatment modalities. However, despite this, it is currently unclear whether the mechanism of action between these different NTP modalities is comparable.

The two major NTP modalities for clinical consideration currently employed are: direct NTP treatment, where NTP is generated in direct contact with the target substrate, and indirect NTP treatment, where a physiological solution is treated and enriched with NTP for a specific duration (commonly referred to as a plasma-treated liquid; PTL) before being introduced to the target substrate. Whereas it is now widely accepted that the anti-cancer effect of NTP is predominantly due to the formation of highly reactive RONS, mainly H_2O_2, NO_2^-, NO_3^-, $^{\bullet}OH$, $^1O_2$, O/O_3 and $^{\bullet}NO$[17,19], the specific RONS that reach and interact with cancerous cells and tumors are highly dependent on the delivery modality[20–22]. The direct NTP treatment method results in a delivery of both long-lived (lifetimes ≥ 1 s; e.g. H_2O_2, NO_2^-, NO_3^-) and short-lived RONS (lifetimes < 1 s; e.g. $^{\bullet}OH$, $^1O_2$, O/O_3, $^{\bullet}NO$)[17]. While this modality is highly efficient in delivering a plethora of biologically active RONS, this approach is constrained to surfaces that can be accessed by the device [23,24]. The indirect NTP treatment method can be used to treat deeper tissue layers, but due to the delay interval between NTP enrichment of the solution and administration to the target substrate, only the long-lived RONS are able to reach the cells[20].

Until today, comparing the cell death signaling mechanisms involved in the two NTP treatment modalities remains challenging, due to the vastly different application parameters, electrical characteristics, and chemical components as well as the large number of regulated cell death (RCD)

pathways[25,26]. So far, the majority of studies evaluating NTP-induced RCD was focused on apoptosis and ICD mechanisms[27–31], representing only 2 of the 12 defined RCD mechanisms[25,26]. We currently hypothesize that NTP can trigger multiple RCD pathways, including, necroptosis, ferroptosis, and even pyroptosis, due to the plethora of different RONS generated by NTP and reacting with various biochemical targets controlling RCD. Moreover, a comparison between direct and indirect NTP treatment modalities can be used to further delineate their respective mechanisms of action.

In this report, we address these long-standing questions, as we investigated the multiple RCD pathways following NTP treatment with both modalities. We used ICD-inducing treatment parameters for both direct and indirect NTP treatment, previously optimized in our lab for different cell lines, to further evaluate the relative contribution of apoptosis, necroptosis, ferroptosis, and pyroptosis RCD mechanisms as their mode of action. We used cell death inhibitors to disrupt different RCD pathways following both direct and indirect NTP treatment and evaluated their ability to rescue cell viability. Key RCD hallmarks were also evaluated to validate pathway-specific activation of apoptosis, pyroptosis, necroptosis, and ferroptosis. While indirect NTP treatment mainly induces apoptosis and ferroptosis as RCD mechanisms, direct NTP treatment leads to the additional activation of the pyroptotic pathway, whereas necroptosis is induced in a cell line-dependent manner for both treatment modalities. The results obtained from this study not only fill major gaps in knowledge and provide valuable insights into the NTP-induced activation of RCD pathways, which holds promise for novel NTP based combination cancer therapies in the future. To our knowledge, this is the first comprehensive study investigating NTP specific targeting of the broad spectrum of RCD pathways. Moreover,

the biochemical approach used here to compare the two main administration modalities of NTP has not previously been carried out and provides a functional method to delineate them.

4.2 Materials and Methods

Cell culture and NTP treatment

For this study, two human melanoma cell lines were used: A375 (ATCC, CRL-1619TM) and SK-MEL-28 (ATCC, HTB-72). Both cell lines were cultured in Dulbecco's Modified Eagle Medium (DMEM) (Gibco™, Life Technologies, 10938-025) supplemented with 10% Fetal Bovine Serum (FBS) (Gibco™, Life Technologies, 10270-106), 100 units/mL penicillin/streptomycin (Gibco™, Life Technologies, 15140-122) and 4 mM L-glutamine (Gibco™, Life Technologies, 25030-024). The cells were incubated at 37°C in a humidified atmosphere with 5% CO_2. For the direct NTP treatment, a microsecond-pulsed dielectric barrier discharge (DBD) plasma system (**Figure 1**, left) was used to generate NTP with a 30 kV pulse, 1-1.5 µs rise-time, and 2 µs pulse width. The cells were seeded in a 24-well plate, 24h prior to treatment, and the cell culture medium was removed from the well just before the treatment. The gap between the electrode and the cells was fixed at 1 mm distance using a z-positioner, following which NTP was discharged directly on the cells for 10 seconds at the defined frequency. Immediately following treatment, 500 µL of fresh cell culture medium was replenished in the well. Based on our previous reports, the energy per pulse for this DBD plasma system was measured to be 1.88 mJ/pulse at a 1 mm application distance[32]. By using a 50, 200, 500 Hz pulse frequency, the total plasma energy delivered for treatment 0.9, 3.8, 9.4 J, respectively .

For the indirect NTP treatment, the cells were seeded in a 96-well plate 24h prior to treatment. NTP-treated PBS, later referred to as plasma-

treated liquid (PTL), was generated using the kINPen IND-LAB plasma system (**Figure 1**, right) to treat 1 mL of phosphate-buffered saline (PBS) (Gibco™, Life Technologies, 14190-144) in a 12-well plate. A gap of 1 cm between the liquid and the tip of the plasma source was used and the gas flow rate was 2 standard liters per minute (slm). The PTL was then added to the cells in a 1:6 ratio for A375 and a 2:7 ratio for SK-MEL-28.

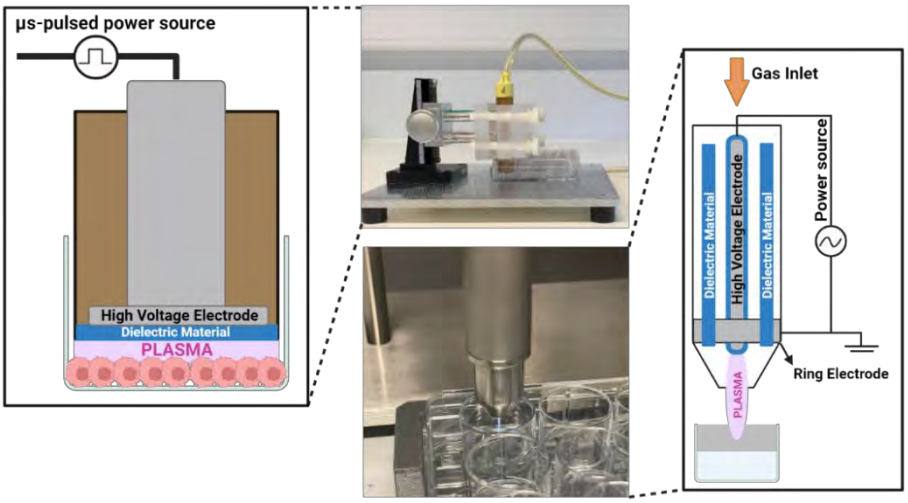

Figure 4.1 Presentation of the different plasma systems used for all the experiments. On the left, a schematic representation of the µs-pulsed DBD plasma system, which is used for direct NTP treatments. On the right, a schematic representation of the kINPen IND-LAB plasma system, which was used for the indirect NTP treatments

Mock treatments

In order to prepare the mock treatments, the concentration of long-lived RONS (H_2O_2, NO_2^-, and NO_3^-) was measured in PBS after exposure to NTP for 12 and 15 minutes, as was done for the indirect NTP treatment. For 12 minute exposure, the concentration of long-lived RONS was 1114 µM of H_2O_2, 58 µM of NO_2^-, and 51 µM of NO_3^-. For 15 minute exposure, the concentration of long-

lived RONS was 1318 μM of H_2O_2, 70 μM of NO_2^-, and 63 μM of NO_3^-. Therefore, mock solutions were made with commercial H_2O_2 (Sigma-Aldrich, H1009), sodium nitrite (Sigma-Aldrich, 237213), and potassium nitrate (Sigma-Aldrich, P8394) dissolved in PBS (without iron, calcium, and magnesium). Mock solutions made using long-lived RONS concentrations from 15 minute exposure were applied to A375 cells in a 1:6 ratio, while mock solutions made using long-lived RONS concentrations from 12 minute exposure were applied to SK-MEL-28 cells in a 2:7 ratio, as was done for the indirect treatment with PTL. We tested two mock solutions for each condition: 1) H_2O_2 only and 2) all the long-lived RONS (H_2O_2, NO_2^-, and NO_3^-).

Kinetic cell death assay

Prior to direct or indirect NTP treatment, the cell culture medium was replaced with medium containing 1 μM of SYTOX Green Nucleic Acid Reagent (Invitrogen, S7020) and 200 mM Hoechst 33342 (Thermo Fisher, 62249). Immediately following NTP treatment, the plate was placed into the Spark Cyto 600 (Tecan, Switzerland) live-cell imager. Fluorescence and brightfield images were captured every 2 hours for 24 hours and the total number of cells (blue object count) and the number of dead cells (green object count) was quantified. Cell death was calculated by:

$$\%\ Cell\ death = 100 - \left(\frac{Blue\ object\ count - Green\ object\ count}{mean(Blue\ object\ count_{untreated})} * 100\right)$$

The mean blue object count of the untreated cells (*Blue object count*$_{untreated}$) was used to normalize the value for cell growth.

Cell death inhibitor assay

To determine which cell death pathways are activated, inhibitors were used to block specific cell death pathways. The cells were seeded in triplicate and incubated for 20 hours at 37°C. After incubation, the cell culture medium was removed and replaced with fresh medium containing 1 µM of SYTOX Green Nucleic Acid Reagent (Invitrogen, S7020) and 200 mM Hoechst 33342 (Thermo Fisher, 62249). Next, the specific cell death inhibitors were added to the wells. To inhibit apoptosis, 10 µM of z-Vad-FMK (Bachem AG, 780051) was used, for pyroptosis 10 µM of Ac-FLTD-CMK (SelleckChem, S9817), for necroptosis 10 µM of Necrostatin-S1 (Nec1s) (Cell Signaling Technology, 17802), and for ferroptosis 1 µM of Ferrostatin-1 (Fer1) (Sigma-Aldrich, SML0583) or 100 µM of Deferoxamine (DFO) (Sigma-Aldrich, D9533). The cells were then incubated for 4 hours at 37°C, after which the cells were treated with either direct or indirect NTP. Fluorescence images were then captured, measured, and analyzed 24 h post NTP treatment using the Spark Cyto 600 (Tecan, Switzerland). To determine the amount of cell death, the following equation was used:

$$\%\ Cell\ viability = \frac{Blue\ object\ count - Green\ object\ count}{mean(Blue\ object\ count_{untreated})} * 100$$

The blue object count corresponds to the total number of cells in the well and the green object count corresponds to the total number of dead cells in the well. This value was again divided by the mean blue object count of the untreated cells (*Blue object count*$_{untreated}$) to normalize for cell growth. The contribution of each RCD pathway following NTP exposure was estimated based on the amount of cell viability recovery with each cell death inhibitor. The difference of NTP-induced cell death, with and without the inhibitors, was then normalized to the amount of NTP-induced cell death without inhibitors to give a relative contribution.

The sum of the measured RCD contribution was calculated based on the four inhibitors, and the remainder was categorized as “other”.

Caspase-3/7 assay

To look further into apoptosis, caspase-3/7 activity was measured using the Incucyte Caspase-3/7 Green Dye for Apoptosis (Sartorius, 4440). The cells were treated with either direct or indirect NTP and incubated at 37°C. After 22 hours, the cell culture medium was removed and replaced with fresh medium containing 200 mM Hoechst 33342 and 5 µM Incucyte Caspase-3/7 Green reagent. After 2 hours of incubation at 37°C, fluorescence images were captured, measured, and analyzed using the Spark Cyto 600 (Tecan, Switzerland). To determine the percentage of caspase-3/7 positive cells, the green object count, corresponding to the caspase-3/7 positive cells was divided by the blue object count, corresponding to the total number of cells in the well.

Annexin V assay

In addition to the caspase-3/7 positivity, annexin V positivity was also measured. The Incucyte® Annexin V Dye for Apoptosis (Sartorius, 4641) was used, together with the Incucyte Cytolight Rapid Green Dye (Sartorius, 4705). The cells were seeded and incubated for 24 h at 37°C after which the Incucyte Cytolight Rapid Green Dye was added (1:20 000 dilution) to each well and incubated for 20 minutes at 37°C. After incubation, the cell culture medium containing the dye was removed and the cells were washed twice with PBS before adding fresh cell culture medium containing the Incucyte Annexin V Dye for Apoptosis (1:200 dilution). Next, the cells were treated with either direct or indirect NTP and incubated for 24 hours at 37°C, after which they were imaged using the Incucyte® ZOOM live-cell imager (Sartorius, Germany). Analysis was performed on the Incucyte software (v2018A) with the removal of 6-8%

of the red signal contributing to the green signal as recommended by the product guide of the Incucyte Annexin V Dye. Annexin V positivity was calculated by dividing the total red object count, corresponding to the annexin V positive cells, by the total green object count, corresponding to the total number of cells.

Caspase 1 assay

To investigate the pyroptotic pathway, caspase-1 activity was measured using the Caspase-Glo 1 Inflammasome Assay (Promega, G9951) according to the manufacturer's instructions. The cells were seeded, NTP treated and incubated at 37°C for 24 h before starting the assay. Each condition was seeded in double triplicates as instructed by the assay manual. As a first step of the assay, the cells were trypsinized and transferred to a white 96-well plate in 100 µL fresh cell culture medium. For direct NTP treatment, the cells were originally seeded in a 24-well plate and were therefore diluted 1:4 when transferred to the white 96-well plate. Secondly, 100 µL of Caspase-Glo 1 reagent was added to half of the samples and 100 µL Caspase-Glo 1 YVAD-CHO reagent was added to the duplicates. The samples were then mixed using a plate shaker for 30 seconds at 500 rpm and incubated for 1 h to allow the luminescent signal to stabilize. Finally, the luminescent signal was read using the Spark Cyto 600 (Tecan, Switzerland) and normalized to the untreated sample to represent the increase in caspase-1 activity.

AlphaLISA

Phosphorylation of MLKL was investigated using the Phospho-MLKL (Ser358) AlphaLISA SureFire Ultra Detection kit (PerkinElmer, ALSU-PMLKL-B500), according to the manufacturer's instructions. Briefly, to prepare the samples, the cells were lysed using the provided lysis buffer and transferred to a 384-well plate. Next, the acceptor mix was added to

all wells and incubated for 1 hour at room temperature. After incubation, the donor mix was added to all wells and incubated in the dark for 2 hours. To analyze the plate, the Spark Cyto 600 (Tecan, Switzerland) was used with standard AlphaLISA settings. The results obtained from the scan were standardized to the total cell count per sample, which was measured prior to lysing of the cells.

Lipid Peroxidation assay

Oxidation of cellular lipids was measured using the Image-iT™ Lipid Peroxidation Kit (Invitrogen, C10445), according to the manufacturer's instructions. In short, the cells were treated with either direct or indirect NTP and incubated for 24 hours. The cells used for the positive controls were incubated with 100 µM cumene hydroperoxide for 1h30. After incubation, the C11-BODIPY dye was added to the wells with a final concentration of 10 µM and incubated for 30 minutes at 37 °C. The cells were washed twice with PBS and once with FACS buffer before flow cytometry was performed with the CytoFLEX (BD). The ratios of the red over green mean fluorescence intensity signals were calculated using the FlowJo v10.8.1 software.

Western blotting

The expression of GPX4 and MLKL was evaluated using western blotting. In short, the cells were treated with either direct or indirect NTP and incubated for 24h at 37°C. After incubation, the cells were washed with cold PBS and lysed using a non-reducing lysis buffer containing Pierce Protease and Phosphatase Inhibitor Mini Tablets (Thermo Fisher, 15662249). The lysates were kept on ice and sonicated twice for 5 seconds. Protein concentration was determined using the Pierce BCA Protein Assay Kit (Thermo Fisher, 23227), according to the manufacturer's instructions. Extracted proteins were then separated,

according to molecular weight, using sodium dodecyl sulphate polyacrylamide gel electrophoresis (SDS-PAGE) gels, followed by electrotransfer to nitrocellulose membranes (Amersham Hybond-ECL, GE Healthcare, USA). Equal amounts of protein and volume were loaded onto a 12.5% polyacrylamide gel. Membranes were blocked in TBS-T (Tris-buffered saline; 0.1% Tween-20), containing 5% non-fat dry milk, for 1 h at room temperature. After blocking, membranes were incubated overnight at 4 °C with the primary antibodies (GPX4, Cell signaling, 52455, 1:1000, anti-β-Actin (ACTB), Santa Cruz, sc-47778, MLKL, Cell signaling, 14993S, 1:1000). The following day, membranes were washed with TBST-T and incubated for 1 h with a horseradish-conjugated secondary antibody (anti-rabbit IgG HRP, Sigma, GENA934-1ML, 1:2000). The signal was revealed using ECL Prime (Amersham, GERPN2232) on an Amersham Imager 680 (GE Life Sciences) and exported and quantified using the Image Studio™ program (LI-COR Biosciences).

Statistics

All statistical differences were analyzed using the linear mixed model with JMP Pro 13 (SAS software). When a significant difference was detected, the post hoc Dunnett's test was performed to calculate the adjusted p value compared to one group (the control or NTP-treated) or a Tukey's honestly significant difference test was performed to compare all conditions to each other. A p value ≤0.05 was considered statistically significant. Data in all graphs are represented as mean ± standard error of the mean (SEM), the number of replicates is indicated in the figure caption, and all figures were prepared in GraphPad Prism (GraphPad Prism 7, GraphPad Prism Software, Inc.).

4.3 Results

4.3.1 Comparison of direct and indirect NTP treatment

In order to determine which RCD pathways were activated in melanoma cells after NTP treatment, different NTP treatment doses were tested on the A375 and SK-MEL-28 human cell lines to define the best treatment conditions for both direct and indirect NTP treatment, based on previously optimized conditions for ICD-induction. For direct NTP treatment, the dose was determined with a range of pulse frequencies, from 50 Hz to 500 Hz (Figure 4.2a), corresponding with a 0.9 to 9.4 J NTP treatment energy. For the indirect treatment with PTL, the dose was determined with a range of treatment duration of PBS, from 7 to 15 minutes, before being added to the cells (Figure 4.2b). PTL was added to cell cultures in a 1:6 ratio for A375 and a 2:7 ratio for SK-MEL-28 based on their different NTP sensitivities, with the SK-MEL-28 showing greater resistance (Appendix 3, Figure A3.1). Untreated PBS was added to the cells at the same PTL ratio, which represented a vehicle control. Cell death was evaluated immediately after treatment, every 2 hours for 24 hours, via quantification of the total amount of live and dead cells, using the Tecan SparkCyto live-cell imager.

A dose-dependent cell death response was observed for both direct and indirect treatment. Here, the higher treatment-resistance of the SK-MEL-28 cells compared to the A375 cells, can be observed in both direct and indirect NTP treatment. For direct treatment, lower NTP doses (50 and 200 Hz) resulted in more A375 cell death (Figure 4.2c) compared to SK-MEL-28 cell death (Figure 4.2d). For indirect treatment, a lower PTL ratio was needed to achieve equivalent A375 (Figure 4.2e) and SK-MEL-28 (Figure 4.2f) cell death. However, direct NTP treatment of both cell line at 500 Hz induced 88.2 $\pm$ 2.1 % and 89.0 $\pm$ 3.5 % cell death for the A375 (Figure 4.2c) and SK-MEL-28 (Figure 4.2d) cells, respectively, at 24

hours. For indirect NTP treatment, the 15-minute treatment induced 80.5 ± 3.2 % cell death for the A375 cells (Figure 4.2e) and nearly 100% cell death for the SK-MEL-28 cells (Figure 4.2f). On the other hand, 12-minute treatment induced 81.5 ± 6.0 % cell death for the SK-MEL-28. Therefore, to further evaluate the different cell death mechanisms of the NTP treatment modalities, these treatment parameters were selected for all subsequent experiments, based on their capacity to induce similar levels of cell death while allowing for down-stream RCD analysis.

The most relevant RCD pathways in the context of cancer and NTP treatment are apoptosis, pyroptosis, necroptosis, and ferroptosis. To provide an initial overview of which of these pathways were activated after direct and indirect NTP treatment, specific inhibitors were used for each pathway: Z-VAD-FMK (apoptosis), Ac-FLTD-CMK (pyroptosis), Nec-1s (necroptosis), and Fer-1 and DFO (ferroptosis). Cell death was measured 24 hours post NTP treatment with live-cell imaging, using a live-death cell stain, and cell viability was calculated.

Following direct NTP treatment, four of the five RCD inhibitors significantly rescued cell viability, suggesting the activation of apoptosis, pyroptosis, and ferroptosis (Figure 4.2g). While NTP treatment alone resulted in 8.7 ± 1.1% and 14.7 ± 1.3 % cell viability for A375 and SK-MEL-28, respectively (Figure 4.2g), inhibition of apoptosis with Z-VAD-FMK increased cell viability for both melanoma cell lines (A375: 14.4 ± 1.0 %, $p=0.0318$; SK-MEL-28: 52.0 ± 3.1 %, $p=0.0012$). The addition of the pyroptosis inhibitor, AC-FLTD-CMK, also significantly increased cell viability after direct NTP treatment, for both A375 (30.5 ± 3.2%, $p\leq0.0001$) and SK-MEL-28 (37.2 ± 1.1%, $p\leq0.0001$) cells, while the necroptosis inhibitor, Nec-1s, did not improve cell viability after treatment. Inhibition of ferroptosis with Fer1 and DFO also led to increased cell viability after treatment for both A375 (14.9 ± 0.8%,

p=0.0188 & 17.0 ± 1.2%, *p=0.0009*, respectively) and SK-MEL-28 (24.7 ± 1.7 %, *p≤0.0001* & 25.3 ± 2.0%, *p≤0.0001*, respectively).

The indirect NTP treatment efficacy, on the other hand, was only modulated by one RCD inhibitor for both cell lines (Figure 4.2h). Without inhibitors, indirect NTP treatment with PTL resulted in 24.7 ± 1.6% cell viability for A375 and 36.2 ± 2.6% cell viability for SK-MEL-28. The addition of Z-VAD-FMK, AC-FLTD-CMK, Nec-1s, and Fer1 did not significantly rescue cell viability after indirect NTP treatment for both cell lines, and AC-FLTD-CMK even appeared to decrease cell viability for SK-MEL-28 cells (23.1 ± 1.9%, *p=0.0038*). DFO clearly improved cell viability significantly for both A375 (74.6 ± 1.8%, *p≤0.0001*) and SK-MEL-28 (73.9 ± 3.5%, *p≤0.0001*) cells after indirect NTP treatment. Since Fer1 and DFO inhibit different stages of the ferroptosis pathway, it appeared that ferroptosis via iron accumulation was a major contributor to indirect NTP-induced RCD.

In order to compare the contribution of different RCD pathways to NTP-induced cell death for the direct and indirect treatment modalities, cell viability following treatment with different inhibitors was normalized to that of NTP treatment without inhibitors (Figure 4.2i). While most inhibitors appeared to recover higher degrees of normalized cell viability following direct NTP treatment compared to indirect treatment (though not statistically significant), AC-FLTD-CMK significantly recovered cell viability for both cell lines (*p≤0.0001*) following direct treatment compared to the indirect modality (Figure 4.2i). This suggests that at equivalent levels of cell death, the induction of pyroptosis could be unique to the direct NTP treatment modality and not the indirect NTP treatment, though more specific and in-depth evaluation is required.

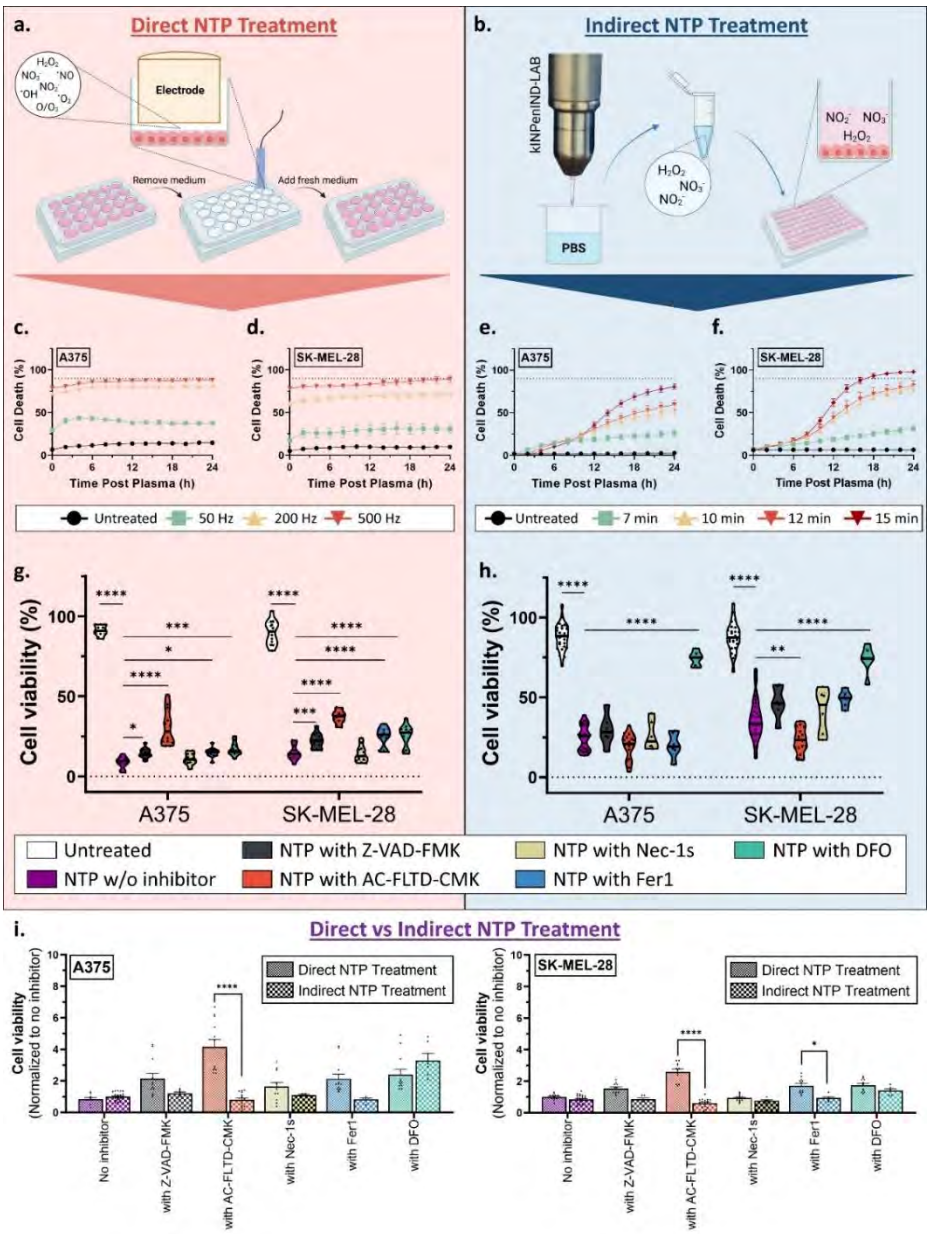

Figure 4.2 Comparing direct and indirect NTP treatment on melanoma cell death pathways. A schematic representation of the **a** direct NTP treatment method and the **b** indirect NTP treatment method is provided. **c** A375 and **d** SK-MEL-28 cells were treated with direct NTP at different frequencies and cell death was monitored continuously, every 2 hours, for 24 hours. PBS was treated with NTP for various durations (7 to 15 minutes), then applied to **e** A375 and **f** SK-MEL-28 cells for indirect NTP treatment, and cell death was also assessed. These data are represented as mean ± SEM (n=3-12). A dashed-line is placed at 90% cell death. To further investigate the RCD pathways induced

by the different modalities of NTP, inhibitors of specific pathways were used. Z-VAD-FMK, AC-FLTD-CMK, necrostatin-1 s (Nec-1s), and ferrostatin-1 (Fer-1) and deferoxamine (DFO) were used to inhibit NTP-induced apoptosis, pyroptosis, necroptosis, and ferroptosis, respectively. Cell viability for A375 and SK-MEL-28 after **g** direct and **h** indirect NTP treatment was then measured. Data are presented as mean ± SEM of at least 3 independent experiments, and each biological sample is shown (n=6-12). Statistical significance was calculated using the generalized linear mixed model. * $p \leq 0.05$, ** $p \leq 0.01$, *** $p \leq 0.001$, **** $p \leq 0.0001$

It is well known that direct NTP treatment exposes the biological target to both short-lived (e.g. •OH, O, •NO) and long-lived (e.g. H_2O_2, NO_2^-, NO_3^-) RONS, while indirect NTP treatment can only deliver the long-lived RONS. Due to the sub-second lifetimes of short-lived RONS and the time between enriching the liquid with NTP and delivery to the target, the only stable RONS delivered by indirect NTP treatment are H_2O_2, NO_2^-, and NO_3^-[33].

In the past, we have demonstrated that the efficacy of direct NTP treatment with the DBD system is not due to the long-lived RONS, but rather the short-lived RONS, which are generated in direct contact with the target tissue[17,34]. However, several reports have shown that long-lived RONS are the main effectors of cell death for indirect NTP[35,36]. Therefore, the significance of indirect NTP treatment over 'mock solutions' made from commercially available long-lived RONS, has been a major topic of debate [33], though the RCD mechanisms of both have not been compared. Here, we also compared the efficacy of indirect NTP treatment with that of mock solutions made up of the same concentration of H_2O_2, NO_2^-, and NO_3^-, as well as the RCD pathways involved.

The concentrations of H_2O_2 was measured to be 1114 µM in PBS after 12 minutes of treatment with NTP and 1318 µM after 15 minutes of treatment. NO_2^- was measured to be 58 µM and 70 µM after 12 and 15 minute treatments, respectively, while NO_3^- was measured to be 51 µM and 63 µM, respectively. A solution of only H_2O_2 and a solution of all

three long-lived RONS (i.e. H_2O_2, NO_2^-, NO_3^-) was made in PBS as mock treatments of indirect NTP. It was very clear that when the H_2O_2 concentrations were the same as that of the PTL used for indirect NTP treatment, equivalent levels of cell death were reached in 24 hours for both cell lines (Figure 4.3a, b). Furthermore, NO_2^- and NO_3^- appeared to have negligible contribution. Therefore, while long-lived RONS cannot account for the efficacy of direct NTP treatment[17], the overall mechanism of PTL, and thus of indirect NTP treatment, does not appear to be more than H_2O_2. Moreover, when comparing the RCD pathways, only DFO significantly recovered cell viability from mock treatment with all the long-lived RONS, which was also significantly greater than that of indirect treatment (Figure 4.3c, d).

The recovery of cell viability with each inhibitor was also used to calculate and compare the contribution of each RCD pathway for treatment-induced cell death. Based on our findings here, indirect NTP treatment with PTL appeared to trigger cell death that closely resembles mock treatment with long-lived RONS of the same concentration (H_2O_2, NO_2^-, and NO_3^- at equivalent concentrations) and was dominated by ferroptosis (Figure 4.3e). In both mock treatments and indirect NTP treatment, ferroptosis appeared to be the dominant cell death modus, as inhibition with DFO recovered the cell viability the most. On the other hand, direct NTP treatment appeared to significantly induce more RCD pathways, and while pyroptosis appeared to dominate (24% for A375 and 26% for SK-MEL-28), the overall RCD distribution was more balanced (Figure 4.3e).

Since cancer cells are prone to adaptation with extensive crosstalk between the RCD pathways, inhibition of one pathway may result in a switch towards another. Therefore, more RCD-specific assays were

used to further delineate the difference between direct and indirect NTP treatment modalities.

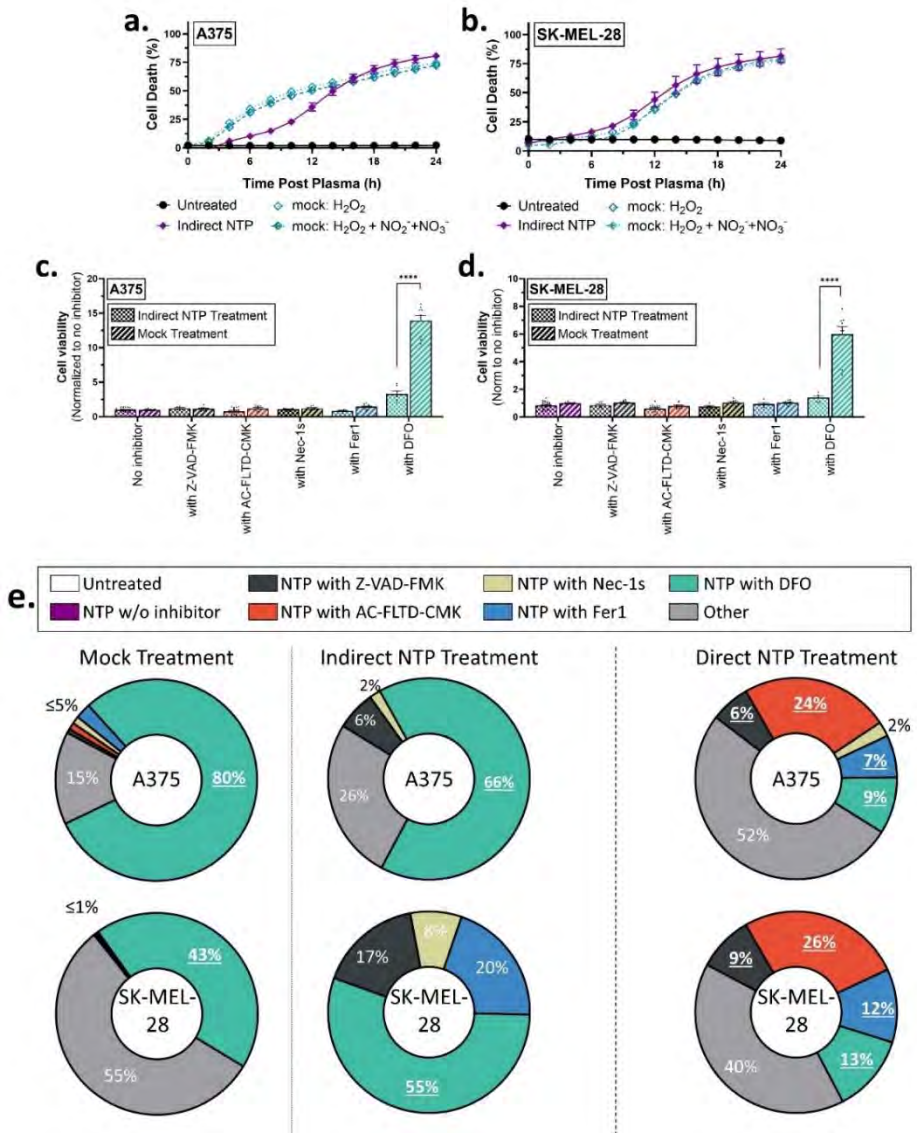

Figure 4.3 Comparing mock treatment with indirect NTP treatment. Mock solutions of H_2O_2 and H_2O_2, NO_2^-, and NO_3^- at equivalent PTL concentrations were made and used to treat both the A375 and SK-MEL-28 cell lines. Cell death was measured every 2 hours post treatment with live-cell imaging and showed that H_2O_2 elicited equivalent levels of cell death at 24 hours, while NO_2^-, and NO_3^- had negligible contributions for both **a** A375 and **b** SK-MEL-28 cells. Similar to indirect NTP treatment, DFO was the only inhibitor able to recover cell viability from mock treatment with all three long-lived RONS (H_2O_2, NO_2^-, and NO_3^-), though the recovery was significantly higher for both **c** A375 and **d**

SK-MEL-28 cells. Data are presented as mean ± SEM of at least 3 independent experiments (n=6-20), and each biological sample is shown for **c**, **d**. Statistical significance was calculated using the generalized linear mixed model. **** $p \leq 0.0001$. **e** Contribution of each RCD pathway to the total amount of cell death for both cell lines was also calculated, based on the increase in cell viability in comparison to NTP treatment without inhibitors. While mock treatment and indirect NTP treatment appeared to induce predominately ferroptosis, as depicted by the significant inhibition by DFO, direct NTP treatment appeared to induce more diverse RCD pathways, with pyroptosis dominating. Percentage values in bold and underlined depict statistical significance (* $p \leq 0.05$) as calculated using the generalized linear mixed model

4.3.2 Apoptosis

To further investigate whether NTP induced apoptosis, the activation of caspase 3/7 was examined. Caspase 3 and 7 are effector caspases that execute apoptosis through the cleavage of multiple structural and regulatory proteins, which are critical for cell survival and maintenance[37]. The melanoma cells were stained with the Incucyte Caspase 3/7 Green Dye and Hoechst 33342, after which they were treated with either direct or indirect NTP treatment; staurosporine was used as a positive control. An increase in caspase 3/7 positivity was observed in both melanoma cell lines for direct NTP treatment (69.2 ± 11.1 % for A375, *p≤0.0001* and 72.3 ± 12.0 % for SK-MEL-28, *p≤0.0001*) and indirect NTP treatment (38.3 ± 1.4 % for A375, *p≤0.0001* and 31.5 ± 8.2 % for SK-MEL-28, *p≤0.0001*)(Figure 4.4a), further evidencing that the apoptotic pathway was activated.

Another hallmark of apoptosis is the loss of plasma membrane symmetry, which was assessed using the annexin V assay. Annexin V binds specifically to phosphatidylserine (PS) residues on the outer plasma membrane as a result of the loss of plasma membrane asymmetry[38]. The percentage of annexin V positive cells was normalized to the positive control with staurosporine. Similarly to the caspase 3/7 results, annexin V positivity increased for both the direct and indirect NTP treatment with a larger increase for the direct NTP treatment (91.1

± 9.7 % for A375, *p≤0.0001* and 89.8 ± 6.9 % for SK-MEL-28, *p≤0.0001*) compared to the indirect NTP treatment (56.0 ± 8.4 % for A375, *p≤0.0001* and 53.6 ± 2.7 % for SK-MEL-28, *p≤0.0001*) (Figure 4.4b). It is important to note that the annexin V assay cannot differentiate between apoptosis and pyroptosis, since the latter also leads to the presentation of PS residues on the outer cell membrane[39].

Taken together, these results further evidence the previous findings that direct NTP treatment activates the apoptotic pathway, while also indicating that the indirect NTP treatment does as well.

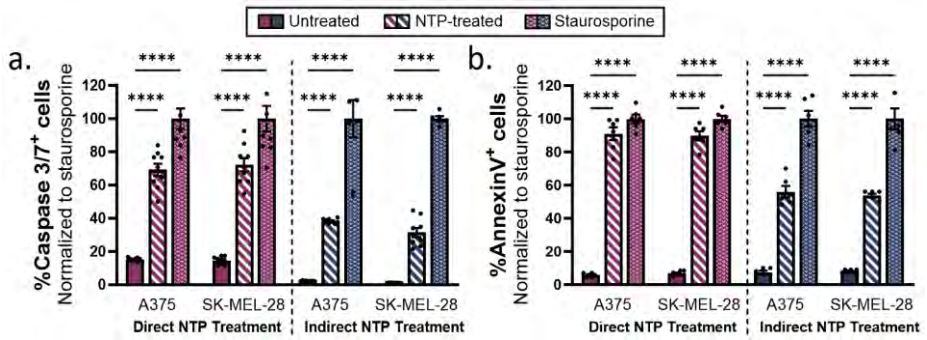

Figure 4.4 Evaluating apoptosis following direct and indirect NTP treatment. **a** Percentage of caspase 3/7 positive cells. **b** Percentage of annexin V positive cells was increased for both direct and indirect NTP treatment. Staurosporine was used as positive control. Data are presented as mean SEM of at least 3 independent experiments (n=6-12), and each biological sample is shown. Statistical significance was calculated using the generalized linear mixed model. **** p ≤ 0.0001

4.3.3 Other caspase-dependent RCD pathways: pyroptosis and necroptosis

Aside from apoptosis, pyroptosis and necroptosis are two additional caspase-dependent RCD mechanisms. Pyroptosis is an inflammatory type of cell death, with a high resemblance to apoptosis, though in contrast to apoptosis, pyroptosis is triggered by the activation of caspase 1, leading to the cleavage of gasdermin D (GSDMD)[40,41]. To verify the observations from the inhibitor experiments, the activation of caspase 1 was assessed 24h after NTP treatment using the Caspase-

Glo 1 inflammasome assay. The results show a significant increase in activated caspase 1 for direct NTP treatment for both A375 (1.3 ± 0.2-fold change, *p=0.0139*) and SK-MEL-28 (1.5 ± 0.2-fold change, *p=0.0018*) melanoma cells (Figure 4.5a). Indirect NTP treatment only induces a slight increase in caspase 1 activity for the A375 cell line (1.2 ± 0.1-fold change, *p=0.0134*), whereas no significant increase is found for SK-MEL-28 cells (1.0 ± 0.1-fold change, *p=0.8368*). Taken together, these results support the findings of the inhibitor experiments (Figure 4.2i), which indicate that direct NTP treatment induces pyroptotic cell death, while indirect NTP treatment does not.

Necroptosis is another non-apoptotic, caspase-dependent type of RCD and often serves as an alternative for apoptosis when caspase-8 is inhibited[37,41,42]. This is mainly mediated by receptor-interacting protein kinase 1 and 3 (RIPK1 and RIPK3) and executed by the phosphorylation of mixed lineage kinase domain-like pseudokinase (MLKL), which is one of the final and critical steps in the necroptotic pathway[37,42,43]. Following both direct and indirect NTP treatment phosphorylation of MLKL significantly increased for the A375 cell line: 1.6 ± 0.2-fold change, *p=0.0258*; and 1.6 ± 0.1-fold change, *p=0.0498*, respectively (Figure 4.5b). However, the SK-MEL-28 cells does not exhibit increased phosphorylation after treatment with both NTP modalities. This difference can be attributed to the considerably lower baseline expression of MLKL in SK-MEL-28 cells compared to the A375 cell line (See Appendix 3, Figure A4.2). These results suggest that both direct and indirect NTP treatment can trigger necroptosis in a cell-dependent manner, given the presence of MLKL in the cells.

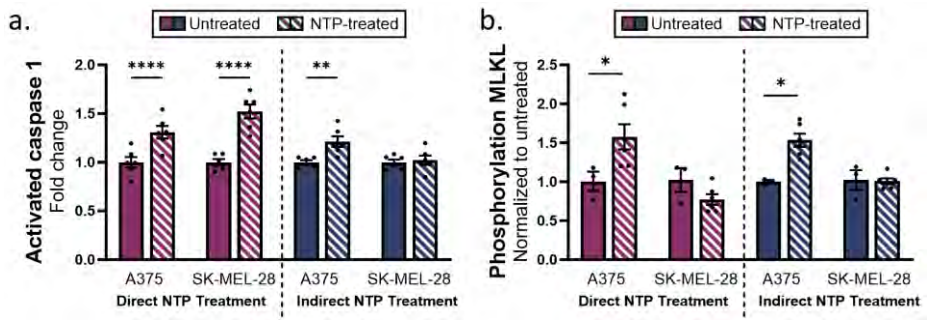

Figure 4.5 Evaluating other caspase-dependent RCD pathways, pyroptosis and necroptosis, following direct and indirect NTP treatment. **a** Caspase 1 activity increased in both melanoma cell lines following direct NTP treatment and only in the A375 melanoma cell line following indirect NTP treatment. **b** Only A375 cells demonstrated significant phosphorylation of MLKL after direct and indirect NTP treatment. Data are presented as mean ± SEM of at least 3 independent experiments (n=4-6), and each biological sample is shown. Statistical significance was calculated using the generalized linear mixed model. * $p \leq 0.05$, ** $p \leq 0.01$, **** $p \leq 0.0001$

4.3.4 Ferroptosis

In contrast to the previously discussed RCD pathways, ferroptosis is an iron-dependent type of cell death, driven by lipid peroxidation, and independent of caspase activity. Although it was only discovered in 2012, this type of cell death has attracted significant attention in cancer research as reports suggest that cancer cells resistant to conventional therapies may be more vulnerable to ferroptosis[44–46].

To assess the activation of the ferroptotic pathway, two key factors were examined, the expression of GPX4 and lipid peroxidation. GPX4 is considered a key player in the ferroptotic pathway, since it is the only GPX that can reduce toxic phospholipid hydroperoxides to non-toxic phospholipids. Therefore, depletion or inactivation of GPX4 results in greater ferroptosis. GPX4 expression following NTP treatment was assessed using western blotting analysis (Figure 4.6a, b). Direct NTP treatment slightly reduced the expression of GPX4 in SK-MEL-28 (0.81 ± 0.06-fold change, *p=0.0483*), whereas no significant change was observed in the A375 cell line (Figure 4.6c). The indirect NTP treatment

did not have an effect on the expression of GPX4 in either of the melanoma cell lines.

We also checked for lipid peroxidation, which mainly affects polyunsaturated fatty acids (PUFAs) and leads to the destruction of lipid bilayers. The melanoma cells were stained 24 h after NTP treatment with the C11-BODIPY dye, a sensitive fluorescent reporter for lipid peroxidation which shifts from red to green fluorescence upon oxidation. Cumene, a ferroptosis inducer, was used as a positive control. For both treatment methods, a decrease in red/green ratio was measured, which indicates an increase in lipid peroxidation (Figure 4.6d). Interestingly, the A375 cell line seems to be more prone to lipid peroxidation in comparison with the SK-MEL-28 cell line (0.66 ± 0.02-fold change, $p \leq 0.0001$; vs 0.83 ± 0.07-fold change, $p=0.0498$ for direct NTP treatment; and 0.39 ± 0.08-fold change, $p \leq 0.0001$; vs 0.79 ± 0.07-fold change, $p=0.0012$ for indirect NTP treatment).

Collectively, even though the expression of GPX4 was barely affected by either direct or indirect NTP treatment, a clear increase in lipid peroxidation was observed. Since lipid peroxidation is the key final step in the ferroptotic pathway, we can conclude that ferroptosis is initiated after NTP treatment.

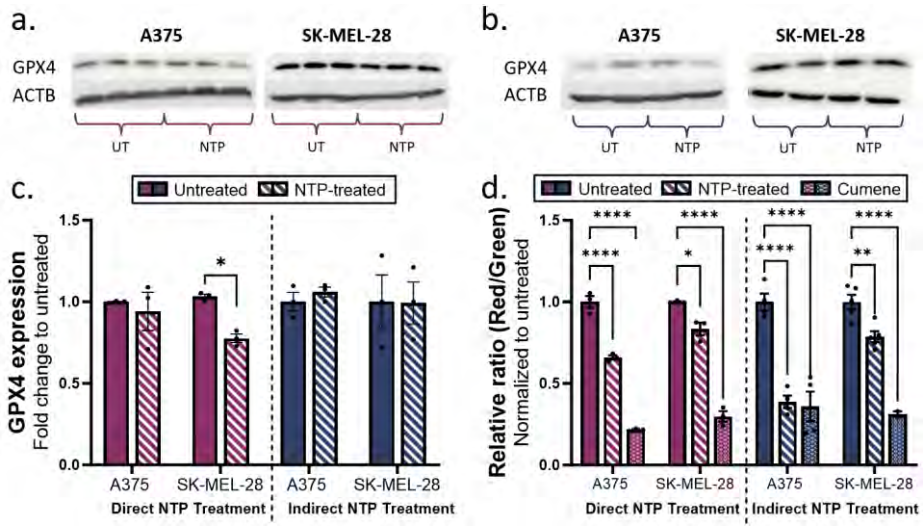

Figure 4.6 Evaluating ferroptosis following direct and indirect NTP treatment. Western blots showing the GPX4 expression in A375 and SK-MEL for **a** direct NTP treatment and **b** indirect NTP treatment. **c** Analysis of the western blotting results for both cell lines following direct and indirect NTP treatment did not show significant changes in GPX4 expression apart from a decrease in SK-MEL-28 cells following direct NTP treatment. **d** Lipid peroxidation analysis of both cell lines, represented as relative ratio (Red/Green), was performed, where the lower the relative ratio, the more lipid peroxidation was observed. Data are presented as mean ± SEM of at least 2 independent experiments (n=2-6), and each biological sample is shown for **c**, **d**. Statistical significance was calculated using the generalized linear mixed model. * $p \leq 0.05$, ** $p \leq 0.01$, **** $p \leq 0.0001$

4.4 Discussion

Although extensive research has been performed, demonstrating the anti-cancer effects of NTP therapy, there is still a major gap in understanding the biochemical cell death mechanisms involved and resolving the ambiguity between the different NTP treatment modalities. Most reports mention apoptosis and necrosis as the major cell death pathways for NTP treatment, with a few studies starting to report on ICD and ferroptosis[18,27–31,47,48], but overall, the other RCD pathways have been largely overlooked. To our knowledge, no studies have investigated necroptosis after NTP and only one study mentioned pyroptosis, despite both being activated via detrimental oxidative stress[49]. In this study, we examined four major RCD pathways (apoptosis, pyroptosis, necroptosis, and ferroptosis) in melanoma cancer cells following NTP treatment, previously defined to induce ICD[12,17,18,50]. Due to the plethora of RONS interacting with the cells during NTP treatment, we hypothesized that multiple RCD pathways are activated following exposure to NTP. Furthermore, we compared the two major modalities of NTP treatment (direct versus indirect treatment) and elucidated distinct RCD responses of each, due to the variable RONS delivered with each treatment modality. Taken together, our study demonstrates that both direct and indirect NTP treatment activate multiple cell death pathways, with distinct variations between direct and indirect NTP treatment, since pyroptosis was exclusively induced by direct treatment (summarized in Figure 4.7 and Table 4.1).

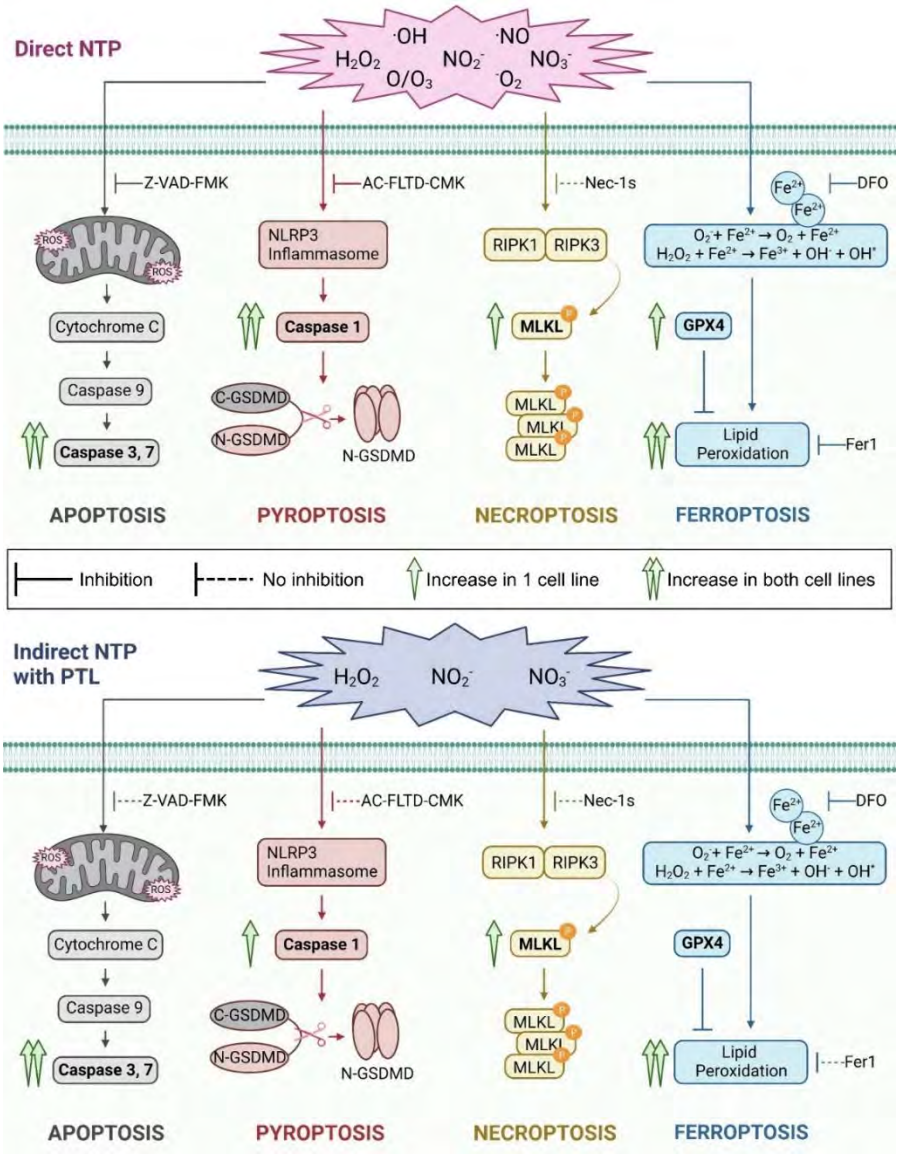

Figure 4.7 Overview of the key biomarkers for each RCD pathway, activated following NTP treatment. Caspase 3/7 expression, indicative for apoptosis, was increased after both direct and indirect NTP treatment. Caspase 1 expression, indicative for pyroptosis, was significantly upregulated after direct NTP treatment, whereas it was only minimally affected following indirect NTP treatment. MLKL phosphorylation was upregulated after both NTP treatment modalities, pointing towards necroptosis. GPX4 expression was slightly affected for direct treatment but not for indirect treatment. Nonetheless, lipid peroxidation was still significantly increased after both NTP treatment modalities, suggesting the occurrence of ferroptosis, and indicating that the basal GPX4 expression is not sufficient to counteract the increase in lipid peroxidation after NTP treatment

Apoptosis is historically the most well-studied RCD pathway, and our results are in-line with previous studies, which report apoptosis induction following NTP treatment with both modalities[23,51–54]. Interestingly, the direct NTP treatment elicited greater caspase 3/7 and annexin V expression compared to indirect treatment, which may stem from the slower response inherent of the indirect NTP treatment. Indeed, caspase 3/7 positivity, measured at 48 h post treatment, was higher compared to that after 24 h (See Appendix 3, Figure A4.3).

Table 4.2 Overview of all NTP-induced RCD responses examined in this study. For apoptosis we examined cell death inhibition with Z-VAD-FMK, together with a change in expression of caspase 3/7 and annexin V. For pyroptosis, we examined cell death inhibition with Ac-FLTD-CMK, together with the activation of caspase 1. For necroptosis, we examined cell death inhibition with Nec-1s, together with the phosphorylation of MLKL. For ferroptosis, we examined cell death inhibition with Fer1 and DFO, together with the expression of GPX4 and an increase in lipid peroxidation

Cell Death	Analysis	Direct NTP Treatment	Indirect NTP Treatment
Apoptosis	Z-VAD-FMK	**	-
	Caspase 3/7	**	**
	Annexin V	**	**
Pyroptosis	Ac-FLTD-CMK	**	-
	Caspase 1	**	*
Necroptosis	Nec-1s	-	-
	Phosphorylated MLKL	*	*
Ferroptosis	Fer-1	**	-
	DFO	**	**
	GPX4	*	-
	Lipid peroxidation	**	**

** indicates this assay showed an effect in both cell lines, * indicates this assay showed an effect in only one cell line, - indicates this assay did not show an affect in either cell line.

In addition to apoptosis, pyroptosis and necroptosis are caspase-dependent RCD pathways of interest in cancer biology. Whereas apoptosis is largely regarded as a silent process that attenuates subsequent immune responses, pyroptosis and necroptosis are reported to trigger the release of alarmins and other proinflammatory signals into the cellular environment to alert and stimulate an immune response[41]. Pyroptosis, as an inflammatory type of RCD, shares several similar features with apoptosis, such as DNA damage and chromatin condensation, but differs in eliciting pore formation and osmotic lysis[40,55]. Pyroptosis is dependent on the activation of caspase-1, which mediates cleavage of GSDMD, which consists of an N-terminal pore-forming domain and a C-terminal regulatory domain[40]. Once GSDMD is cleaved, the N-terminal domain translocates into the plasma membrane, where it forms pores, which facilitate the secretion of pro-inflammatory content (e.g. IL-1β and IL-18) and cause cell lysis[40]. Our findings indicate that activation of the pyroptotic pathway occurs following direct NTP treatment, as evidenced by the substantial increase in caspase 1 activity (Figure 4.5a), and supported by the significant reduction in cell death upon addition of a caspase 1/4/5 inhibitor (Figure 4.2g). Since pyroptosis was not as prevalent following indirect NTP treatment, the short-lived RONS may be critical for triggering the activation of the pyroptotic pathway, as they are only present in the direct treatment [56]. In the case of indirect NTP treatment, the interaction between the cells and RONS is limited to the long-lived and stable species (i.e. H_2O_2, NO_2^-, NO_3^-), which could lead to a milder inflammatory response. Furthermore, it has been shown that the effect of pyroptosis can vary in different tissues and depends on the genetic background, which might explain the different response in the two cell lines after indirect NTP treatment[40]. The additional induction of pyroptosis can provide an advantage for direct

NTP treatment over indirect NTP treatment, as it can enhance the efficacy of NTP against cancer and overcome certain therapy-resistant pathways.

In contrast to apoptosis and pyroptosis, it is the inhibition of caspase-8 which triggers necroptosis, rather than the activation of caspases[41,57]. Caspase-8, an initiator caspase of apoptosis, inhibits necroptosis through the cleavage of RIPK1, and when caspase-8 is depleted, RIPK1 promotes necroptosis by interacting with RIPK3 to form the necrosome[41,57]. This is necessary to mediate the phosphorylation of MLKL, which will thereafter lead to cell lysis. Despite the ineffectiveness of Nec-1s, a RIPK1 inhibitor, in recovering cell viability after NTP treatment, our further findings demonstrate an increase in MLKL phosphorylation for the A375 cell line, indicating a cell-dependent activation of the necroptotic pathway following both direct and indirect NTP treatment. Conversely, the SK-MEL-28 cell line exhibited no discernible increase in phosphorylation of MLKL, which can be explained by its comparatively lower basal expression of MLKL.

In contrast to the previous three cell death pathways, ferroptosis is not caspase-dependent but iron-dependent. Free intracellular iron can react with H_2O_2 through Fenton reactions, leading to peroxidation of polyunsaturated fatty acids in the cell membrane. These oxidized lipids would then generate more toxic free radicals, resulting in more oxidized lipids and oxidative damage[45]. Our results show limited modulation in GPX4 expression after direct NTP treatment and no change following indirect NTP treatment (Figure 4.6c). GPX4 is a phospholipid hydroperoxidase and is considered a master regulator of ferroptosis, as it converts lipid hydroperoxides into non-toxic lipid alcohols, thereby preventing ferroptosis[45]. Although GPX4 expression remained largely unaffected by NTP, we still observed a significant increase in lipid

peroxidation for the cell lines following both treatment modalities (Figure 4.6d). Whether NTP treatment may inhibit GPX4 enzymatic activity needs further verification counteract this peroxidation. Alternatively, both treatment modalities excess reactive RONS including hydrogen peroxide which can directly promote lipid peroxidation. Furthermore, it has been hypothesized that cells with a higher mesenchymal phenotype are more susceptible to ferroptosis[46]. Rossi *et al*, calculated the melanoma aggressiveness score (MAGS), which is based on proliferation, migration, and invasion, for A375 and SK-MEL-28, and they showed that the A375 cell line was more migratory and invasive compared to the SK-MEL-28 cell line. When examining our results, we observed that the SK-MEL-28 cell line had a higher basal expression of GPX4 (Figure 4.6a,b), which indeed indicates a greater resistance against ferroptosis. Furthermore, our results showed a larger increase in lipid peroxidation for the A375 cell line, confirming the higher sensitivity to ferroptosis. Our results therefore support the hypothesis that the mesenchymal state influences the susceptibility for ferroptosis.

Although these RCD pathways are the spearhead of many anti-cancer therapies, they often face a dual nature. For instance, despite the advantage of harnessing the cell's inherent apoptotic pathway to trigger cell death, cancer cells, and especially melanoma cells, often show overexpression of anti-apoptotic proteins, which increases the chance of developing resistance against this type of cell death[58,59]. Berthenet *et al* reported that when the apoptotic stimuli do not reach a lethal threshold in melanoma cells, these cells even become more proliferative and migratory[60]. Similar to apoptosis, pyroptosis can have a dual impact on cancer progression, either promoting or inhibiting tumorigenesis, depending on the type of inflammation[61,62]. Whereas acute inflammation can initiate immune surveillance and humoral immunity, chronic

inflammation can lead to cell survival, proliferation, metastasis, and therapy resistance[63]. Nevertheless, recent studies have shown that utilizing pyroptosis to trigger anti-cancer immunity is feasible and has clinical potential for melanoma[62,64]. For example, Erkes *et al* showed that the combination of a BRAFi/MEKi treatment (currently FDA-approved for BRAF-mutated melanoma patients) with stimulation of the pyroptotic pathway, represents a potential salvage therapy for more resistant patients. Since resistance to BRAF/MEKi therapy is associated with poor intratumoral T cell activation, stimulation of this immune response by triggering pyroptosis showed an improved response[65]. Furthermore, necroptosis is also known to elicit a strong immunogenic response. Aaes *et al* reported that necroptotic cancer cells are able to cross-prime cytotoxic $CD8a^+$ cells *in vivo* in the form of a vaccination assay and induced a strong tumor antigen-specific production of IFN-γ *in vitro*[66]. However, some controversy exists on whether targeting this RCD pathway is feasible and clinically relevant since numerous key molecules in the necroptotic signaling pathway have been found to be downregulated in different types of cancer cells, suggesting that cancer cells can quite easily evade necroptosis to survive. Indeed, the downregulation of RIPK3, which is commonly found in melanoma cells, correlated with a poor prognosis and was found to enhance tumor progression and cancer metastasis[67,68].

Finally, ferroptosis is also considered a double-edged sword in cancer therapy. As a more novel RCD pathway, it quickly gained significant interest as it was shown that therapy-resistant cells were more prone to this pathway[69]. However, recent studies show that inducing ferroptosis in cancer cells can lead to immune tolerance[44,70]. Indeed, Wiernicki *et al*. reported that, despite the emission of ICD-associated DAMPs, ferroptosis decreased the phagocytic potential and maturation of DCs

and dampens antigen cross-presentation, altogether impairing DC-mediated anti-tumor immunity[71]. Since evasion of RCD, one of the most important hallmarks of cancer, leads to a rapid development of resistance against specific therapies, researchers are starting to look into combination therapies that target multiple cell death pathways simultaneously. For instance, Cheng *et al* showed that Ophiopogonin B can help to alleviate cisplatin-induced apoptosis-resistance by inducing pyroptotic cell death[72]. Guo *et at* reported that GW4064, a synthetic FXR agonist, enhanced pyroptosis of HT-29 and SW620 cells, which increased the sensitivity to oxaliplatin, an apoptosis-inducing chemotherapy[73]. This study demonstrated that a single NTP treatment can activate multiple cell death pathways, which might provide significant advantage in minimizing the risk of therapy resistance and enhancing therapeutic efficacy. Whether NTP can simultaneously trigger multiple cell death pathways within the same cell, or whether different cell death pathways are activated in a spatial mosaic pattern in the 2D-3D cell culture microenvironment[74,75], needs further investigation by single cell omics applications.

As research into the biochemical mechanisms of NTP-induced cell death is becoming more in-depth, it is still critical to consider the clinical application for the different treatment modalities. While direct treatment delivers a plethora of short- and long-lived RONS to the treatment target, it is currently limited to treatment of superficial tumors and lesions that are easily accessible with the device. Therefore, clinical studies have been limited to superficial tumor lesions and skin diseases[76,77]. However, more sophisticated NTP devices, including an endoscopic-like NTP device, are being developed to deliver direct treatment to tumors inside the body[78]. Others have suggested to apply direct NTP treatment to tumor beds following surgical procedures, though this method is still to

be tested. Indirect NTP treatment, with plasma-treated liquids, has been another treatment modality to circumvent the limitations of direct treatment and reach tumors inside the body[79–81]. However, the delivery of only long-lived RONS with indirect NTP treatment has recently come under fire. Indeed, our previous work has questioned the practical delivery of PTL, as various body fluids would quickly inactivate any remaining RONS left in the liquid when introduced into the body[22]. Therefore, injection or profusion site of PTL would have to be carefully calculated in relation to the treatment target. Furthermore, PTL in physiological, inorganic solutions does not appear to possess any usefulness or added benefit beyond commercially available RONS solutions[33]. Indeed, our initial comparison of indirect NTP treatment with mock solutions also suggested that the H_2O_2 produced by indirect NTP treatment with PTL accounts for the induced cell death and follows similar RCD pathways (ferroptosis) (Figure 4.3). In our opinion, based on existing literature and the comparisons made here, we believe that PTL has very low clinical translational value. Recently, a new modality of NTP delivery has been emerging to "hybridize" the advantages of both direct NTP treatment with PTLs: plasma-treated hydrogels (PTH)[82]. In contrast to PTLs, the varied chemistry of polymers provides potential for modified reactivity with NTP and form organic RONS. Therefore, PTHs might also allow for more localized, diverse, and prolonged RONS generation for deep tissue tumors. As this NTP modality becomes more mature, it will also be crucial to investigate the biochemical mechanisms of induced cell death and evaluate clinical translation.

4.5 Conclusion

Overall, the findings obtained from this study highlight the molecular discrepancies and consequential ramifications regarding regulated cell death associated with direct and indirect NTP treatment in the context of cancer therapy. Collectively, the activation of multiple RCD pathways presents a promising avenue for mitigating treatment resistance and amplifying therapeutic efficacy. Profoundly understanding the NTP-induced RCD pathways holds significant potential for the development of strategic combination therapies designed to simultaneously target multiple RCD pathways, thereby fostering an enhanced potential for inducing cancer cell toxicity. These findings hold great promise for advancing the field of plasma oncology.

4.6 References

1. Faramarzi F, Zafari P, Alimohammadi M, Moonesi M, Rafiei A, Bekeschus S. Cold Physical Plasma in Cancer Therapy: Mechanisms, Signaling, and Immunity. *Oxid Med Cell Longev*. 2021;2021. doi:10.1155/2021/9916796

2. Graves DB. Low temperature plasma biomedicine: A tutorial review. *Phys Plasmas*. 2014;21(8). doi:10.1063/1.4892534

3. Keidar M. Plasma for cancer treatment. *Plasma Sources Sci Technol*. 2015;24(3). doi:10.1088/0963-0252/24/3/033001

4. Huang J, Chen W, Li H, et al. Deactivation of A549 cancer cells in vitro by a dielectric barrier discharge plasma needle. *J Appl Phys*. 2011;109(5). doi:10.1063/1.3553873

5. Kim SJ, Chung TH, Bae SH, Leem SH. Induction of apoptosis in human breast cancer cells by a pulsed atmospheric pressure plasma jet. *Appl Phys Lett*. 2010;97(2). doi:10.1063/1.3462293

6. Hattori N, Yamada S, Tori K, et al. Effectiveness of plasma treatment on pancreatic cancer cells. *Int J Oncol*. 2015;47(5):1655-1662. doi:10.3892/ijo.2015.3149

7. Tanaka H, Mizuno M, Ishikawa K, et al. Plasma-Activated Medium Selectively Kills Glioblastoma Brain Tumor Cells by Down-Regulating a Survival Signaling Molecule, AKT Kinase. *Plasma Med*. 2011;1(3-4):265-277. doi:10.1615/PlasmaMed.2012006275

8. Leduc M, Guay D, Leask RL, Coulombe S. Cell permeabilization using a non-thermal plasma. *New J Phys*. 2009;11. doi:10.1088/1367-2630/11/11/115021

9. Vermeylen S, De Waele J, Vanuytsel S, et al. Cold atmospheric plasma treatment of melanoma and glioblastoma cancer cells. *Plasma Processes and Polymers*. 2016;13(12):1195-1205. doi:10.1002/ppap.201600116

10. Vandamme M, Robert E, Dozias S, et al. *Response of Human Glioma U87 Xenografted on Mice to Non Thermal Plasma Treatment*.; 2011. https://hal.archives-ouvertes.fr/hal-00683299

11. Brullé L, Vandamme M, Riès D, et al. Effects of a Non Thermal Plasma Treatment Alone or in Combination with Gemcitabine in a MIA PaCa2-luc Orthotopic Pancreatic Carcinoma Model. *PLoS One*. 2012;7(12). doi:10.1371/journal.pone.0052653

12. Lin A, De Backer J, Quatannens D, et al. The effect of local non-thermal plasma therapy on the cancer-immunity cycle in a melanoma mouse model. *Bioeng Transl Med*. 2022;7(3). doi:10.1002/btm2.10314

13. Troitskaya O, Golubitskaya E, Biryukov M, et al. Non-thermal plasma application in tumor-bearing mice induces increase of serum hmgb1. *Int J Mol Sci*. 2020;21(14):1-14. doi:10.3390/ijms21145128

14. Metelmann HR, Seebauer C, Miller V, et al. Clinical experience with cold plasma in the treatment of locally advanced head and neck cancer. *Clin Plasma Med*. 2018;9:6-13. doi:10.1016/j.cpme.2017.09.001

15. Yan D, Horkowitz A, Wang Q, Keidar M. On the selective killing of cold atmospheric plasma cancer treatment: Status and beyond. *Plasma Processes and Polymers*. 2021;18(10). doi:10.1002/ppap.202100020

16. Lin A, Truong B, Fridman G, Fridman A, Miller V. *Immune Cells Enhance Selectivity of Nanosecond-Pulsed DBD Plasma Against Tumor Cells*. Vol 7.; 2017. www.begellhouse.com

17. Lin A, Gorbanev Y, De Backer J, et al. Non-Thermal Plasma as a Unique Delivery System of Short-Lived Reactive Oxygen and Nitrogen Species for Immunogenic Cell Death in Melanoma Cells. *Advanced Science*. 2019;6(6). doi:10.1002/advs.201802062

18. Van Loenhout J, Boullosa LF, Quatannens D, et al. Auranofin and cold atmospheric plasma synergize to trigger distinct cell death mechanisms and immunogenic responses in glioblastoma. *Cells*. 2021;10(11). doi:10.3390/cells10112936

19. Wende K, von Woedtke T, Weltmann KD, Bekeschus S. Chemistry and biochemistry of cold physical plasma derived reactive species in liquids. *Biol Chem*. 2019;400:19-38. doi:10.1515/hsz-2018-0242

20. Dubuc A, Monsarrat P, Virard F, et al. Use of cold-atmospheric plasma in oncology: a concise systematic review. *Ther Adv Med Oncol*. 2018;10. doi:10.1177/1758835918786475

21. Biscop E, Lin A, Van Boxem W, et al. Influence of cell type and culture medium on determining cancer selectivity of cold atmospheric plasma treatment. *Cancers (Basel)*. 2019;11(9). doi:10.3390/cancers11091287

22. Lin A, Biscop E, Breen C, Butler SJ, Smits E, Bogaerts A. Critical evaluation of the interaction of reactive oxygen and nitrogen species with blood to inform the clinical translation of nonthermal plasma therapy. *Oxid Med Cell Longev*. 2020;2020. doi:10.1155/2020/9750206

23. Malyavko A, Yan D, Wang Q, et al. Cold atmospheric plasma cancer treatment, direct: Versus indirect approaches. *Mater Adv*. 2020;1(6):1494-1505. doi:10.1039/d0ma00329h

24. Yan D, Malyavko A, Wang Q, Lin L, Sherman JH, Keidar M. Cold atmospheric plasma cancer treatment, a critical review. *Applied Sciences (Switzerland)*. 2021;11(16). doi:10.3390/app11167757

25. Liu W, Jin W, Zhu S, Chen Y, Liu B. Targeting regulated cell death (RCD) with small-molecule compounds in cancer therapy: A revisited review of apoptosis, autophagy-dependent cell death and necroptosis. *Drug Discov Today*. 2022;27(2):612-625. doi:10.1016/j.drudis.2021.10.011

26. Galluzzi L, Vitale I, Aaronson SA, et al. Molecular mechanisms of cell death: Recommendations of the Nomenclature Committee on Cell Death 2018. *Cell Death Differ*. 2018;25(3):486-541. doi:10.1038/s41418-017-0012-4

27. Gaur N, Kurita H, Oh JS, et al. On cold atmospheric-pressure plasma jet induced DNA damage in cells. *J Phys D Appl Phys*. 2021;54(3). doi:10.1088/1361-6463/abb8ab

28. Siu A, Volotskova O, Cheng X, et al. Differential effects of cold atmospheric plasma in the treatment of malignant glioma. *PLoS One*. 2015;10(6). doi:10.1371/journal.pone.0126313

29. Arndt S, Wacker E, Li YF, et al. Cold atmospheric plasma, a new strategy to induce senescence in melanoma cells. *Exp Dermatol*. 2013;22(4):284-289. doi:10.1111/exd.12127

30. Kim CH, Bahn JH, Lee SH, et al. Induction of cell growth arrest by atmospheric non-thermal plasma in colorectal cancer cells. *J Biotechnol*. 2010;150(4):530-538. doi:10.1016/j.jbiotec.2010.10.003

31. Arndt S, Fadil F, Dettmer K, et al. Cold atmospheric plasma changes the amino acid composition of solutions and influences the anti-tumor effect on melanoma cells. *Int J Mol Sci*. 2021;22(15). doi:10.3390/ijms22157886

32. Lin A, Biscop E, Gorbanev Y, Smits E, Bogaerts A. Toward defining plasma treatment dose: The role of plasma treatment energy of pulsed-dielectric barrier discharge in dictating in vitro biological responses. *Plasma Processes and Polymers*. 2022;19(3). doi:10.1002/ppap.202100151

33. Tampieri F, Gorbanev Y, Sardella E. Plasma-treated liquids in medicine: Let's get chemical. *Plasma Processes and Polymers*. Published online June 7, 2023. doi:10.1002/ppap.202300077

34. Lin A, Truong B, Patel S, et al. Nanosecond-Pulsed DBD Plasma-Generated Reactive Oxygen Species Trigger Immunogenic Cell Death in A549 Lung Carcinoma Cells through Intracellular Oxidative Stress. *Int J Mol Sci*. 2017;18(5):966. doi:10.3390/ijms18050966

35. Girard PM, Arbabian A, Fleury M, et al. Synergistic Effect of H2O2 and NO2 in Cell Death Induced by Cold Atmospheric He Plasma. *Sci Rep*. 2016;6(1):29098. doi:10.1038/srep29098

36. Sklias K, Santos Sousa J, Girard PM. Role of Short- and Long-Lived Reactive Species on the Selectivity and Anti-Cancer Action of Plasma Treatment In Vitro. *Cancers (Basel)*. 2021;13(4):615. doi:10.3390/cancers13040615

37. Koren E, Fuchs Y. Modes of regulated cell death in cancer. *Cancer Discov*. 2021;11(2):245-265. doi:10.1158/2159-8290.CD-20-0789

38. Van Engeland M, Nieland LJW, Ramaekers FCS, Schutte B, Reutelingsperger CPM. Annexin V-affinity assay: A review on an apoptosis detection system based on phosphatidylserine exposure. *Cytometry*. 1998;31(1):1-9. doi:10.1002/(SICI)1097-0320(19980101)31:1<1::AID-CYTO1>3.0.CO;2-R

39. Shlomovitz I, Speir M, Gerlic M. Flipping the dogma - Phosphatidylserine in non-apoptotic cell death. *Cell Communication and Signaling*. 2019;17(1). doi:10.1186/s12964-019-0437-0

40. Yu P, Zhang X, Liu N, Tang L, Peng C, Chen X. Pyroptosis: mechanisms and diseases. *Signal Transduct Target Ther*. 2021;6(1). doi:10.1038/s41392-021-00507-5

41. Bertheloot D, Latz E, Franklin BS. Necroptosis, pyroptosis and apoptosis: an intricate game of cell death. *Cell Mol Immunol*. 2021;18(5):1106-1121. doi:10.1038/s41423-020-00630-3

42. Yan G, Elbadawi M, Efferth T. Multiple cell death modalities and their key features (Review). *World Acad Sci J*. 2020;2(2):39-48. doi:10.3892/wasj.2020.40

43. Peng F, Liao M, Qin R, et al. Regulated cell death (RCD) in cancer: key pathways and targeted therapies. *Signal Transduct Target Ther*. 2022;7(1). doi:10.1038/s41392-022-01110-y

44. Dang Q, Sun Z, Wang Y, Wang L, Liu Z, Han X. Ferroptosis: a double-edged sword mediating immune tolerance of cancer. *Cell Death Dis*. 2022;13(11). doi:10.1038/s41419-022-05384-6

45. Wu Y, Yu C, Luo M, et al. Ferroptosis in Cancer Treatment: Another Way to Rome. *Front Oncol*. 2020;10. doi:10.3389/fonc.2020.571127

46. Liu X, Zhang Y, Wu X, et al. Targeting Ferroptosis Pathway to Combat Therapy Resistance and Metastasis of Cancer. *Front Pharmacol*. 2022;13. doi:10.3389/fphar.2022.909821

47. Sato K, Shi L, Ito F, et al. Nonnthermal plasma specifically kills oral squamous cell carcinoma cells in a catalytic Fe(II))dependent manner. *J Clin Biochem Nutr*. 2019;65(1):8-15. doi:10.3164/jcbn.18891

48. Jo A, Bae JH, Yoon YJ, et al. Plasma-activated medium induces ferroptosis by depleting FSP1 in human lung cancer cells. *Cell Death Dis*. 2022;13(3). doi:10.1038/s41419-022-04660-9

49. Yang X, Chen G, Yu KN, et al. Cold atmospheric plasma induces GSDME-dependent pyroptotic signaling pathway via ROS generation in tumor cells. *Cell Death Dis*. 2020;11(4). doi:10.1038/s41419-020-2459-3

50. Van Loenhout J, Flieswasser T, Boullosa LF, et al. Cold atmospheric plasma-treated PBS eliminates immunosuppressive pancreatic stellate cells and induces immunogenic cell death of pancreatic cancer cells. *Cancers (Basel)*. 2019;11(10). doi:10.3390/cancers11101597

51. Turrini E, Laurita R, Stancampiano A, et al. Cold Atmospheric Plasma Induces Apoptosis and Oxidative Stress Pathway Regulation in T-Lymphoblastoid Leukemia Cells. *Oxid Med Cell Longev*. 2017;2017. doi:10.1155/2017/4271065

52. Eggers B, Marciniak J, Memmert S, et al. Influences of cold atmospheric plasma on apoptosis related molecules in osteoblast-like cells in vitro. *Head Face Med*. 2021;17(1). doi:10.1186/s13005-021-00287-x

53. Wang Y, Mang X, Li X, Cai Z, Tan F. Cold atmospheric plasma induces apoptosis in human colon and lung cancer cells through modulating mitochondrial pathway. *Front Cell Dev Biol*. 2022;10. doi:10.3389/fcell.2022.915785

54. Arndt S, Fadil F, Dettmer K, et al. Cold atmospheric plasma changes the amino acid composition of solutions and influences the anti-tumor effect on melanoma cells. *Int J Mol Sci*. 2021;22(15). doi:10.3390/ijms22157886

55. Qi S, Wang Q, Zhang J, Liu Q, Li C. Pyroptosis and Its Role in the Modulation of Cancer Progression and Antitumor Immunity. *Int J Mol Sci*. 2022;23(18). doi:10.3390/ijms231810494

56. Mittal M, Siddiqui MR, Tran K, Reddy SP, Malik AB. Reactive oxygen species in inflammation and tissue injury. *Antioxid Redox Signal*. 2014;20(7):1126-1167. doi:10.1089/ars.2012.5149

57. Wu Y, Dong G, Sheng C. Targeting necroptosis in anticancer therapy: mechanisms and modulators. *Acta Pharm Sin B*. 2020;10(9):1601-1618. doi:10.1016/j.apsb.2020.01.007

58. Mattia G, Puglisi R, Ascione B, Malorni W, Carè A, Matarrese P. Cell death-based treatments of melanoma:conventional treatments and new

therapeutic strategies review-Article. *Cell Death Dis*. 2018;9(2). doi:10.1038/s41419-017-0059-7

59. Pfeffer CM, Singh ATK. Apoptosis: A target for anticancer therapy. *Int J Mol Sci*. 2018;19(2). doi:10.3390/ijms19020448

60. Berthenet K, Castillo Ferrer C, Fanfone D, et al. Failed Apoptosis Enhances Melanoma Cancer Cell Aggressiveness. *Cell Rep*. 2020;31(10). doi:10.1016/j.celrep.2020.107731

61. Wei X, Xie F, Zhou X, et al. Role of pyroptosis in inflammation and cancer. *Cell Mol Immunol*. 2022;19(9):971-992. doi:10.1038/s41423-022-00905-x

62. Xia X, Wang X, Cheng Z, et al. The role of pyroptosis in cancer: pro-cancer or pro-"host"? *Cell Death Dis*. 2019;10(9). doi:10.1038/s41419-019-1883-8

63. Singh N, Baby D, Prasad Rajguru J, B Patil P, S Thakkannavar S, Bhojaraj Pujari V. Inflammation and cancer. *Ann Afr Med*. 2019;18(3):121-126.

64. Qi S, Wang Q, Zhang J, Liu Q, Li C. Pyroptosis and Its Role in the Modulation of Cancer Progression and Antitumor Immunity. *Int J Mol Sci*. 2022;23(18). doi:10.3390/ijms231810494

65. Erkes DA, Cai W, Sanchez IM, et al. Mutant BRAF and MEK inhibitors regulate the tumor immune microenvironment via pyroptosis. *Cancer Discov*. 2020;10(2):255-269. doi:10.1158/2159-8290.CD-19-0672

66. Aaes TL, Kaczmarek A, Delvaeye T, et al. Vaccination with Necroptotic Cancer Cells Induces Efficient Anti-tumor Immunity. *Cell Rep*. 2016;15(2):274-287. doi:10.1016/j.celrep.2016.03.037

67. Gong Y, Fan Z, Luo G, et al. The role of necroptosis in cancer biology and therapy. *Mol Cancer*. 2019;18(1). doi:10.1186/s12943-019-1029-8

68. Geserick P, Wang J, Schilling R, et al. Absence of RIPK3 predicts necroptosis resistance in malignant melanoma. *Cell Death Dis*. 2015;6(9). doi:10.1038/cddis.2015.240

69. Liu X, Zhang Y, Wu X, et al. Targeting Ferroptosis Pathway to Combat Therapy Resistance and Metastasis of Cancer. *Front Pharmacol*. 2022;13. doi:10.3389/fphar.2022.909821

70. Kepp O, Kroemer G. Is ferroptosis immunogenic? The devil is in the details! *Oncoimmunology*. 2022;11(1). doi:10.1080/2162402X.2022.2127273

71. Wiernicki B, Maschalidi S, Pinney J, et al. Cancer cells dying from ferroptosis impede dendritic cell-mediated anti-tumor immunity. *Nat Commun*. 2022;13(1). doi:10.1038/s41467-022-31218-2

72. Cheng Z, Li Z, Gu L, et al. Ophiopogonin B alleviates cisplatin resistance of lung cancer cells by inducing Caspase-1/GSDMD dependent pyroptosis. *J Cancer*. 2022;13(2):715-727. doi:10.7150/jca.66432

73. Guo J, Zheng J, Mu M, et al. GW4064 enhances the chemosensitivity of colorectal cancer to oxaliplatin by inducing pyroptosis. *Biochem Biophys Res Commun*. 2021;548:60-66. doi:10.1016/j.bbrc.2021.02.043

74. Wang Y, Pandian N, Han JH, et al. Single cell analysis of PANoptosome cell death complexes through an expansion microscopy method. *Cellular and Molecular Life Sciences*. 2022;79(10):531. doi:10.1007/s00018-022-04564-z

75. Khatib SA, Ma L, Dang H, et al. Single-cell biology uncovers apoptotic cell death and its spatial organization as a potential modifier of tumor diversity in HCC. *Hepatology*. 2022;76(3):599-611. doi:10.1002/hep.32345

76. Metelmann HR, Seebauer C, Miller V, et al. Clinical experience with cold plasma in the treatment of locally advanced head and neck cancer. *Clin Plasma Med*. 2018;9:6-13. doi:10.1016/j.cpme.2017.09.001

77. Friedman PC, Miller V, Fridman G, Lin A, Fridman A. Successful treatment of actinic keratoses using nonthermal atmospheric pressure plasma: A case series. *J Am Acad Dermatol*. 2017;76(2):349-350. doi:10.1016/j.jaad.2016.09.004

78. Decauchy H, Pavy A, Camus M, Fouassier L, Dufour T. Cold plasma endoscopy applied to biliary ducts: feasibility risk assessment on human-like and porcine models for the treatment of cholangiocarcinoma. *J Phys D Appl Phys*. 2022;55(45):455401. doi:10.1088/1361-6463/ac8c4d

79. Nakamura K, Yoshikawa N, Mizuno Y, et al. Preclinical Verification of the Efficacy and Safety of Aqueous Plasma for Ovarian Cancer Therapy. *Cancers (Basel)*. 2021;13(5):1141. doi:10.3390/cancers13051141

80. Tanaka H, Bekeschus S, Yan D, Hori M, Keidar M, Laroussi M. Plasma-Treated Solutions (PTS) in Cancer Therapy. *Cancers (Basel)*. 2021;13(7):1737. doi:10.3390/cancers13071737

81. Freund E, Liedtke KR, Gebbe R, Heidecke AK, Partecke LI, Bekeschus S. *In Vitro* Anticancer Efficacy of Six Different Clinically Approved Types of Liquids Exposed to Physical Plasma. *IEEE Trans Radiat Plasma Med Sci*. 2019;3(5):588-596. doi:10.1109/TRPMS.2019.2902015

82. Živanić M, Espona-Noguera A, Lin A, Canal C. Current State of Cold Atmospheric Plasma and Cancer-Immunity Cycle: Therapeutic Relevance

and Overcoming Clinical Limitations Using Hydrogels. *Advanced Science*. 2023;10(8). doi:10.1002/advs.202205803

Appendix 3

Appendix 3.1 Optimizing the optimal PTL ratio for SK-MEL-28

During the cell death kinetics experiments, we noted that SK-MEL-28 exhibited greater resistance to the treatment, requiring a higher NTP dose for cytotoxicity induction compared to A375. We examined varying volumes of PTL in combination with 150 µL of cell culture medium, resulting in PTL:Medium ratios of 1:6, 2:7, 3:8, 4:9, and 1:2. Among these, the 2:7 ratio displayed the most favorable dose-response pattern (Figure A3.1B), prompting us to select these conditions for subsequent experiments.

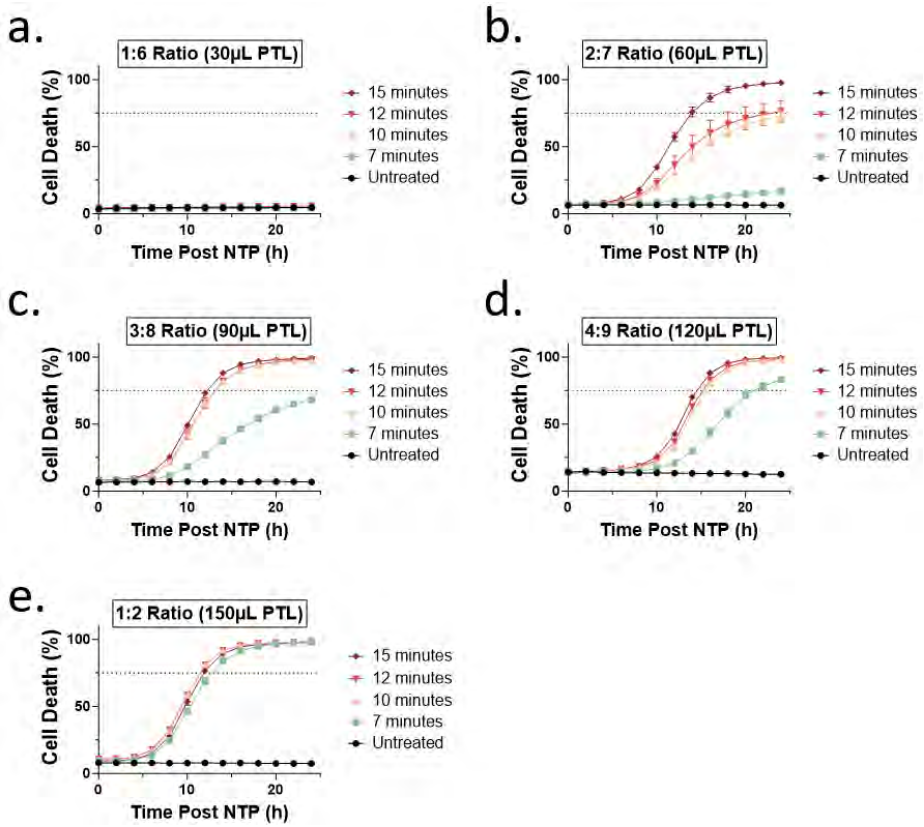

Figure A3.1 Percentage of cell death versus time post plasma for SK-MEL-28 for the optimization of the ratio for cell death kinetics experiments. pPBS is added to the cells in a ratio of a. 1:6, b. 2:7, c. 3:8, d. 4:9 and e. 1:2. The different treatments of PBS are shown in the legend by the number of minutes the PBS was treated with plasma. The vehicle is shown as untreated in the legend

Appendix 3.2 Baseline MLKL expression in A375 and SK-MEL-28

Different response in MLKL phosphorylation were found in both cell lines. To investigate these different responses, we evaluated the baseline expression of MLKL for both cell lines using Western Blotting. We observed that A375 has a higher basal expression of MLKL, explaining the augmented MLKL phosphorylation and therefore higher susceptibility to necroptosis.

Figure A8.2 Western blots showing the baseline expression of MLKL for A375 and SK-MEL-28

Appendix 3.3 Caspase 3/7 positivity 48h after indirect NTP treatment

To follow up a possible delayed effect for the indirect NTP treatment regarding apoptosis induction, we examined the caspase 3/7 expression at 24h and 48h post NTP treatment. We indeed observed that 48h post NTP treatment, caspase 3/7 positivity was increased in comparison to 24h after treatment.

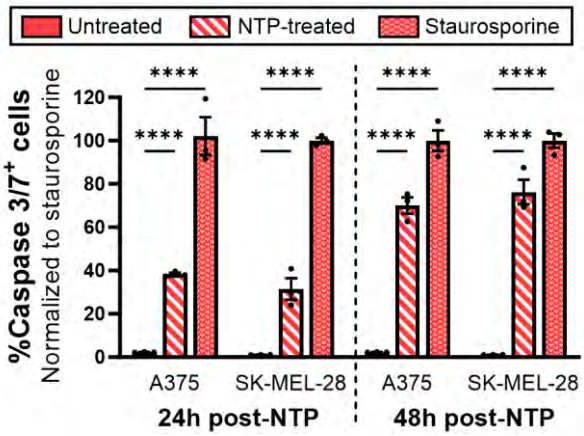

Figure A3.3 The percentage of caspase 3/7 positive cells following indirect NTP treatment. The experiment was performed in triplicate and the data is presented as mean ± SEM. Statistical significance was calculated using the generalized linear mixed model. **** $p \leq 0.0001$

CHAPTER 5

Dose-Dependent Induction of Epithelial-Mesenchymal Transition in 3D melanoma Models by Non-Thermal Plasma Treatment.

This Chapter is submitted to Cancer Communications as:

Eline Biscop, Edgar Cardenas De La Hoz, Hanne Verswyvel, Joey De Backer, Ho Wa Lau, Wim Vanden Berghe, Evelien Smits, Annemie Bogaerts and Abraham Lin. Dose-Dependent Induction of Epithelial-Mesenchymal Transition by Non-Thermal Plasma Treatment in 3D Melanoma Spheroids and *In Ovo* Tumors.

Abstract

Despite the very promising results, the potential role of NTP in triggering the epithelial-mesenchymal transition (EMT) and its subsequent impact on cancer cell migration remain unexplored. In this Chapter, we investigate NTP-induced EMT initiation and progression by evaluating six key EMT biomarkers in combination with functional assays to assess changes in migration in melanoma cells using both a Chicken Chorioallantoic Membrane (CAM) model and a 3D spheroid model. Furthermore, we elucidate the dose-dependent effects of NTP on EMT induction. We demonstrate that high NTP treatments exhibit a significant EMT response and enhanced migration, while low NTP doses induce no such changes. Our findings highlight the important role of NTP treatment parameters in influencing EMT responses. The insights obtained in this study offer a foundation for clinical optimization, harnessing the cancer-killing potential of NTP, while safeguarding against undesirable EMT-related outcomes.

5.1 Introduction

Although the cancer-killing potential of NTP through the induction of oxidative stress seems very promising, extensive research from both experimental and clinical studies indicates that RONS can also play an important role in promoting various stages of tumor formation and progression, dependent on their mutagenic potential and ability to interact with signaling pathways regulating cell proliferation, motility, invasiveness and survival[1,2]. Moreover, increasing evidence suggests that oxidative stress plays a crucial role in promoting cell invasion and metastasis through the activation of stimuli associated with epithelial-mesenchymal transition (EMT)[1]. EMT is a morphogenesis process first described by researchers studying embryonic and organ development[3]. Later it was shown that EMT also plays an important role in adult tissue regeneration and cancer metastasis, leading to a continuous surge in research attention[3]. In the context of cancer, EMT represents a transition from an epithelial phenotype towards a mesenchymal phenotype during which the cancer cells lose their apical-basal polarity and acquire more migratory and invasive properties[3,4]. As implied by its name, EMT is a transition process wherein cells go through different states along the E-M spectrum before attaining a fully mesenchymal phenotype, also called EMT plasticity[5–7]. Consequently, this generates an extensive phenotypic heterogeneity within the tumor, resulting in increased adaptability and resistance, granting cancer cells a survival advantage[8,9].

Given the proven connection between oxidative stress and EMT, in this Chapter, we aim to investigate whether NTP would initiate this transition and whether we could modify the response by altering the NTP treatment parameters. To do this, we performed a comprehensive study of six key EMT biomarkers to analyze their expression post NTP treatment and, moreover, looked into a change in migratory capacities

of the cells in two different 3D cancer models, the spheroid model and the Chicken Chorioallantoic Membrane (CAM) *in ovo* model. Our results elucidate the dose-dependent nature of the NTP-induced EMT response. Whereas high NTP treatments clearly initiate EMT, low NTP treatments trigger no such response. These findings highlight the importance of optimizing NTP treatment parameters, thereby delineating a promising foundation for clinical refinement.

5.2 Materials and methods

Cell culture

For this study, three human melanoma cell lines were used: A375 (ATCC, CRL-1619TM), SK-MEL-28 (ATCC, HTB-72) and Malme-3M (ATCC, HTB-64). All cell lines were cultured in Dulbecco's Modified Eagle Medium (DMEM) (Gibco™, Life Technologies, 10938-025) supplemented with 10% Fetal Bovine Serum (FBS) (Gibco™, Life Technologies, 10270-106), 100 units/mL penicillin/streptomycin (Gibco™, Life Technologies, 15140-122) and 4 mM L-glutamine (Gibco™, Life Technologies, 25030-024). The cells were maintained at 37°C in a humidified atmosphere with 5% CO_2.

3D spheroid model

For the generation of 3D spheroids, the cells were seeded in an ultra-low attachment 96-well plate (Corning B.V. Life Sciences, 7007). Cell suspensions were made with 5000 cells/spheroid for SK-MEL-28 and 7000 cells/spheroid for Malme-3M and supplemented with 2% GFR Matrigel (Corning B.V. Life Sciences, 354-230). Different seeding concentrations were used for the different cell lines in order to obtain spheroids with a diameter of approximately 500 µm at the start of the experiments. For the A375 cell line, no spheroids could be generated due to the incapability of this cell line to form compact spheres. After

seeding, the spheroids were centrifuged at 1000 RPM for 10 minutes at 4°C. Subsequently, they were incubated for three days at 37 °C in a humidified incubator with 5% CO_2 prior to their use in experiments.

3D CAM in-ovo model

Fertilized chicken eggs (embryonic development (ED) day 4) were incubated in a horizontal position at 37 °C and 65% humidity in an egg incubator with automatic turning function (Ova-Easy 100, Brinsea, Veenendaal, The Netherlands). On ED day 5, the upper pole of the egg was disinfected and pierced with a 20G sterile needle (BD) after which it was sealed with medical tape (Leukosilk S, Covamed Farma BVBA, Marke, Belgium). Following the piercing, the eggs were put in a vertical position in the egg incubator (turning function off) to promote the relocation of the air chamber to the upper pole. At ED day 7, the upper pole of the egg was cut off to expose the CAM, and a 1 x 1 mm filter paper soaked in diethyl ether was briefly applied on a vascular region on the CAM. At this region, a sterile silicon ring (ID = 5 mm, OD = 6 mm) was placed on the CAM and 2 x 10^6 cells for A375 and SK-MEL-28 or 6 x 10^6 cells for Malme-3M, mixed with 15µL GFR Matrigel, were loaded into the ring. The eggs were sealed with Tegaderm (3D) and placed back in the incubator for four days. On ED day 11, the Tegaderm was cut and the tumors were treated with either direct NTP or an EMT-supplement. For the EMT-supplement, a second sterile plastic ring (ID = 7 mm, OD = 8.5 mm) was placed around the first ring and 20 µL of StemXVivo EMT Inducing Media Supplement (100X) (Biotechne, CCM017) was loaded into the ring. The eggs were sealed with Tegaderm and incubated until the end of the experiment. On ED day 14, the tumors were excised and weighted on a precision balance (Mettler Toledo, Fischer, Merelbeke, Belgium) after which the chicken embryos were further dissected to collect the liver, lungs and a lower part of the CAM for further analysis.

All steps outside the incubator were carried out using a heat block (set at 37 °C) with a custom-made egg-shaped aluminum adapter.

NTP treatment

The same FE-DBD as described in Chapter 4 was used. For the treatment of spheroids, the spheroid was transferred to an empty 96-well plate in 3µL of medium prior to treatment. The gap between the electrode and the spheroid was fixed at 1 mm distance using a z-positioner, following which NTP was discharged directly on the cells for 10 seconds at various frequencies, ranging between 100 Hz and 700 Hz. Immediately following treatment, 100 µL of fresh cell culture medium was replenished in the well. For the treatment of the *in ovo* tumors, the gap between the electrode and the tumor was set at approximately 2-4 mm distance. Fixing at an exact distance was not possible for this model due to the varying egg size and occasional movement of the embryo. After fixing the gap, NTP was discharged directly onto the tumor for 10 seconds at 700 Hz, following which the eggs were sealed again. As a positive control for EMT induction, the StemXVivo EMT Inducing Media Supplement, later referred to as EMT-supplement, was used. This EMT-supplement contains the following premium quality proteins and high performance neutralizing antibodies to induce EMT: Recombinant Human Wnt-5a, Recombinant Human TGF-β1, Anti-Human E-cadherin, Anti-Human sFRP-1 and Anti-Human Dkk-1.

Immunofluorescence on 3D spheroids and in ovo tumors

To assess several key EMT biomarkers, immunofluorescent stainings were performed on both 3D spheroids and tumors collected from the *in ovo* model. The spheroids were collected 1 day, 4 days and 7 days after NTP treatment and fixed overnight in 4% paraformaldehyde (PFA) at 4°C. The fixed spheroids were transferred to molds of 4% agarose, following which they were dehydrated and embedded in paraffin

overnight. *In ovo* tumors were collected 3 days after NTP treatment and fixed with 4% PFA at room temperature prior to dehydration and paraffin embedding. For both embedded spheroids and *in ovo* tumors, sections of 5 µm were cut. The slides were deparaffinized and rehydrated, following which antigen retrieval was done using a citrate buffer (10 mM, pH6) for 20 min at 96°C. After a 30 min cooldown, the cells were washed twice in tris buffer saline with 2.5% Triton X-100 (TBS) for 5 minutes. Subsequently the slides were blocked for 2h with TBS containing 10% goat serum (Abcam, ab7481) for vimentin and ZEB1 and 10% donkey serum (Abcam, ab7475) for E-cadherin, N-cadherin, SNA1 and Twist. After blocking, the primary antibody was applied, diluted in TBS containing 1% goat or donkey serum, depending on the antibody, and incubated overnight at 4 °C. Following primary antibodies were used: E-cadherin (Abcam, ab76055, 1:200), N-cadherin (Thermo Fisher, MA5-15633, 1:200), Vimentin (Abcam, ab92547, 1:500), SNAI1 (Santa Cruz Biotechnology, sc-271977, 1:100), ZEB1 (Abcam, ab203829, 1:250) and Twist (Abcam, ab175430, 1:200). The next day, the slides were washed twice in TBS and incubated with the secondary antibody in the dark for 1 hour at room temperature. The following secondary antibodies were used: Goat Anti-Rabbit IgG (H+L) Alexa Fluor 488 (Abcam, ab150077) and Donkey Anti-Mouse IgG (H+L) Highly Cross-adsorbed Alexa Fluor 594 (Thermo Fisher, A21203). The slides for vimentin and ZEB1 were additionally chemically bleached with Sudan Black B in 70% ethanol for 30 minutes to reduce autofluorescence, following which the slides were washed 3 times in TBS. All slides were mounted with VECTASHIELD HardSet antifade mounting medium with DAPI (Vectorlabs, Burlingame, CA, USA).

Spheroid migration

In order to evaluate cell migration in a more functional matter, a spheroid migration assay was performed. In this assay, the treated spheroids were transferred to a collagen-coated 96-well plate in 300µL growth factor reduced medium (2% FBS instead of 10% FBS). The spheroids were incubated for 30 minutes to allow them to adhere to the coated surface before starting the imaging. To investigate cell migration out of the spheroids, images were collected every 4 hours for a duration of 3 days using the Tecan Spark Cyto 600 (Tecan, Switzerland). These images were subsequently analyzed using the Orbits software.

RNA isolation and cDNA conversion

To isolate the RNA from the liver, lungs and lower CAM of the chicken embryos, the RNeasy Plus Mini Kit (Qiagen, 74034) was used according to the manufacturer's instructions. The RNA was then quantified using the Qubit 4 Fluorometer following which cDNA conversion was performed using Superscript II Reverse Transcriptase (Thermo Fisher, 18061-022) according to the manufacturer's instructions.

Real-time PCR

Amplification of cDNA was performed using the GoTaq Flexi DNA Polymerase assay (Promega M829B) with the Techne Prime Thermal Cycler. The following conditions were used during PCR: 95 °C for 2 min, 35 cycles of: 95 °C for 0.5 min, 60 °C for 0.5 min and 72 °C for 1 min; 72 °C for 5 min. The reference gene β-2 microglubulin (B2M, GeneID: 567) was used to selectively prime human cDNA.

Statistical analysis

All statistical differences were analyzed using the linear mixed model with JMP Pro 13 (SAS software). When a significant difference was detected, the post hoc Dunnett's test was performed to calculate the adjusted p value compared to the control. A p value of <0.05 was considered statistically significant. Data in all graphs are represented as mean ± standard error of the mean (SEM), the number of replicates is indicated in the legend, and all figures were prepared in GraphPad Prism (GraphPad Prism 10.0.1, GraphPad Prism Software, Inc.).

5.3 Results

5.3.1 Investigation of key EMT biomarkers after NTP treatment in the 3D CAM in ovo model

EMT is a complex multifaceted cellular process involving many changes in cell biology, protein expression and physiology[1]. It constitutes changes of cell behavior that involve the loss of certain epithelial characteristics and the gain of certain mesenchymal traits. In order to fully comprehend the impact of NTP on EMT progression, we assessed the expression of six key EMT biomarkers following NTP treatment using the 3D chicken CAM *in ovo* model. This model provides an *in vivo*-like environment that closely resembles physiological conditions, making it an excellent preclinical model to study cancer metastasis in a considerably shorter time compared to murine models (14 days instead of 4-10 weeks)[10]. In short, the cancer cells are seeded on top of the CAM at day 7 and grow until day 11 to form a small solid tumor (Fig. 5.1A), following which it was treated with NTP (700 Hz, 10 s). Three days after the treatment, the tumors were collected, weighted, fixed and embedded in paraffin for sectioning. As shown in figure 5.1B, the 700 Hz NTP treatment induced a cytotoxic response in all three melanoma cell lines, as evidenced by the significant reduction in tumor weight when

compared to the untreated tumors. After sectioning of the tumors, immunofluorescent stainings were used to examine the expression of the EMT biomarkers. One of the most important hallmarks of EMT is the so-called “cadherin switch”, which represents the downregulation of E-cadherin and upregulation of N-cadherin on the cell membrane surface[6,11]. Whereas E-cadherin is one of the most important molecules regulating cell-cell adhesion in epithelial tissues, N-cadherin endows tumor cells with enhanced migratory and invasive capacity. Our results show that NTP treatment induced a downregulation in E-cadherin expression in all three cell lines (0.64 ± 0.04-fold change for A375, $p \leq 0.0001$; 0.72 ± 0.02-fold change for SK-MEL-28, $p \leq 0.0001$; and 0.83 ± 0.03 for Malme-3M, $p = 0.0121$) (Fig 5.1C), together with an upregulation in N-cadherin expression (1.46 ± 0.06-fold change for A375, $p = 0.0002$; 1.71 ± 0.06-fold change for SK-MEL-28, $p \leq 0.0001$; and 1.32 ± 0.05-fold change for Malme-3M, $p = 0.0250$) (Fig. 5.1D). These results are in line with the positive control, the EMT-supplement, indicating that NTP indeed promotes EMT.

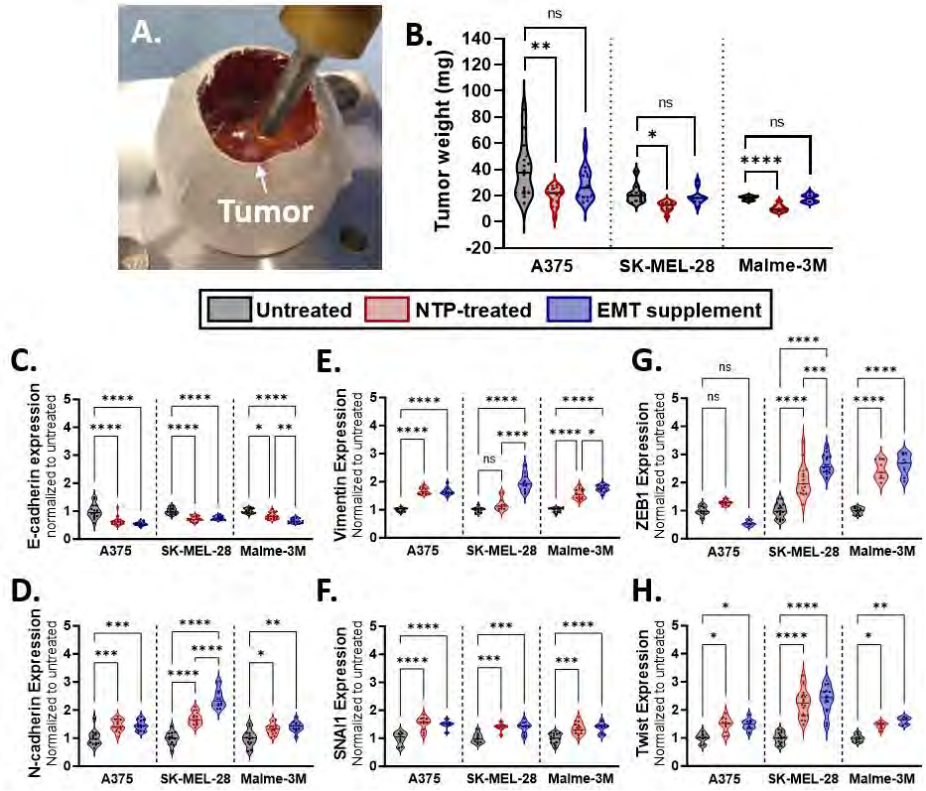

Figure 5.1 NTP-induced EMT response in tumors collected from the CAM *in ovo* model. A. Image showing the NTP treatment of the tumor, which is grafted on top of the CAM. B. Cytotoxic response of NTP treatment represented as reduction in tumor weight. C-H. Results from immunofluorescent stainings of six key EMT biomarkers (C. E-cadherin, D. N-cadherin, E. Vimentin, F. SNAI1, G. Twist, and H. ZEB1) in sections of the tumors collected from the CAM *in ovo* model. As a positive control, an EMT-inducing supplement was used. The results are normalized to the untreated sample. All experiments were performed at least in triplicate and the data is represented as mean ± SEM. Statistical significance was calculated using the generalized linear mixed model. * $p \leq 0.05$, ** $p \leq 0.01$, *** $p \leq 0.001$, **** $p \leq 0.0001$

Although the cadherin switch is an important hallmark of EMT, this alone might not be sufficient to trigger EMT-associated changes in cellular motility. Aside from the cadherin switch, vimentin has also shown to be an excellent indication for EMT[4,6]. Vimentin is a type III intermediate filament predominantly found in mesenchymal cells and is known to maintain cellular integrity and provide resistance against mechanical stress by providing a viscoelastic framework. Hence, increased

expression of vimentin undoubtedly promotes cancer cell migration[4]. The analysis of vimentin expression showed an upregulation for A375 (1.68 ± 0.04-fold change, $p \leq 0.0001$) and Malme-3M (1.56 ± 0.05-fold change, $p \leq 0.0001$), but not for SK-MEL-28, although there seems to be an increasing trend (Fig. 5.1E). These results are also in-line with the results obtained using the EMT-supplement, further supporting the hypothesis that NTP promotes EMT.

Lastly, we investigated the transcriptional factors that regulate EMT, which are mainly the Snail, ZEB and Twist families[12]. Altogether they act to suppress the expression of epithelial markers such as E-cadherin, as well as activate mesenchymal markers among which N-cadherin and Vimentin. In general, SNAI1, also known as Snail, is primarily known to be the major inducer of EMT as it can directly regulate the expression of E-cadherin and Vimentin but also stimulates the activation of Twist and ZEB1, which are subsequently mainly involved in upholding the mesenchymal phenotype[3]. With regard to SNAI1, we observed an increase in expression for all three cell lines (1.53 ± 0.07-fold change for A375, $p \leq 0.0001$; 1.40 ± 0.04-fold change for SK-MEL-28, $p = 0.0007$; and 1.35 ± 0.05-fold change for Malme-3M, $p = 0.0002$), comparable to that of the EMT-inducing supplement (Fig. 5.1F). Furthermore, also ZEB1 and Twist seem upregulated for SK-MEL-28 (ZEB1: 2.0 ± 0.1-fold change, $p \leq 0.0001$; Twist: 2.3 ± 0.1-fold change, $p \leq 0.0001$) and Malme-3M (ZEB1: 2.4 ± 0.1-fold change, $p \leq 0.0001$; Twist: 1.40 ± 0.05-fold change, $p = 0.0144$), whereas the A375 tumors only showed an upregulation for Twist expression (1.47 ± 0.08-fold change, $p = 0.0254$) (Fig. 5.1G, 5.1H). Since these transcription factors are often found to be co-expressed in different combinations during EMT, the absence of one of them is not necessarily a sign that EMT does not occur[6,13].

Taken together, these findings imply that NTP treatment triggers an EMT response, as evidenced by the activation of the cadherin switch, the upregulation of vimentin and the activation of the three main EMT transcription factors. Nevertheless, it should be noted these findings only represent one time point after NTP treatment. As mentioned before, EMT is a transition process, which transfers through different hybrid phases before attaining a fully mesenchymal phenotype. However, during these hybrid phases, the cells can also recover and return to their initial epithelial state before becoming fully mesenchymal[5]. Whereas the results from this model clearly indicate that EMT is initiated, no conclusions can be made regarding the progression of the EMT process. To do this, we would have to look at the expression at a later time point, which is not possible with the CAM model. Due to ethical considerations, it is not allowed to keep the eggs alive for more than 14 days, which makes analysis at a later time point impossible. Therefore, to answer the questions regarding the progression of NTP-induced EMT, we continued this study using the 3D spheroid model.

5.3.2 Investigating EMT progression and NTP-dose dependence in the 3D spheroid model

To examine the progression of EMT after NTP treatment, we evaluated the expression of the six markers at day 1, day 4 and day 7 after NTP treatment, using a low NTP treatment dose (200 Hz) and a high NTP treatment dose (700 Hz). These two NTP treatment conditions were chosen due to their ability to elicit a significant cytotoxic response in both cell lines (Fig. 5.2A, 5.2B). We only used the SK-MEL-28 and Malme-3M cell lines for these experiments since A375 did not form tight spheroids. Similarly, we started with the analysis of the cadherin switch. Interestingly, there appears to be an initial spike in E-cadherin expression for both cell lines and NTP doses, although the increase for

Malme-3M for the 200 Hz treatment is not statistically significant (200 Hz treatment: 2.2 ± 0.2-fold change for SK-MEL-28, p = 0.0481; 700 Hz treatment: 1.8 ± 0.2-fold change for SK-MEL-28, p = 0.0469, and 1.6 ± 0.1-fold change for Malme-3M, p = 0.0193), indicating an increase in cell adhesion (Fig. 5.2C, 5.2I). However, by day 4, the expression diminished and aligned with that of the untreated sample. By day 7 a strong downregulation of E-cadherin was observed for both cell lines for the high NTP-dose (0.31 ± 0.07 for SK-MEL-28, p = 0.0013, and 0.4 ± 0.1 for Malme-3M, p = 0.0241), whereas, despite the declining trend, no significant downregulation of E-cadherin was observed for the low NTP-dose. When looking at the N-cadherin expression, an upregulation can be observed for the high NTP-dose by day 4 for Malme-3M (1.6 ± 0.1-fold change, p = 0.0215) and even more by day 7 for both cell lines (1.8 ± 0.1-fold change for SK-MEL-28, p = 0.0156; and 1.8 ± 0.2-fold change for Malme-3M, p = 0.0440) (Fig. 5.2D, 5.2J). The low NTP-dose, however, does not significantly alter the expression of N-cadherin.

Furthermore, analysis of the vimentin expression showed that only the high NTP dose induced an increase in vimentin expression by day 4 for both cell lines (4.6 ± 0.5-fold change for SK-MEL-28, p = 0.0029; and 4.9 ± 0.4-fold change for Malme-3M, p = 0.0059) (Fig. 5.2E, 5.2K). Interestingly, the expression decreased again by day 7 and, for SK-MEL-28, even completely returned to the baseline level. Similarly to the cadherin switch, the low NTP treatment had negligible impact on vimentin expression.

Lastly, we examined the expression of the three EMT transcription factors. Regarding the expression of SNAI1, we observed an increase already at day 1 for the SK-MEL-28 spheroids for both the low NTP treatment (1.85 ± 0.08-fold change, p = 0.0127) and the high NTP treatment (2.00 ± 0.07, p = 0.0061), which stayed until day 4, but then

slightly decreased again by day 7 (Fig. 5.2F). However, neither NTP treatment had an impact on SNAI1 expression in the Malme-3M spheroids (Fig. 5.2L). For Twist and ZEB1, however, the two cell lines did respond similarly to NTP treatment. More specifically, Twist expression appears to be only affected by the high NTP treatment, with the highest upregulation at day 1 (2.4 $\pm$ 0.3-fold change for SK-MEL-28, $p = 0.0481$ and 2.1 $\pm$ 0.2 for Malme-3M, $p = 0.0373$), followed by a gradual return to baseline levels by day 7 (Fig. 5.2G, 5.2M). Furthermore, ZEB1 expression was upregulated by day 4 after following the high NTP treatment of both cell lines (2.7 $\pm$ 0.3-fold change for SK-MEL-28, $p = 0.0478$, and 2.7 $\pm$ 0.2-fold change for Malme-3M, $p = 0.0159$) (Fig. 5.2H, 5.2N). Similar to Twist, this effect was reduced back to its baseline level by day 7.

Altogether, these results imply that the 700 Hz NTP treatment triggers an EMT response, as evidenced by the activation of the cadherin switch, the upregulation of vimentin and the activation of the three main EMT transcription factors. However, these responses seem to be temporary and most of the biomarkers we investigated returned to their baseline levels by day 7, implying that the cells might only go through a partial EMT instead of reaching a fully mesenchymal phenotype. In contrast, the 200 Hz NTP treatment did not trigger a response for most EMT biomarkers, yet did induce a cytotoxic response, suggesting that using lower NTP treatment doses could circumvent these issues and be more attractive from a clinical perspective.

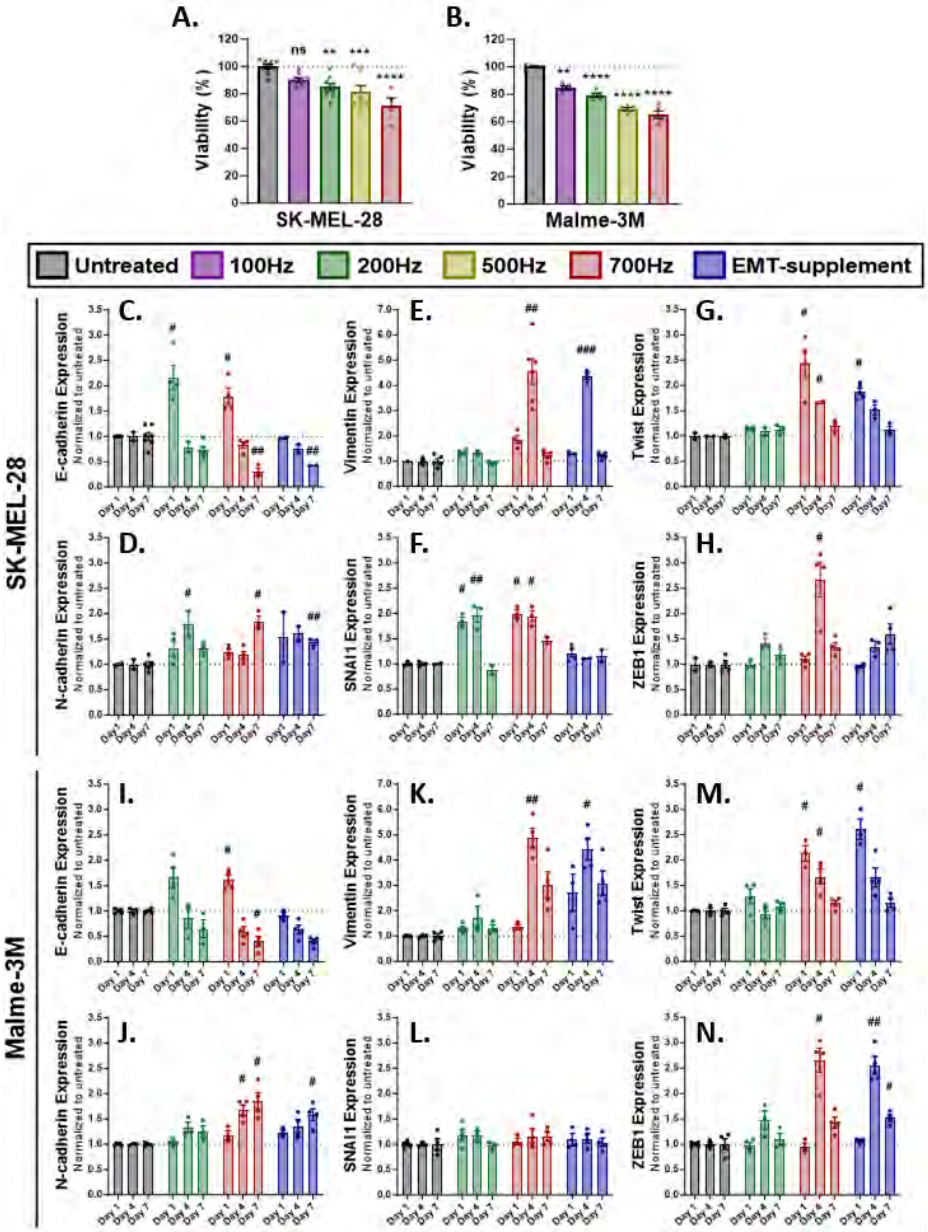

Figure 5.2 NTP-induced EMT response in 3D melanoma spheroids. A. Cytotoxic response of different NTP doses on SK-MEL-28 spheroids. B. Cytotoxic response of different NTP doses on Malme-3M spheroids. C.-H. Results from immunofluorescent stainings of six key EMT biomarkers (C. E-cadherin, D. Vimentin, E. Twist, F. N-cadherin, G. SNAI1, and H. ZEB1) in SK-MEL-28 spheroids comparing a 200 Hz and 700 Hz NTP treatment. As a positive control, an EMT-inducing supplement was used. I.-N. Results from immunofluorescent stainings of six key EMT biomarkers (C. E-cadherin, D. Vimentin, E. Twist, F. N-cadherin, G. SNAI1, and H. ZEB1) in Malme-3M spheroids. The results from C.-N. are normalized to the untreated sample of the

same time point and alterations in expression are assessed by calculating statistical significance between the treated sample and the untreated sample from the same time point. The untreated samples are used to indicate the baseline expression at each time point. All experiments were performed at least in triplicate and the data is represented as mean ± SEM. Statistical significance between the treated samples and the untreated samples from the same time point was calculated using the generalized linear mixed model. # $p \leq 0.05$, ## $p \leq 0.01$, ### $p \leq 0.001$

5.3.3 Migratory properties in both 3D melanoma models post-NTP treatment

Whereas the expression of the key EMT biomarkers is a valuable indicator of EMT progression, defining EMT exclusively on the basis of the expression of molecular markers underrepresents the enormous complexity and plasticity of EMT[6]. To complement this data, we performed more functional assays to investigate whether NTP-induced EMT could indeed provide the cells with enhanced migratory capacities. To examine the migratory capacities of the tumor cells in the CAM *in ovo* model, we collected several organs from the chicken embryo to check for metastasis. For this, we collected the liver, the lungs and the lowest part of the CAM (furthest away from the tumor site) immediately after tumor removal. After RNA isolation, we used RT-PCR to check the presence of human RNA in the organs of the chicken embryo. To start, we used embryo organs from an egg without a tumor to test eight primers for cross-reactivity with the chicken cells, namely B2M, HMBS, ALTB, HPRT1, TBP, SDHA, YWHAZ and UBC. From these, only B2M and HMBS gave a positive result for the human control sample without showing any reactivity with the chicken samples. Since B2M gave the brightest signal, we continued with this primer. In total, we collected samples from six eggs per condition for each cell line. When examining the results, we noticed that even for the untreated tumors there was some human RNA present in most of the samples (Fig. 5.3A). Due to large variations in the replicates, no statistical differences were found.

Nevertheless, we notice some trends in the heatmap for all three cell lines (Fig. 5.3A). In the samples from the lung and lower CAM, it seems like there is more human RNA detected in the NTP-treated samples compared to the untreated samples. Furthermore, there appears to be less human RNA in the liver samples in comparison to the lung and lower CAM samples for all three cell lines. Overall, these outcomes illustrate that the cancer cells are able to migrate away from the primary tumor on top of the CAM into the chicken embryo. Furthermore, while not statistically significant, it appears that NTP-treated cancer cells exhibit enhanced migratory capacities, confirming the previous findings that NTP can stimulate EMT, consequently enhancing migration.

To examine migratory capabilities in the 3D spheroid model, we performed a 3D migration assay by transferring the spheroids to a collagen-coated plate immediately after treatment, following which they were monitored every four hours for three days. Analysis was performed using the Orbits analysis software, which is able to recognize and calculate the area of the migrating tumor cells (Fig. 5.3B). For the SK-MEL-28 spheroids, a substantial increase in migration can be observed for the 700 Hz treatment, comparable to that of the positive control (Fig. 5.3C). However, the 200 Hz-treated spheroids did not show an increase in migration, indicating that the lower NTP treatment has a negligible impact on EMT initiation. The Malme-3M spheroids, however, did not show any alterations in migratory capacities in response to the NTP treatments. Even the positive control did not affect the migration in any of the repeats. This can potentially be explained by the relative instability of the Malme-3M spheroids in comparison to the SK-MEL-28 spheroids. Taken together, these findings support in part the previous observations that the high NTP treatment induces EMT and thereby enhances the

migratory capabilities of the cells, whereas the low NTP treatment did not trigger an EMT-inducing response.

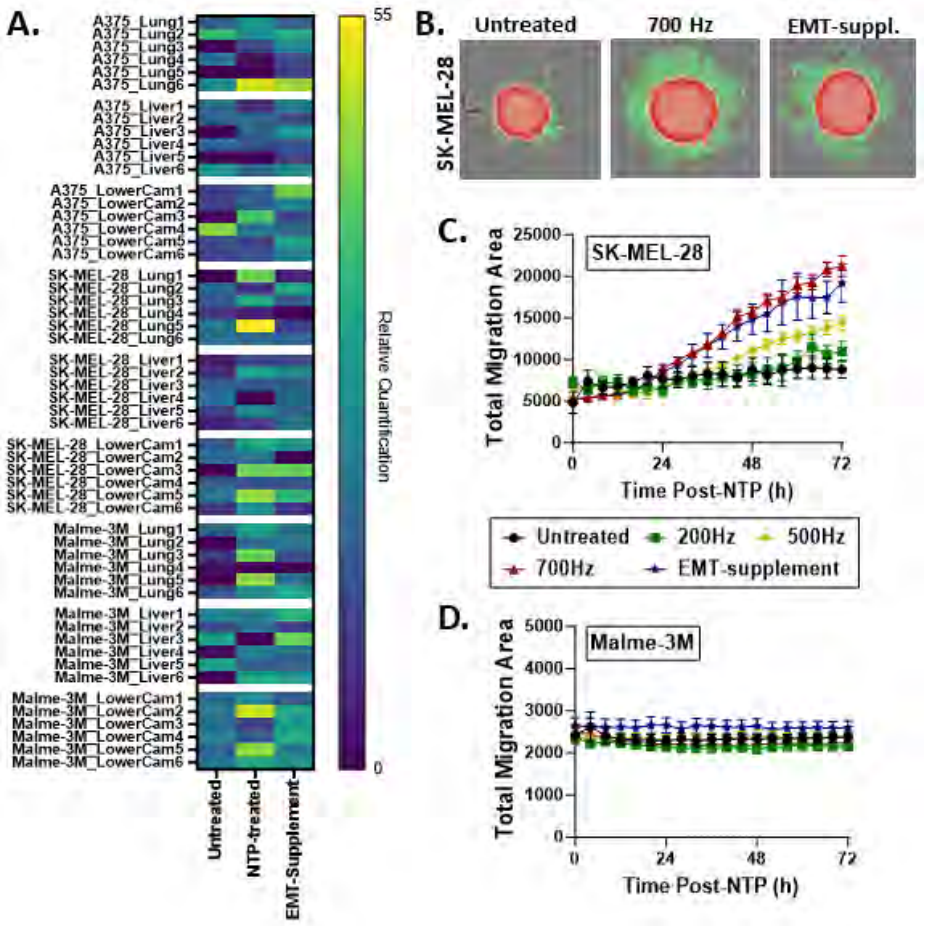

Figure 5.3 Functional assays to investigate enhanced migration post-NTP treatment. A. Heatmap showing the presence of human RNA in different organs of the chicken embryo, indicating metastasis from the primary tumor site. B. Representation of the analysis for the 3D spheroid migration software, analyzed by the Orbits Analysis Software. The red masking represents the spheroid and the green masking represents the migration area out of the spheroid. C.-D. Results from the 3D spheroid migration assay for C. SK-MEL-28 and D. Malme-3M. As a positive control, an EMT-inducing supplement was used. All experiments were performed at least in triplicate and the data is represented as mean ± SEM

5.4 Discussion

Although oxidative stress-inducing therapies, like NTP, hold significant promise as therapies for cancer, the dual nature of oxidative stress is often disregarded. Indeed, the majority of studies exploring NTP as a novel therapy for cancer report remarkable results in terms of cytotoxicity, selectivity and NTP's ability to trigger an immunogenic response, whereas almost no studies investigate its potential to induce EMT, and, consequently, its influence on the migratory capabilities of the cells. In this study, we evaluated the expression of six key EMT biomarkers in melanoma cancer cells, using both the CAM *in ovo* model and the 3D spheroid model. To confirm our findings, a functional assay was performed for both 3D models, assessing the enhanced migratory capabilities of the cancer cells post-NTP treatment. Taken together, our study demonstrates that NTP initiates an EMT-inducing response for the high NTP treatment dosage, whereas the low NTP dosage does not affect the EMT status or migratory capabilities of the cells, yet still inducing a toxic response.

The chick embryo chorioallantoic membrane (CAM) model has been widely used as a relatively simple and cost-efficient approach to study angiogenesis and metastasis. Because of the highly vascularized nature of the CAM, tumor grafting is relatively easy with a high reproducibility, and, moreover, it mimics the physiological cancer cell environment due to the presence of extracellular matrix proteins like fibronectin, laminin, collagen type I and integrin $\alpha_V\beta_3$[14,15]. While the use of this model dates back to studies from 1949, its re-emergence as an inventive alternative to murine models has sparked renewed attention within the cancer research community[10]. We used this model for the formation of tumors for three melanoma cell lines, A375, SK-MEL-28 and Malme-3M, and assessed several key EMT biomarkers, as well as the formation of

metastasis in the chicken embryo. Our results indicate that EMT is initiated after NTP treatment, as evidenced by activation of the cadherin switch, upregulation of vimentin and upregulation of the three major EMT transcription factors. These results are further supported by an elevated trend of metastasis in the lungs and lower CAM of the chicken embryo. While the outcomes from this model undeniably establish the initiation of EMT, drawing conclusions about the progression of this process remains limited since these findings are only representative of one specific time point following NTP treatment. To evaluate further, an examination at different time points would be necessary, which is not possible with the CAM model, since the survival of the eggs beyond day 14 is prohibited due to ethical constraints. Therefore, to address the question concerning the progression of NTP-induced EMT, we extended our study using the 3D spheroid model. In this model, we compared two NTP dosages (200 Hz vs. 700 Hz) and examined the responses at distinct time points following NTP treatment (day 1, day 4 and day 7). We demonstrated that the low NTP treatment had a negligible impact on EMT initiation. This was observed not only through the evaluation of the EMT biomarkers but also in the assessment of migration after treatment. In contrast, the 700 Hz treatment did trigger an EMT response, as evidenced by the activation of all six key biomarkers in both cell lines, as well as enhanced migratory characteristics after treatment but only for SK-MEL-28. This can potentially be explained by the relative instability of the Malme-3M spheroids in comparison to the SK-MEL-28 spheroids. Given that the 3D migration assay requires quite a lot of transferring of the spheroids, it is plausible that the experiment itself induced substantial stress on the spheroids. We should therefore be careful before claiming that EMT is not induced in these spheroids.

However, the alterations in the EMT biomarkers seem to be temporary and most of the biomarkers returned to their baseline expression by day 7, implying that the cells might only go through a partial EMT instead of reaching a fully mesenchymal phenotype. Nevertheless, it should be noted that these are the results from a single treatment. It is probable that subjecting the cells to repetitive 700 Hz NTP treatments, resulting in a more sustained EMT stimulation, might potentially drive the cells to progress further and attain a fully mesenchymal phenotype. Taken together, these findings highlight the importance of choosing the most optimal NTP treatment conditions. Whereas higher NTP treatment doses induce more cell death, they might simultaneously trigger several adverse effects like enhanced metastatic potential. In contrast, using lower NTP doses might lead to fewer side effects, however, due to their lower toxicity, they may require repetitive treatments. While this is not really a significant concern for superficial tumors, it might be an important limitation for the treatment of tumors situated within the body, which require a combination of surgery to access the tumor site.

Given that the induction of EMT is a relatively commonly found side effect in conventional therapies like chemotherapy and radiotherapy, increasing efforts are being made to search for opportunities to interfere with the EMT pathway and develop anti-EMT adjuvant therapies[1,16]. However, this is very challenging due to the high plasticity and heterogeneity of the various pathways involved[7]. Most of the currently available anti-EMT drugs are focused on blocking upstream inducers of EMT such as TGF-β[4,17]. However, the majority of these blockers are broad-spectrum inhibitors, being non-specific to cancer cells and therefore often causing side-effects[4]. An alternative anti-EMT approach is targeting the EMT transcription factors[4,17]. A study showed that genetically silencing the transcription factors could reduce the

metastatic burden and resistance to chemotherapy in a pancreatic cancer mouse model, showing its potential as valuable targets[12,18]. However, some controversy exists due to the traditional classification of transcription factors as “undruggable” as it is a nuclear event which is not readily accessible for drugs[17,19]. Furthermore, another strategy is to target active biomarkers of EMT[17,19]. For example, one could use biologically active compounds against vimentin, fibronectin and N-cadherin, promoting the transition back into an epithelial phenotype. Although this appears very promising, defining the precise therapeutic window for these type of drugs is critical as it might also accelerate metastasis of disseminated cells[17]. Despite the many challenges of developing anti-EMT therapies, there are currently several promising drugs at various stages of clinical trials, capable of targeting EMT markers. For instance, trabedersen, an antisense therapy capable of blocking protein translation of TGF-β mRNA, showed encouraging preliminary results in patients with stage IV pancreatic cancer, malignant melanoma, colorectal cancer and brain cancer[19,20]. Furthermore, salinomycin, an ionophore antibiotic, was shown to downregulate vimentin, while upregulating E-cadherin in colorectal cancer cells, reversing doxorubicin-induced EMT and restoring chemosensitivity *in vitro* and *in vivo*[21]. Moreover, several clinical cases showed reduced tumor metastasis in patients with metastatic breast cancer, metastatic ovarian cancer and metastatic head-and-neck squamous cell carcinoma[22].

In summary, despite notable progress, targeting or suppressing EMT remains very challenging. Developing anti-cancer therapies that do not alter the EMT state of the cancer cells offers therefore major benefits. As shown by our results, optimizing the treatment parameters of NTP

therapy could majorly impact its response on EMT induction, thereby highlighting the clinical potential of using lower NTP treatment doses.

5.5 Conclusions

While NTP holds remarkable potential as an anti-cancer therapy, its capacity to induce EMT and, subsequently, impact cell migration has been largely overlooked. This study provides a comprehensive overview of NTP-induced EMT initiation and progression in melanoma by evaluating the expression of six key EMT biomarkers together with the assessment of changes in migration following NTP treatment. We revealed that a high NTP treatment dose triggered a significant EMT response and enhanced migration following treatment, whereas a low NTP dose did not alter the EMT state of the cells. Overall, our findings demonstrate that optimizing the NTP dose holds the key to improving its therapeutic potential, thus highlighting the significance of these insights into the clinical translation of NTP.

5.6 References

1. Giannoni E, Parri M, Chiarugi P. EMT and oxidative stress: A bidirectional interplay affecting tumor malignancy. *Antioxid Redox Signal*. 2012;16(11):1248-1263. doi:10.1089/ars.2011.4280

2. Chatterjee R, Chatterjee J. ROS and oncogenesis with special reference to EMT and stemness. *Eur J Cell Biol*. 2020;99(2-3). doi:10.1016/j.ejcb.2020.151073

3. Ribatti D, Tamma R, Annese T. Epithelial-Mesenchymal Transition in Cancer: A Historical Overview. *Transl Oncol*. 2020;13(6). doi:10.1016/j.tranon.2020.100773

4. Huang Y, Hong W, Wei X. The molecular mechanisms and therapeutic strategies of EMT in tumor progression and metastasis. *J Hematol Oncol*. 2022;15(1). doi:10.1186/s13045-022-01347-8

5. Pastushenko I, Blanpain C. EMT Transition States during Tumor Progression and Metastasis. *Trends Cell Biol*. 2019;29(3):212-226. doi:10.1016/j.tcb.2018.12.001

6. Yang J, Antin P, Berx G, et al. Guidelines and definitions for research on epithelial–mesenchymal transition. *Nat Rev Mol Cell Biol*. 2020;21(6):341-352. doi:10.1038/s41580-020-0237-9

7. Ye X, Weinberg RA. Epithelial-Mesenchymal Plasticity: A Central Regulator of Cancer Progression. *Trends Cell Biol*. 2015;25(11):675-686. doi:10.1016/j.tcb.2015.07.012

8. Sinha D, Saha P, Samanta A, Bishayee A. Emerging concepts of hybrid epithelial-to-mesenchymal transition in cancer progression. *Biomolecules*. 2020;10(11):1-22. doi:10.3390/biom10111561

9. Jolly MK, Mani SA, Levine H. Hybrid epithelial/mesenchymal phenotype(s): The ‘fittest’ for metastasis? *Biochim Biophys Acta Rev Cancer*. 2018;1870(2):151-157. doi:10.1016/j.bbcan.2018.07.001

10. Domenico Ribatti. *The Chick Embryo Chorioallantoic Membrane in the Study of Angiogenesis and Metastasis*.; 2010.

11. Loh CY, Chai JY, Tang TF, et al. The e-cadherin and n-cadherin switch in epithelial-to-mesenchymal transition: Signaling, therapeutic implications, and challenges. *Cells*. 2019;8(10). doi:10.3390/cells8101118

12. Debnath P, Huirem RS, Dutta P, Palchaudhuri S. Epithelial-mesenchymal transition and its transcription factors. *Biosci Rep*. 2022;42(1). doi:10.1042/BSR20211754

13. Jägle S, Dertmann A, Schrempp M, Hecht A. ZEB1 is neither sufficient nor required for epithelial-mesenchymal transition in LS174T colorectal cancer cells. *Biochem Biophys Res Commun*. 2017;482(4):1226-1232. doi:10.1016/j.bbrc.2016.12.017

14. Ribatti D. The CAM assay in the study of the metastatic process. *Exp Cell Res*. 2021;400(2). doi:10.1016/j.yexcr.2021.112510

15. Pawlikowska P, Tayoun T, Oulhen M, et al. Exploitation of the chick embryo chorioallantoic membrane (CAM) as a platform for anti-metastatic drug testing. *Sci Rep*. 2020;10(1). doi:10.1038/s41598-020-73632-w

16. Santos Ramos F, Wons L, João Cavalli I, M.S.F. Ribeiro E. Epithelial-mesenchymal transition in cancer: An overview. *Integr Cancer Sci Ther*. 2017;4(3). doi:10.15761/icst.1000243

17. Jonckheere S, Adams J, De Groote D, Campbell K, Berx G, Goossens S. Epithelial-Mesenchymal Transition (EMT) as a Therapeutic Target. *Cells Tissues Organs*. 2022;211(2):157-182. doi:10.1159/000512218

18. Sakata J, Utsumi F, Suzuki S, et al. *Inhibition of ZEB1 Leads to Inversion of Metastatic Characteristics and Restoration of Paclitaxel Sensitivity of Chronic Chemoresistant Ovarian Carcinoma Cells*. Vol 8.; 2017. www.impactjournals.com/oncotarget

19. Zhang N, Ng AS, Cai S, Li Q, Yang L, Kerr D. Novel therapeutic strategies: targeting epithelial–mesenchymal transition in colorectal cancer. *Lancet Oncol*. 2021;22(8):e358-e368. doi:10.1016/S1470-2045(21)00343-0

20. D'Cruz O, Lee C, Trieu V, Hwang L. Synergistic antitumor effects of OT-101 (trabedersen), a transforming growth factor-beta 2 (TGF-β2) antisense oligonucleotide (ASO) and chemotherapy in preclinical tumor models. *Annals of Oncology*. 2017;28:v583-v584. doi:10.1093/annonc/mdx390.034

21. Zhou Y, Liang C, Xue F, et al. Salinomycin decreases doxorubicin resistance in hepatocellular carcinoma cells by inhibiting the β-catenin/TCF complex association via FOXO3a activation. *Oncotarget*. 2015;6(12):10350-10365. doi:10.18632/oncotarget.3585

22. Qi D, Liu Y, Li J, Huang JH, Hu X, Wu E. Salinomycin as a potent anticancer stem cell agent: State of the art and future directions. *Med Res Rev*. 2022;42(3):1037-1063. doi:10.1002/med.21870

CHAPTER 6

General Conclusions and Future Perspectives

6.1 General Conclusions

Over the years, our understanding of NTP as a novel therapy for cancer has consistently evolved thanks to the persistent efforts of a growing plasma-oncology scientific community. Years of multidisciplinary research have proven the potential of NTP to trigger a cytotoxic response in many cancer types, both *in vitro*, *in vivo* and even in pilot clinical studies. Furthermore, it was found that NTP, when combined with other cancer therapies, can synergistically augment toxicity and enhance their selectivity and efficacy against resistant tumors[1-4]. However, in order to effectively use NTP in the clinic, a better understanding of the impact of oxidative stress-responses following NTP treatment is necessary.

In this thesis, I started with unraveling the ability of NTP to selectively killing cancer cells (**Chapter 2**). As an oxidative-stress inducing therapy, NTP is often claimed to be selective but in many cases it has been misconcluded due to discrepancies in culturing conditions and cell types. I showed that several factors, like cell culture medium, cancer type and even cell type, can have a major influence of cancer cell selectivity. Since the influence of the cell culture medium was less important for direct NTP treatment, I used this treatment modality to analyze the selectivity of treatment for two cancer types: melanoma and glioblastoma. I showed that direct NTP treatment preferentially affected cancer cells at lower intensity treatments, suggesting that selectivity depends on optimizing NTP treatment conditions to exploit the differences between normal and cancerous tissue. Interestingly, the perks of using low dose NTP treatments were further supported by the findings in **Chapter 5**, revealing that low NTP treatments did not trigger an EMT-inducing response, in contrast to the impact of high NTP treatments.

As it became clear in Chapter 2, many factors can influence the stability of NTP-derived RONS. This raised some questions regarding the stability of these RONS in more clinically relevant fluids. In **Chapter 3**, I explored the scavenging potential of various blood components following the two NTP modalities. This study, marking the first examination of NTP-derived RONS in blood, addresses the knowledge gap concerning the interaction between NTP-derived RONS and clinical substrates. Notably, our results revealed that RONS were scavenged up to a fixed concentration, irrespective of the initial RONS quantities generated by the two NTP modalities. This implies that the scavenging action of dissolved proteins and lipids in blood plasma is only partial. The inclusion of cellular and platelet components in whole blood further contributed to RONS scavenging. Specifically, H_2O_2 exhibited significant scavenging capacity within blood plasma. In contrast, the rapid quenching of H_2O_2 by processed whole blood primarily stemmed from the enzymatic mechanisms in red blood cells, safeguarding hemoglobin from oxidative changes. This observation highlights the role of hemoglobin in preventing the formation of potentially toxic ferryl hemoglobin. Overall, this study highlighted the importance of understanding the behavior of NTP-derived RONS in clinical substrates and their subsequent by-products for the safe clinical translation of this technology. While both direct and indirect NTP treatment exhibit translational potential, their mechanisms vary due to the nature of the species they deliver, influencing their potential for specific clinical applications.

In order to further unravel the difference between the underlying mechanisms of how the two NTP modalities kill the cells, I investigated which regulated cell death (RCD) pathways were activated following both direct and indirect NTP treatment, focusing on apoptosis,

necroptosis, pyroptosis and ferroptosis (**Chapter 4**). I demonstrated that both direct and indirect NTP treatment were able to activate apoptosis, necroptosis and ferroptosis, whereas only direct NTP treatment activated the pyroptotic pathway. The intricate nature of these RCD pathways, each with dual roles in cancer progression and therapy, necessitates careful consideration for their targeted manipulation. Activating these pathways collectively could hold the key to combatting therapy resistance. As researchers explore combination therapies targeting multiple cell death pathways, the insights provided by this study into the diverse responses to NTP treatment will undoubtedly contribute to the development of more effective and strategic therapeutic approaches in the future.

Besides the many advantages of oxidative stress-inducing therapies such as NTP, it should be acknowledged that oxidative stress can be a key driver promoting tumor metastasis and drug resistance. In **Chapter 5**, I delved into this often neglected aspect by investigating the impact of NTP treatment on epithelial-mesenchymal transition (EMT)-related biomarkers and migratory capabilities using both the CAM *in ovo* model and the 3D spheroid model. The CAM model revealed NTP's ability to initiate EMT, evidenced by the activation of key EMT biomarkers and an elevated trend in metastasis in the lungs and lower CAM of the chicken embryo. In contrast, the 3D spheroid model demonstrated distinct EMT responses at different time points following NTP treatment, emphasizing the importance of studying the progression of NTP-induced EMT over time. These observations highlight the significance of selecting the optimal NTP treatment conditions to balance cytotoxicity and adverse effects such as enhanced metastatic potential.

6.2 Future perspectives of NTP treatment for cancer

In this thesis, I aspired to elucidate several fundamental questions regarding the dual role of oxidative stress induced by NTP treatment of cancer. Taken together, my findings support the promising potential of NTP as a valuable addition to conventional cancer strategies. However, there are still several important aspects to be figured out before clinical application is possible.

The main challenge, in my opinion, that needs to be addressed in order to really progress towards clinical implementation is uniformity and dose standardization. Upon reviewing the literature and participating in conferences, it becomes evident that many researchers use custom-made plasma sources. While they all fall under the category of a plasma jet or DBD, the configuration and generation of RONS differ greatly across different setups. As was shown in Chapters 2 and 5 of this thesis, the specific array of RONS delivered to the cells, and even more crucially the concentration of these species, greatly influences the outcome of the treatment. Given the diverse range of plasma sources used by researchers, defining a standardized dosing regime is very challenging. Addressing this predicament would allow for a better dose standardization, promote more collaborations among researchers and increase the supporting evidence essential to convince clinicians of the therapeutic potential of NTP treatment.

Another challenge is the delivery method for the treatment of tumors deep within the body. While NTP treatment is straightforward for superficial tumors such as skin cancer and head and neck cancer, addressing non-superficial tumors poses greater challenges due to accessibility issues. One potential strategy involves integrating NTP with surgical procedures, enabling the eradication of lingering cancer cells

within surgical sites or addressing tumor regions that are challenging to excise. Another approach could be to use plasma-treated liquids (PTL). This indirect approach allows for the treatment of deeper located tumors using injections or catheters without the need of surgery, resulting in a minimally invasive treatment[5]. However, only the long-lived species would reach the tumor, possibly limiting the cytotoxic effect. Moreover, researchers are raising the question whether NTP is really necessary to make these solutions[5]. Since it mainly relies on the interaction of the tumor with the long-lived species, H_2O_2, NO_2^- and NO_3^-, why not just mix these chemicals to obtain a similar effect. Indeed, several studies have proven that such mock solutions have the same biological effects as the corresponding plasma-treated ones[6–8].

Despite these challenges, massive leaps have been made in the path towards clinical application for NTP and pilot clinical studies have already been performed to assess its potential. In 2018, Metelmann *et al*. used the kINPen MED to treat patients with locally advanced head and neck squamous cell carcinoma[9]. Their findings indicated a reduction in the need for pain medication and a decrease in odor, along with improvements in social function and emotional well-being. Furthermore, Canady *et al*. recently conducted a Phase I trial using the Canady Helios Cold Plasma device in combination with surgical resection to treat patients with stage IV or recurrent solid tumors[10]. Their results demonstrated that the combination of NTP treatment and surgery is not only safe but also exhibits selectivity for cancer cells. These outcomes hold great promise for effectively controlling local and regional recurrences in cancer patients.

6.3 References

1. Lafontaine J, Boisvert JS, Glory A, Coulombe S, Wong P. Synergy between non-thermal plasma with radiation therapy and olaparib in a panel of breast cancer cell lines. *Cancers (Basel)*. 2020;12(2). doi:10.3390/cancers12020348

2. Liedtke KR, Freund E, Hermes M, et al. Gas plasma-conditioned ringer's lactate enhances the cytotoxic activity of cisplatin and gemcitabine in pancreatic cancer in vitro and in ovo. *Cancers (Basel)*. 2020;12(1). doi:10.3390/cancers12010123

3. Almeida ND, Klein AL, Hogan EA, et al. Cold Atmospheric Plasma as an Adjunct to Immunotherapy for Glioblastoma Multiforme. *World Neurosurg*. 2019;130:369-376. doi:10.1016/j.wneu.2019.06.209

4. Van Loenhout J, Boullosa LF, Quatannens D, et al. Auranofin and cold atmospheric plasma synergize to trigger distinct cell death mechanisms and immunogenic responses in glioblastoma. *Cells*. 2021;10(11). doi:10.3390/cells10112936

5. Tampieri F, Gorbanev Y, Sardella E. Plasma-treated liquids in medicine: Let's get chemical. *Plasma Processes and Polymers*. Published online June 7, 2023. doi:10.1002/ppap.202300077

6. Girard PM, Arbabian A, Fleury M, et al. Synergistic Effect of H2O2 and NO2 in Cell Death Induced by Cold Atmospheric He Plasma. *Sci Rep*. 2016;6(1):29098. doi:10.1038/srep29098

7. Sklias K, Santos Sousa J, Girard PM. Role of Short- and Long-Lived Reactive Species on the Selectivity and Anti-Cancer Action of Plasma Treatment In Vitro. *Cancers (Basel)*. 2021;13(4):615. doi:10.3390/cancers13040615

8. Jirešová J, Scholtz V, Julák J, Šerá B. Comparison of the Effect of Plasma-Activated Water and Artificially Prepared Plasma-Activated Water on Wheat Grain Properties. *Plants*. 2022;11(11):1471. doi:10.3390/plants11111471

9. Metelmann HR, Seebauer C, Miller V, et al. Clinical experience with cold plasma in the treatment of locally advanced head and neck cancer. *Clin Plasma Med*. 2018;9:6-13. doi:10.1016/j.cpme.2017.09.001

10. Canady J, Murthy SRK, Zhuang T, et al. The First Cold Atmospheric Plasma Phase I Clinical Trial for the Treatment of Advanced Solid Tumors: A Novel Treatment Arm for Cancer. *Cancers (Basel)*. 2023;15(14):3688. doi:10.3390/cancers15143688

Summary

Cancer is the second leading cause of death worldwide and has become an important factor affecting people's heath and quality of life for decades. Although conventional therapies like chemotherapy, surgery, radiation and immunotherapy have advanced significantly in recent years, issues regarding the development of resistance remain very challenging. Therefore, the development of innovative therapies remains critical in the fight against this horrible disease.

The last two decades, researchers have demonstrated the potential of non-thermal plasma (NTP) as a valuable addition to conventional therapies. NTP is a partially ionized gas, consisting of various reactive oxygen and nitrogen species (RONS). These RONS can interact with the cells and trigger an oxidative stress response, leading to cell death. Whereas oxidative stress-inducing therapies are very promising, the dual nature of a pro-oxidant environment should be carefully considered when developing a novel therapy.

After providing a general introduction on NTP in Chapter 1, I examined the potential of NTP as a selective treatment for glioblastoma and melanoma in Chapter 2. I revealed that many experimental factors can greatly influence the outcome of the experiments, making the assessment of selectivity very challenging. For direct NTP treatment, I was able to examine the selective response and demonstrated that lower NTP doses were able to selectively target the cancer cells, with a lesser effect on their healthy counterparts.

In Chapter 3, I investigated the stability of the long-lived RONS, specifically H_2O, NO_2^- and NO_3^-, in three clinically relevant solutions, namely phosphate-buffered saline, blood plasma and whole blood. I demonstrated that both blood plasma and whole blood were able to significantly scavenge the NTP-derived RONS. These findings illustrate the importance of understanding the behavior of NTP-derived RONS to ensure a reliable clinical application.

Furthermore, in Chapter 4, I characterized the different regulated cell death pathways that are activated following NTP treatment. I demonstrated that both direct and indirect NTP treatment are able to activate apoptosis, necroptosis and ferroptosis, whereas the induction of pyroptosis was exclusively observed following direct NTP treatment. This response highlights the potential of NTP as a multidimensional treatment, lowering the risk of resistance development.

Finally, in Chapter 5, I shifted the attention towards the potential drawbacks of oxidative stress-inducing therapies, investigating the enhanced metastatic potential following NTP treatment. I revealed that a high NTP dose triggered an EMT-inducing response, followed by enhanced migration, whereas a low NTP dose exhibited no impact on the migratory behavior of the cancer cells. These findings highlight the importance of optimizing the NTP parameters to obtain an optimal treatment regime with minimal side effects.

Summarized key findings:

- → NTP selectivity is often misconcluded in literature due to discrepancies in treatment factors. When analyzed properly, I found a slightly selective response for lower treatment doses for direct treatment, though the biological relevance might be minimal.
- → Long-lived RONS are inactivated in blood plasma and whole processed blood, limiting the clinical application of indirect NTP treatment.
- → Both direct and indirect NTP treatment are able to activate multiple RCD pathways, including apoptosis, necroptosis, ferroptosis, and for direct NTP treatment also pyroptosis, minimizing the risk of resistance development.
- → High NTP doses do not only induce a high cytotoxic response, but they also trigger an EMT response, enhancing the metastatic potential of the cells. Since low doses do not trigger this effect, using repetitive lower NTP doses might hold greater clinical potential for clinical translation.

Overall, the results presented in this thesis highlight the importance of optimizing the NTP treatment parameters. Whereas high NTP treatments appear to be interesting due to their high cytotoxic response, using low repetitive NTP treatments might hold more clinical potential, due to their ability to selectively target cancer cells without enhancing the metastatic potential. However, it should be noted that repeated treatments are only feasible for superficial tumors, while for other tumors supplementary surgical interventions would be required. In Chapter 6, I provide a general conclusion to the previous chapters and reveal several challenges for the future perspective of NTP treatment for cancer.

Samenvatting

Kanker is wereldwijd de op een na belangrijkste doodsoorzaak en heeft decennialang een belangrijke invloed gehad op de gezondheid en levenskwaliteit van patiënten. Hoewel conventionele therapieën zoals chemotherapie, chirurgie, bestraling en immuuntherapie de afgelopen jaren aanzienlijke vooruitgang hebben geboekt, blijven problemen met betrekking tot de ontwikkeling van resistentie zeer uitdagend. De ontwikkeling van innovatieve therapieën is daarom nog steeds essentieel in de strijd tegen deze vreselijke ziekte.

In de afgelopen jaren hebben onderzoekers het potentieel van niet-thermisch plasma (NTP) aangetoond als veelbelovende aanvulling op conventionele therapieën. NTP is een gedeeltelijk geïoniseerd gas, bestaande uit verschillende reactieve zuurstof- en stikstofdeeltjes. Deze reactieve deeltjes kunnen interageren met de kankercellen, waar ze de oxidatieve balans verstoren en celdood kunnen veroorzaken. Hoewel therapieën die oxidatieve stress veroorzaken zeer veelbelovend zijn, moet de dubbele aard van een pro-oxidatieve tumoromgeving zorgvuldig worden overwogen bij de ontwikkeling van een nieuwe therapie.

Na een algemene inleiding over NTP in Hoofdstuk 1, heb ik in Hoofdstuk 2 het potentieel van NTP onderzocht als een selectieve behandeling voor glioblastoom en melanoom. Ik heb aangetoond dat veel experimentele factoren een aanzienlijke invloed kunnen hebben op de resultaten, wat de evaluatie van de selectiviteit zeer uitdagend maakt. Voor de directe NTP-behandeling was ik in staat om de selectieve

reactie te onderzoeken en aan te tonen dat lagere NTP-dosissen in staat waren om de kankercellen selectief te behandelen, met een minder cytotoxisch effect op hun gezonde tegenhangers.

In Hoofdstuk 3 heb ik de stabiliteit onderzocht van de langlevende reactieve zuurstof- en stikstofdeeltjes, meer specifiek H_2O_2, NO_2^- en NO_3^-, in drie klinisch relevante oplossingen, namelijk een fosfaat-gebufferde zoutoplossing, bloedplasma en volledig bloed. Ik heb aangetoond dat zowel bloedplasma als volledig bloed in staat waren om de gegenereerde reactieve zuurstof- en stikstofdeeltjes aanzienlijk te verminderen. Deze resultaten benadrukken het belang om te begrijpen wat er met de NTP-gegenereerde deeltjes gebeurd in het lichaam om een veilige klinische behandeling mogelijk te maken.

In Hoofdstuk 4 ben ik nagegaan welke gereguleerde celdoodmechanismen geactiveerd worden na behandeling met NTP. Ik heb aangetoond dat zowel directe als indirecte NTP behandeling apoptose, necroptose en ferroptose kunnen activeren, terwijl de inductie van pyroptose uitsluitend werd waargenomen na directe NTP behandeling. Dit resultaat benadrukt het potentieel van NTP als een multivariabele behandeling, wat de kans op de ontwikkeling van resistentie tegen deze behandeling kleiner maakt.

Tot slot heb ik in Hoofdstuk 5 de aandacht verlegd naar de mogelijke nadelen van het veroorzaken van oxidatieve stress. Meer specifiek heb ik onderzocht of NTP in staat is om de migrationele eigenschappen van de kankercellen te beïnvloeden. Ik toonde aan dat een hoge NTP-dosis een reactie van epitheliale-naar-mesenchymale overgang op gang bracht, gevolgd door een verhoogde migratie, terwijl een lage NTP-dosis geen invloed had op het migratiegedrag van de kankercellen. Dit benadrukt het belang om de behandelingscondities te optimaliseren om

maximale schade aan te brengen aan de tumor met minimale bijwerkingen.

Belangrijkste bevindingen samengevat:

- → NTP-selectiviteit wordt in de literatuur vaak verkeerd geïnterpreteerd vanwege discrepanties in behandelingsfactoren. Bij een goede analyse vond ik een lichte selectieve respons voor lagere behandelingsdoses voor directe behandeling, hoewel de biologische relevantie minimaal zou kunnen zijn.
- → Langlevende reactieve zuurstof- en stikstofdeeltjes worden geïnactiveerd in bloedplasma en verwerkt bloed, waardoor de klinische toepassing van indirecte NTP-behandeling beperkt is.
- → Zowel directe als indirecte NTP behandeling is in staat om meerdere celdoodmechanismen te activeren, waaronder apoptose, necroptose, ferroptose, en voor directe behandeling ook pyroptose, waardoor de kans op de ontwikkeling van resistentie kleiner is.
- → Hoge NTP dosissen kunnen niet alleen een hoge cytotoxische respons induceren, maar ze activeren ook een toenemend metastatisch karakter van de cellen. Aangezien lage dosissen dit effect niet uitlokken, zou het gebruik van herhaalde lagere NTP dosissen een groter klinisch potentieel kunnen hebben.

Samenvattend tonen de resultaten gepresenteerd in dit proefschrift het belang van het optimaliseren van de parameters van de NTP-behandeling. Hoewel hoge NTP-dosissen interessant lijken vanwege hun sterke cytotoxische respons, hebben herhaalde lage NTP-behandelingen mogelijk meer klinisch potentieel vanwege hun vermogen om selectief kankercellen aan te vallen zonder hun migratiegedrag te beïnvloeden.

List of Publications/Conferences

First Author Publications

"The Influence of Cell Type and Culture Medium on Determining Cancer Selectivity of Non-Thermal Plasma Treatment", **Biscop E**., Lin A., Van Boxem W., Van Loenhout J., De Backer J., Deben C., Dewilde S., Smits E., Bogaerts A. Cancers 11(9) (2019) IF: 6.639

DOI: 10.3390/cancers11091287

"Critical Evaluation of the Interaction of Reactive Oxygen and Nitrogen Species with Blood to Inform the Clinical Translation of Non-Thermal Plasma Therapy", **Biscop E**., Lin A., Breen C., Butler S. J., Smits, E., Bogaerts A. Oxidative Medicine and Cellular Longevity Vol 2020, 9750206 (2020) IF: 7.31

DOI: 10.1155/2020/9750206

Under Submission

"Characterization of Regulated Cancer Cell Death Pathways Induced by the Different Modalities of Non-Thermal Plasma Treatment: Apoptosis, Pyroptosis, Necroptosis, and Ferroptosis", **Biscop E**., Baroen J., De Backer J., Vanden Berghe W., Smits, E., Bogaerts A., Lin. A

"Dose-Dependent Induction of Epithelial-Mesenchymal Transition by Non-Thermal Plasma Treatment in 3D Melanoma Spheroids and *In Ovo* Tumors", **Biscop E**., Cardenas De La Hoz E., Verswyvel H., De Backer J., Lau H.W., Vanden Berghe W. Smits, E., Bogaerts A., Lin A.

As Co-author

"Toward Defining Plasma Treatment Dose: The Role of Plasma Treatment Energy of Pulsed-Dielectric Barrier Discharge in Dictating In Vitro Biological Responses", Lin A., **Biscop E**., Gorbanev Y., Smits E., Bogaerts A. Plasma Processes and Polymers 19(3) (2021) IF: 3.877

DOI: 10.1002/ppap.202100151

"Acquired Non-Thermal Plasma Resistance Mediates a Shift Towards Aerobic Glycolysis and Ferroptotic Cell Death in Melanoma", Lin A., Sahun M., **Biscop E**., Verswyvel H., De Waele J., De Backer J., Theys C., Cuypers B., Laukens K., Vanden Berge W., Smits E., Bogaerts A. Drug Resistance Updates Vol 67, 100914 (2023) (16 pages)

DOI : 10.1016/j.drup.2022.100914

Conference Contributions – Oral Presentations

- Frontiers in Redox Biochemistry and Medicine (FiRBaM) 2019, Greifswald Germany: Does plasma induce EMT type 3?
- Chemistry Conference for Young Scientists (ChemCYS) 2020, Blankenberge Belgium: Does cold atmospheric plasma induce epithelial-mesenchymal transition in cancer cells?
- 1st International CAM Conference 2022, Online: The effect of NTP on epithelial-mesenchymal transition of melanoma cells in the 3D Chicken Chorioallantoic Membrane model
- 9th International Conference on Plasma Medicine (ICPM9) 2022, Utrecht The Netherlands: Elucidating non-thermal plasma-induced cell death mechanisms for direct and indirect treatment conditions
    - **Awarded Best Student Paper Award**

Conference Contributions – Poster Presentations

- 6th International Workshop on Plasma for Cancer Therapy (IWPCT) 2019, Antwerp Belgium: Selectivity of plasma treatment for cancer and the influence of the cell culture medium
- Belgian Association for Cancer Research (BACR) 2019, Antwerp: Selectivity of plasma treatment for cancer and the influence of the cell culture medium
- 7th International Workshop on Plasma for Cancer Therapy (IWPCT) 2021, Online: The effect of non-thermal plasma on epithelial-mesenchymal transition
- European Association for Cancer Research (EACR) 2022, Sevilla Spain: The effect of non-thermal plasma on epithelial-mesenchymal transition in a 3D melanoma model
- UA Cancer Research Day 2022, Antwerp Belgium: The effect of non-thermal plasma on epithelial-mesenchymal transition in a 3D melanoma model

Other Science-Promoting Activities

- Organizing the workshop “Proefkot” to promote science to children between 9 and 13 years old. (November 2019, October 2020 and Februari 2021)
- Organizing the workshop “Doe Chemie”, to promote chemistry to high school students who passed the first round of the “chemistry olympiad” (Januari 2020, Januari 2021)
- Part of the support team of the Kekule lectures at the University of Antwerp as part of Jong-KVCV (2019-2020, 2021-2022)
- Part of the organizing committee of ChemCYS 2020 and CRF-ChemCYS 2022, an international conference or young scientists in Blankenberge